Copyright Warning & Restrictions

The copyright law of the United States (Title 17, United States Code) governs the making of photocopies or other reproductions of copyrighted material.

Under certain conditions specified in the law, libraries and archives are authorized to furnish a photocopy or other reproduction. One of these specified conditions is that the photocopy or reproduction is not to be "used for any purpose other than private study, scholarship, or research." If a, user makes a request for, or later uses, a photocopy or reproduction for purposes in excess of "fair use" that user may be liable for copyright infringement,

This institution reserves the right to refuse to accept a copying order if, in its judgment, fulfillment of the order would involve violation of copyright law.

Please Note: The author retains the copyright while the New Jersey Institute of Technology reserves the right to distribute this thesis or dissertation

Printing note: If you do not wish to print this page, then select "Pages from: first page # to: last page #" on the print dialog screen

ABSTRACT

OPTIMIZING SPEED PROFILES FOR SUSTAINABLE TRAIN OPERATION WITH WAYSIDE ENERGY STORAGE SYSTEMS

by
Leon A. Allen

Large hauling capability and low rolling resistance has put rail transit at the forefront of mass transportation mode sustainability in terms of congestion mitigation and energy conservation. As such, rail vehicles are one of the least energy-intensive modes of transportation and least environmentally polluting. Despite, these positives, improper driving habits and wastage of the braking energy through dissipation in braking resistors result in unnecessary consumption, extra costs to the operator and increased atmospheric greenhouse gas emissions.

This study presents an intelligent method for the optimization of the number and locations of wayside energy storage system (WESS) units that maximize the net benefits of the operation of a rail line. First, the optimized speed profiles with and without WESS is determined for a single alignment segment. Then, using the speed profiles obtained as an input, the number and locations of the WESS units that maximize the net benefit is determined for an entire rail line. The energy recovery methods used comprise optimal coasting, regenerative braking, and positioning of the energy storage devices to achieve maximum receptivity. Coasting saves energy by maintaining motion with propulsion disabled, but this increases the total travel time. Regenerative braking converts the kinetic

energy of the train into electrical energy for the powering of subsequent acceleration cycles and although it does not affect travel time, it reduces the time available for coasting, indicative of a tradeoff. The study entails the design of a model that simulates the movement of the train over an existing alignment section while considering alignment topography, speed limits, and train schedule. Since on-time performance is the priority of railroad operations, the simulator instructs the driver to operate according to several motion regimes to optimize the energy consumption while maintaining schedule.

The model consists of several time-varying inputs which add increased levels of complexity to the problem. This, in addition to its combinatorial nature, necessitates a heuristic algorithm to solve it, because traditional analytical solution methods are deficient. The optimization problem is solved by applying Genetic Algorithms (GA) because of their ability to search for a global solution in a complex multi-dimensional space. This strategy adds sustainability and reduces the carbon footprint of the operator. A case study is conducted on a single segment of a commuter rail line and yields a 34% energy reduction. The case study is extended to an entire line with multiple segments where the aim is to optimize the locations of wayside energy storage devices (WESS) for maximum economic benefit. It was found that out of the 10 alignment segments in the study, a maximized benefit of over $600,000 was achieved with WESS units installed on only three of those segments.

The methods derived in this study can be used to generate speed profiles for planning purposes, to assist in recovery from service disruptions, to plan for infrastructural

upgrades related to energy harvesting or to assist in the development of Driver Advisory Systems (DAS).

OPTIMIZING SPEED PROFILES FOR SUSTAINABLE TRAIN OPERATION WITH WAYSIDE ENERGY STORAGE SYSTEMS

by
Leon A. Allen

A Dissertation
Submitted to the Faculty of
New Jersey Institute of Technology
in Partial Fulfillment of the Requirements for the Degree of
Doctor of Philosophy in Transportation

John A. Reif, Jr. Department of Civil and Environmental Engineering

May 2022

APPROVAL PAGE

OPTIMIZING SPEED PROFILES FOR SUSTAINABLE TRAIN OPERATION WITH WAYSIDE ENERGY STORAGE SYSTEMS

Leon A. Allen

Dr. Steven I-Jy Chien, Dissertation Advisor — Date
Professor of Civil and Environmental Engineering, NJIT

Dr. Lazar Spasovic, Committee Member — Date
Professor of Civil and Environmental Engineering, NJIT

Dr. Janice R. Daniel, Committee Member — Date
Professor of Civil and Environmental Engineering, NJIT

Dr. Joyong Lee, Committee Member — Date
Associate Professor of Civil and Environmental Engineering, NJIT

Dr. Athanassios Bladikas, Committee Member — Date
Associate Professor of Mechanical and Industrial Engineering, NJIT

BIOGRAPHICAL SKETCH

Author: Leon A. Allen

Degree: Doctor of Philosophy

Date: May 2022

Undergraduate and Graduate Education:

- Doctor of Philosophy in Transportation
  New Jersey Institute of Technology, Newark, New Jersey, 2022

- Master of Science in Electrical and Computer Engineering
  New York Institute of Technology, Old Westbury, New York, 2005

- Bachelor of Engineering (Electrical), University of Guyana, Guyana, South America, 1999

Major: Transportation

Presentations and Publications:

(a) Journal publications

Allen, L. and Chien, S., "Optimizing Locations of Energy Storage Devices and Speed Profiles for Sustainable Urban Rail Transit", *Journal of Infrastructure Systems,* Submitted March 10, 2022. (Under review).

Allen, L. and Chien, S., Application of Regenerative Braking with Optimized Speed Profiles for Sustainable Train Operation, *Journal of Advanced Transportation*, vol. 2021, Article 8555372, htttps://10.1155/2021/8555372.

Allen, L. A., and Chien, S. I., Rail Energy Improvement by Combining Coasting and Regenerative Braking, *International Journal of Railway Technology*, 7(4), 1-22, 2018. doi: 10.4203/ijrt.7.4.1.

(b) Conference papers

Allen, L. and Chien, S., "Optimizing the Placement of Energy Storage Devices to Maximize the Net Present Value in Rail Transit Operations", *Proceedings of the Fifth International Conference on Railway Technology: Research, Development and Maintenance*, Montpellier, France, 2022, J. Pombo (Editor), Stirlingshire, UK: Civil Comp Press, Submitted April 15, 2022. (Under review).

Allen, L. and Chien, S., Maximizing Regenerative Braking in Rapid Transit Operations on an Alignment Comprising Short Interstation Spacings, *Proceedings of the 98th Annual Meeting, Transportation Research Board*, Washington, DC, 2019.

Allen, L. and Chien, S., Reducing Rail Energy Consumption through Coasting and Regenerative Braking, *Proceedings of the 96th Annual Meeting, Transportation Research Board*, Washington, DC, 2017.

Allen, L. A. and Chien, S. I., Examination of the Contributions of Coasting and Regenerative Braking to the Efficiency of Electric Rail Vehicles, *Proceedings of the Third International Conference on Railway Technology: Research, Development and Maintenance*, J. Pombo (Editor), Stirlingshire, UK: Civil Comp Press, 2016, paper 290. doi: 10.4203/ccp.110.290.

Allen, L., and Chien S., Optimization of Rail Energy Conservation Through the Adoption of Various Coasting Strategies: A Case Study of Long Island Rail Road's Flatbush Branch, *Proceedings of the Transportation Research Board 93rd Annual Meeting*, Washington, DC, 2014.

(c) Presentations

Allen, L., Optimizing Speed Profiles for Sustainable Train Operation with Wayside Energy Storage Systems, *NJIT Graduate Students' Association Research Day*, Newark, New Jersey, November 2021.

Allen, L., and Chien, S., Optimized Speed Profiles for Sustainable Train Operation with Regenerative Braking, *New Jersey Department of Transportation Research Showcase*, Newark, New Jersey, October 2020.

To all people of color (particularly immigrants) who aspire to reach the pinnacle of success, despite the odds stacked against them.

ACKNOWLEDGEMENTS

First, I would like to thank Almighty God with whom all things are possible, for seeing me through this journey.

I am also thankful to my dissertation advisor Dr. Steven I-Jy Chien for believing in me and for his encouragement, guidance, and support throughout this process.

I would like to express sincere gratitude to the members of my dissertation committee: Dr. Lazar Spasovic, Dr. Janice R. Daniel, Dr. Joyong Lee and Dr. Athanassios Bladikas for their willingness to sit on my committee and their insightful inputs into my research.

I am also grateful for the support from the U.S. Department of Veterans Affairs, the Long Island Rail Road and the New Jersey Institute of Technology for affording me this opportunity.

Thanks also to my fellow graduate students who have helped me along the way, especially Dr. Slobodan Gutesa, Dr. Zijia Zhong and Dr. Celina Semaan.

To my fellow colleagues at the Long Island Rail Road, Dr. Baidyanath Sahay and, Mr. Terrence Joseph P.E., and my former career counselor and motivator Dr. Clayton Q. Bacchus, I'm forever grateful for your assistance, advice and stimulating conversations.

To my family members who gave me unwavering support from the inception to the completion of my Ph. D. My parents, Lea, and Joyce (who are both with their heavenly

father); my sister, Anne; and my children: Jamaal, Jasmine, Daryl and Makeba, thank you for your love and support.

TABLE OF CONTENTS

Table of Contents
(Continued)

Chapter **Page**

Table of Contents
(Continued)

LIST OF TABLES

List of Tables

(Continued)

LIST OF FIGURES

List of Figures
(Continued)

VARIABLE DEFINITIONS

Variable	Definition	Variable	Definition
A	Cross-sectional area of the railcar (ft^2);	P	Principal of capital ($)
A_T	Total interest payment ($)	P_r	Total motor power (hp)
a^t	Applied acceleration at time *t* (ft/s^2);	P^t	Total power at time *t* (kWh);
a_{ap}	Applied acceleration (ft/s)	P_L^t	Transmission Line Losses at time *t*
a_{av}	Available acceleration (ft/s)	q	Repayment period for loan (Years)
a_{max}	Maximum allowed acceleration (ft/s)	R_D	Remaining distance for safe stop
B	Company budget ($)	R^t	Train resistance at *time t* (lbf);
B^t	Braking force at time t (lbf)	R_c^t	Coasting Resistance at time *t* (lbf);
b_{cr}	Minimum braking distance (ft);	R_u^t	Unit train resistance at time *t* (lbf);
b^t	Brake rate (ft/s)	r	Interest rate (%)
C	WESS cost ($)	r_1	Electricity rates at summer peak ($/kWh)
C_I	WESS Installation cost	r_2	Electricity rates at winter peak ($/kWh)
C_E	Annual energy cost without WESS ($)	r_N	Electricity rates at off- peak ($/kWh)
$C_{E'}$	Annual energy cost with WESS ($)	r_u	Unit line resistance (Ohms)
C_M	Annual maintenance cost ($)	r^t	Line resistance at time t Ohms)
E_a	Energy consumed during accel. (kWh);	S	Station spacing (ft);
E_c	Energy consumed during coasting (kWh);	s_{cr}	Minimum station spacing (ft);
E_F	Fitness value (kWh)	s^0	Initial distance (ft)
E_r	Total energy regenerated (kWh);	s^T	Distance at destination (ft)

E_T	Total energy consumed (kWh);	s^t	Travel distance in time *t* (ft);
E'_T	Energy consumed in accel and cruising	T	Max. allowable travel time (s);
e_{ij}	Annual energy consumed without WESS (kWh)	TB	Total Benefit ($)
e'_{ij}	Annual energy consumed with WESS (kWh)	TC	Total Costs ($)
e_L	Incremental line loss (kWh)	t	Incremental travel time (s);
e_r	Incremental energy regenerated	t_a	Duration acceleration regime (s)
e^t	Energy consumed at time *t* (kWh);	t_b	Duration of braking regime (s)
F^t	Tractive effort at time *t* (lbf);	t_c	Duration of cruising regime (s)
F_a^t	Adhesive force at time *t* (lbf);	V	Line voltage (V)
F_c^t	Tractive force for cruising at time *t* (lbf);	V_c	Coasting termination speed (ft/s)
F_m^t	Motor force at time *t* (lbf);	v^0	Initial speed (ft/s)
f_1	Train frequency at summer peak (trains)	v^T	Final speed (ft/s)
f_2	Train frequency at winter peak (trains)	v^t	Speed at time *t* (ft/s);
f_N	Of-peak train frequency (trains)	$v_{m\alpha}$	Maximum allowable speed (ft/s)
G^t	Gradient of alignment section at time *t* (%);	W	Net train weight (tons);
g	Acceleration due to gravity (lbf)	w	Weight of train (lbs)
l	Time steps in inter-station segment (steps)	y	Index of installed WESS
M	Number of rail segments (segments)	ΔT	Length of time step (s)
M_e	Mass for rotating components (lbf);	η	Motor efficiency;
m	Mass of the train (tons)	η_r	Regeneration Coefficient;
NB	Annual net benefit ($)	μ^t	Adhesive coefficient at *t*;
N^t	Normal reaction force (lbf);	θ^t	Alignment inclination at *t* (degree)
n	Total axles per train unit (axles);	ρ	Coefficient of rotating masses

CHAPTER 1

INTRODUCTION

1.1 Background

Large hauling capability and low rolling resistance has put rail transport at the forefront of mass transportation mode sustainability. In the case of electric rail vehicles, they are indispensable in metropolitan areas as a means of moving passengers whether through elevated, surface, or subterranean travel in a clean and pollution-free manner. They have been known to have high energy efficiencies compared to the other modes of transportation and play a leading role in reliability. However, with the advent of the automobile and creation of the Interstate Highway System in the 1950's, a steady decline in passenger rail ridership was initiated (Northeast Maglev, 2018). For decades, the private car was the choice mode of the average commuter in the United States due the convenience provided by its use. Consequently, with the U.S. population doubling since the 1950s (Pew Research Center, 2014), increased vehicle ownership, and marginal capacity increases, highway congestion became more prevalent. This, together with urban gridlock and concerns about the environment in relation to carbon monoxide and greenhouse gas emissions have fueled renewed interest in rail travel. Federal, state and local officials are making a collective effort to discourage private vehicle use and promote mass transit, since rail vehicles have one of the lowest greenhouse gas emissions of any transportation mode as shown in Figure 1.1. This initiative has seen vehicle miles driven declining since 2004 even though the

economy has shown improvement (Grisby, 2013); an indication that the switching of modes was not entirely due to economic circumstances. Also of note is the fact that a 34% growth was recorded in the number of trips taken on transit for the years 2005 to 2011 (APTA, 2012).

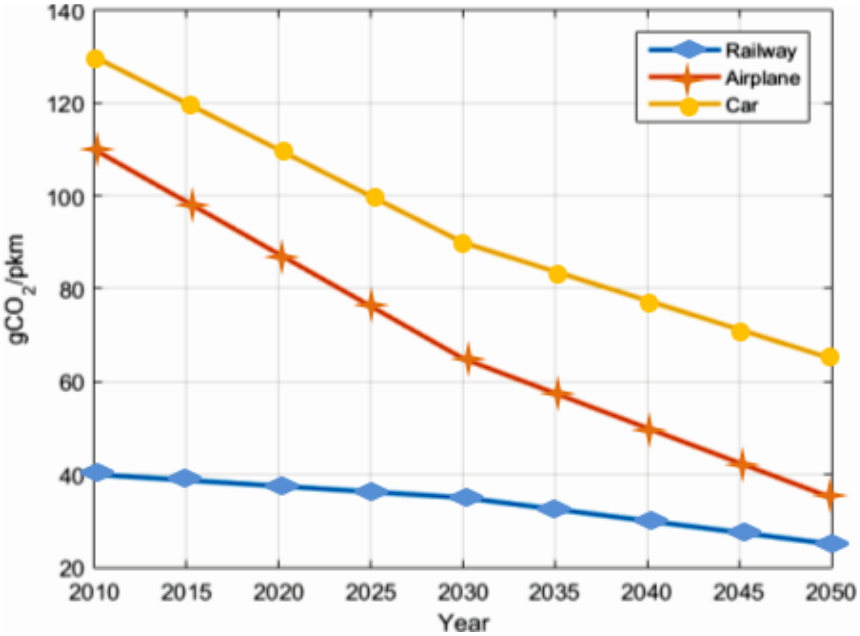

Figure 1.1 Projected CO_2 Emissions for Major Transportation Modes.
Source: Frilli et al. (2017)

Passenger rail is one of the most reliable transportation modes for both interurban and intra-urban travel and their high capacity, safety and fuel economy has set them apart from other modes. Despite this, they consume an exceptionally high amount of energy on acceleration, and therefore the number of stops a train makes has a major influence on energy demand. From a theoretical standpoint, the most energy-efficient trip would be one

devoid of any intermediate stops (International Union of Railways, 2003). Except for streetcars, they do not compete with other surface transportation modes for use of streets or highways. This advantage allows them to travel at higher average speeds without outside interference from regular traffic signals or other transportation modes, allowing the train to experience almost constant fluidity. Despite their superiority in terms of energy efficiency, the leadership in sustainability enjoyed by rail vehicles is projected to be reduced by 50% by the year 2050 due to technological improvements related to the efficiencies of cars and airplanes as shown in Figure 1.1 (Frilli et al., 2017). Thus, railways will have to significantly improve on efficiency in order to confront future challenges. More than 60% of total rail energy consumed is absorbed by traction (Howlett and Pudney, 1995) and presently, rail operators are seeking ways to reduce their energy consumptions in order to reduce overall costs.

1.1.1 Electric Braking

A popular method used to save energy in railroad operations involves the capture and reuse of the braking energy of the trains. Braking in rail vehicles is focused on keeping the kinetic energy of the train under control. Consequently, it is mainly concerned with enabling deceleration, controlling downhill acceleration or to immobilize the train in a standing position. Electric braking consists of two main types – rheostatic and regenerative braking. In both braking types, the traction motor acts as a generator, converting the kinetic energy of the train into electric energy. Figure 1.2 illustrates the principle of rheostatic braking.

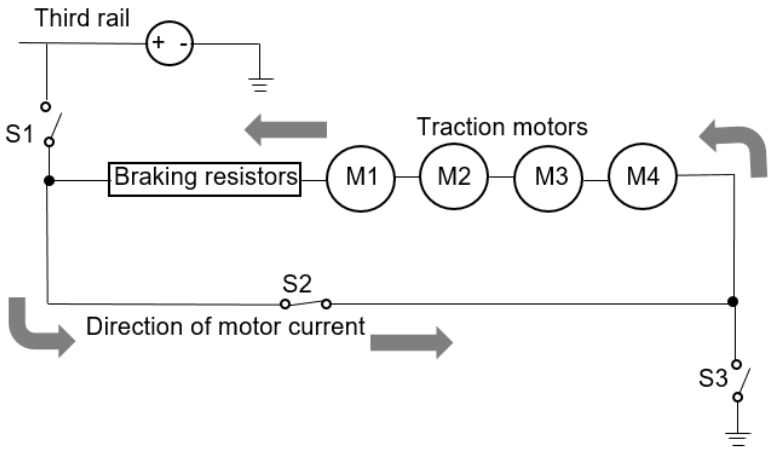

Figure 1.2 Rheostatic braking.

It occurs when energy is regenerated in the absence of a suitable load to absorb it. In that case, a localized area of high voltage would be created, and protective devices would be activated to prevent a fault condition. In Figure 1.2, this is done by the opening of switch S1, and the current, the square of which is proportional to the energy, flows through the braking resistors. The train is therefore electrically disconnected from the third rail and the energy is dissipated in the braking resistors in the form of heat and radiated to the surrounding air. This energy can never be recovered, but if there is a load present, then regenerative braking would be possible. The braking resistors would be isolated from the braking resistor circuit and the traction motors would be directly electrically connected to the third rail (catenary) as shown in Figure 1.3. The motor current flows from the motors directly to the third rail, from where it could then be absorbed by a load in the same electrical section. The load could either be another train accelerating in the same electrical

section as the braking one, or either a wayside energy storage system (WESS) or an on-board energy storage system (OBESS) positioned to absorb the regenerated energy.

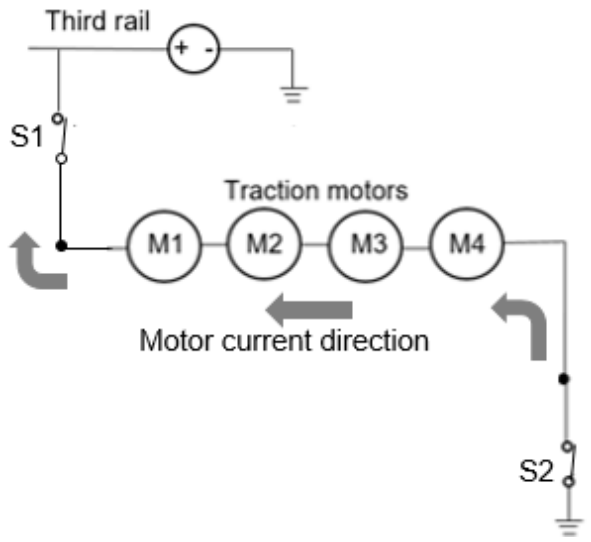

Figure 1.3 Regenerative braking.

1.1.1.1 Train-to-Train Regeneration. When regeneration intended for another train When regeneration intended for another train is to be accomplished, the receiving train must be in the same electrical section. In addition, the acceleration of the receiving train must be synchronized with the braking of the regenerating train. Figure 1.4 shows two trains arriving at Station 1 at different times. Train 1 and Train 2 are not simultaneously braking and accelerating and are therefore not synchronized because Train 1 was immobilized at Station 1 when Train 2 was braking but departed after Train 2 arrived. The braking energy of Train 2 would be absorbed by its braking resistors and no energy transfer would have been possible to power the acceleration of Train 1 out of the station.

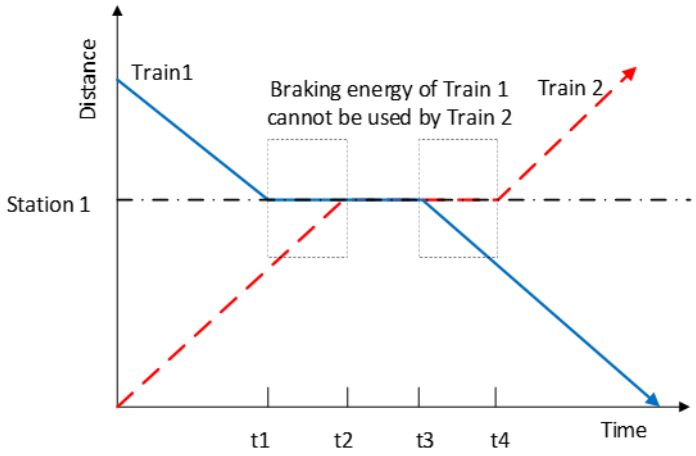

Figure 1.4 Trains 1 and 2 unsynchronized.

When the train movements are synchronized, the departure of one train from the station coincides with the arrival of the other. Figure 1.5 illustrates this, where the arrival time of Train 1 is synchronized with the departure time of Train 2. The energy is transferred from Train 1 to Train 2 via the third rail and is used for acceleration out of the station and potentially to power on-board auxiliary loads.

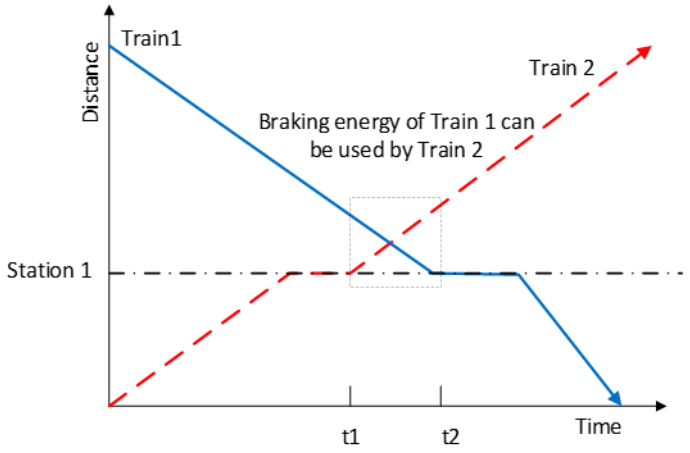

Figure 1.5 Synchronization between Trains 1 and 2.

1.1.1.2 Regeneration to Energy Storage Devices. One of the challenges faced by regenerative braking as a means of saving energy is receptivity. Another nearby, train has to accelerate and absorb the energy being regenerated by a braking train. If this is not the case, the energy is dissipated in the braking resistors as heat and can never be recovered. The solution to the dilemma of receptivity is energy storage, so that the energy is available whenever a demand arises. The energy storage devices could be chemical (batteries) , mechanical (flywheels) or electrostatic (ultra-capacitors) which have various advantages over each other. Table 1.1 shows recent energy storage applications by transit agencies across the US.

Table 1.1 Recent Energy Storage Applications

Transit Agency	**Rail Type**	**Storage Technology**	**Application**
Sacramento Regional Transit District	Light Rail	Battery	Voltage Support
Sacramento Regional Transit District	Light Rail	Ultracapacitors	Regenerative Braking
MTA- New York City Transit	Heavy Rail	Flywheel	Voltage Support
MTA- New York City Transit	Heavy Rail	Battery	Regenerative Braking
Los Angeles MTA	Heavy Rail	Flywheel	Regenerative Braking , Substation Replacement
Washington Metro Area Transit	Heavy Rail	Battery	Regenerative Braking
Southeastern PA Transportation Authority	Heavy Rail	Battery	Regenerative Braking

Source: Lamontagne (2013)

Passenger rail systems are important infrastructural additions for the movement of passengers in urban and suburban settings, and WESS units are significant infrastructural inclusions for energy recovery. What is needed is a model to optimize the speed profiles of the train while considering the specifications of the train and alignment parameters in order to reduce energy consumption and greenhouse gas emissions. Previous studies suggested regenerative braking as a strategy for reducing energy consumption; the cost of which could exceed expectation forcing the operator to increase fares or reduce service. This study proposes a method to optimize the number and location of WESS units which maximize the benefit achieved with the inclusion of optimal speed profiles

1.2 Problem Statement

Urban growth and congestion on highways are resulting in increased passenger demands for rail travel. In densely populated areas such as the New York metropolitan area and Chicago, ridership has increased steadily over the years, especially when gas prices rise (Nowak and Savage, 2013), as also shown in Figure 1.6. To keep up with demand, rail operators need to increase capacity by increasing train length and/or service frequency. These improvements consume more fuel/energy and trigger environmental concerns. It was observed that 25% of all passenger rail systems was powered by fossil fuels in 2020 (International Energy Agency, 2021), therefore reducing consumption also reduces harmful environmental emissions.

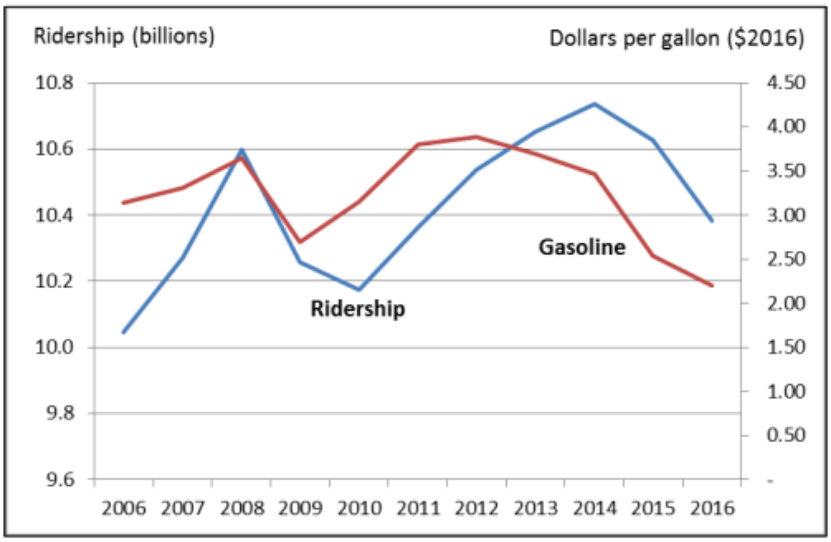

Figure 1.6 Transit ridership compared with gasoline prices.
Source: American Public Transportation Association, Transit Ridership Report, U.S. Energy Information Administration, Monthly Energy Review (June 2017), Table 9.4.

Rail travel is one of the least energy-intensive modes of transportation and demand is constantly increasing due to the many advantages afforded to the travelling public. For instance, in some cities, free transfers from trains to buses, the avoidance of traffic congestion and reliability are some of the reasons that passengers may opt for public transit. In spite of this, frequent starts/stops, rheostatic braking and inadequate power management all contribute to sub-optimal power consumption and increased operating expenses. The problem is further compounded by steadily diminishing budgets over the years and the volatility in the price of petroleum fuels as indicated in Figure 1.7. This volatility is more prevalent in times of international conflict, for example, the Organization of Petroleum Exporting Countries' oil embargo in 1973, the Iranian Revolution in 1979 and Operation

Desert Storm in 1990. These events triggered sudden increases in the price of oil and saw transit ridership experiencing significant increases.

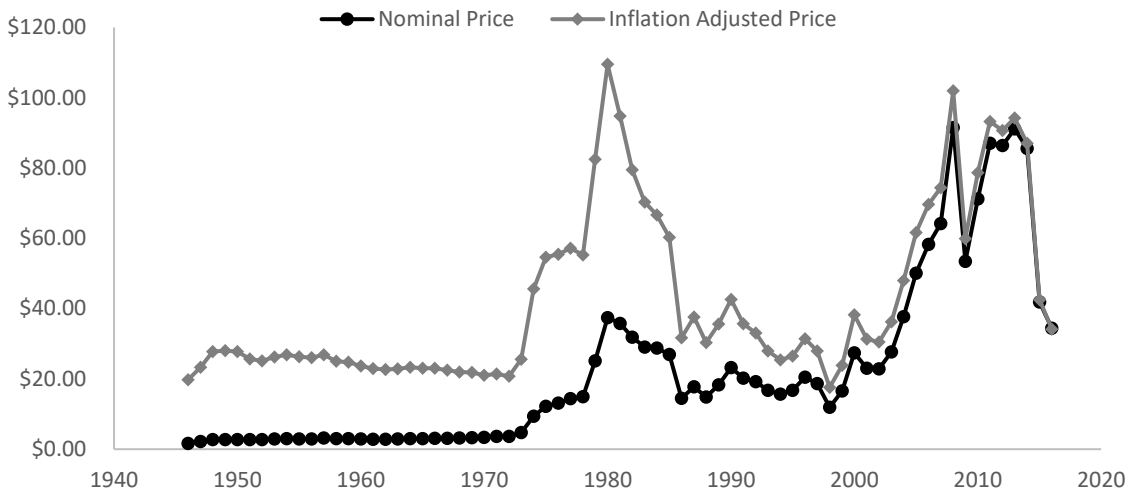

Figure 1.7 Historic crude oil prices.
Source: US Energy Information Administration (2010)

Added to the economic reasons for reducing oil consumption, the planet also benefits environmentally. Air pollution and global warming are directly attributable to the combustion of fossil fuels in air, resulting in the release of greenhouse agents such as carbon dioxide (CO_2) and environmental pollutants such as nitrogen oxides (NO_x). According to the United States Energy Information Administration (2020), in 2018, 75% of the human sources of CO_2 emissions resulted from the combustion of fossil fuels. This is especially so in the electricity generation sector where 0.85 lb. of CO_2 is emitted for each kWh of electricity generated. A comparison of the quantity of electricity generated and the resulting CO_2 emitted by fossil fuel type is shown in Table 1.2.

Table 1.2 Electricity Generated and CO_2 Emitted by Fuel Type for the year 2000

Fuel Type	**Energy Generated (million kWh)**	**CO_2 Emitted (tons)**	**Pounds CO_2/kWh**
Coal	757,763	845	2.23
Natural Gas	1,402,438	635	0.91
Petroleum	13,665	15	2.13

Source: U.S. Energy Information Administration (2021)

These findings indicate that although electric trains do not emit pollutants at the point of consumption, their contribution to atmospheric pollution is significant. Statistics show that about 67% of the electricity generated in the U.S. is derived from fossil fuel consumption (Thomas, 2015), which invariably contributes to worldwide deaths as a result of respiratory illnesses (Table 1.3). The remaining 33% of U.S. electricity generation comes from nuclear energy which provides 21%, and renewable energy sources which supply 12% (U.S. Energy Information Administration, 2020). Given the slow pace of development of renewables, it is unlikely that they would replace fossil fuels in the near or medium term. As such, it is imperative that the use of fossil fuel-based energy be tempered as much as possible to counteract the threat of global warming. This can begin with the transportation sector, since fossil fuels accounted for 95% of all the energy used for transportation in the U.S. with highway vehicles consuming approximately 8.5 million barrels of fuel per day (Texas Transportation Institute (TTI), 2011). Since private automobiles are the largest contributor to pollution emanating from the transportation sector, giving priority to the reduction in the use of this mode can help with this problem.

In return, city agencies may have to make transit attractive to private car commuters by offering incentives to entice them to use public transportation instead of their cars.

Table 1.3 Projected Annual Deaths due to Urban Air Pollution 2001- 2020

REGION	PROJECTED DEATHS
Established Market Economies	20,000
Former Socialist Economies	200,000
China	590,000
India	460,000
East Asia and the Pacific	150,000
Latin America and the Caribbean	130,000
South Asia	120,000
Middle East Crescent	90,000
Sub-Saharan Africa	60,000
World Total	1,820,000

Source: Worldwatch Institute
http://www.worldwatch.org/global-fossil-fuel-consumption-surges. Retrieved March 20, 2014

Consequently, improving the level of service of public transportation to create a more attractive and robust system could trigger a modal shift from private car to mass transit. This would play an especially important role in the reduction of highway congestion and the reduction of carbon emissions into the atmosphere.

1.3 Objectives and Work Scope

The objective of this research is to provide a novel method for the optimization of energy consumed by electric rail vehicles. It would consider the energy that could potentially be saved through coasting, and that that could be harvested through regenerative braking. In consideration of regenerative braking energy storage on the wayside (beside the track), it

will determine the number and locations of the energy storage devices required to minimize the cost to the operator. First, kinematic equations will be applied to simulate the energy consumption. Then, a genetic algorithm (GA) will be developed to optimize the speed profiles which minimize the energy consumption with and without a wayside energy storage (WESS) unit for a rail transit line. Finally, a model will be developed to optimize the locations of the WESS units that maximize the net benefit.

The methods actually entail the development of two models; the first to optimize the speed profiles of an electric train using coasting and regenerative braking, and the second to optimize the locations of the energy storage devices for maximum economic benefit. These models are developed while considering the alignment geometry, expected travel time and maximum operating speed. They would minimize the energy consumed by the train, mitigate the environmental effects caused by carbon dioxide (CO_2) emissions and reduce costs to the operator. In the first model, a simulator will be developed to mimic the movement of the train along the alignment through all the motion regimes (e.g. acceleration, cruising, coasting and braking). It will consider physical alignment constraints such as gradient and coefficient of friction, the train specifications, and operational constraints such as travel time and speed limit. It will examine four distinct scenarios as a basis for determining the optimal speed profiles which minimize the energy consumption of the train.

Scenario I: The baseline case where the train minimizes its travel time, and no energy optimization strategy is applied will be developed and used as a benchmark for the other three cases. This scenario simulates the event where the train is behind schedule, and it is required to minimize the travel time to reduce the delay.

Scenario II: Coasting only is applied. This scenario depicts the case where the train is running ahead of schedule, but the regenerative braking system is either inactive or unreceptive. It therefore applies the maximum possible amount of coasting.

Scenario III: Regenerative braking only is applied. This scenario is a depiction of a case where the train is late but can capture and store its braking energy using the WESS.

Scenario IV: Both coasting and regenerative braking are combined and optimally applied. Here, the train is ahead of schedule and has the regenerative braking system active, so that the algorithm can select optimal amounts of coasting and regenerative braking to optimize the energy consumption.

Since the model consists of multiple variables which are continuously varying, analytical methods are not sufficient to solve the problem and therefore Genetic Algorithms (GA) will be used to search for a solution. The expectation is that by synergizing coasting and regenerative braking, the fuel economy and sustainability of railroad operations will be greatly improved. The proposed model will allow the train to operate using minimum energy if the train is early or on time, or minimum travel time if the train is running behind schedule. The operation would therefore be able to recover from delays and service disruptions.

In the second model, a simulation will be conducted on a multi-segment alignment section, using the methods that optimized speed profile in the first model. Then, those results will be used to determine the total benefits while considering the electricity rates during the respective travel periods. Finally, a linear programming algorithm will be developed to determine the number of WESS units and their positions along the alignment that maximize the net benefits. The methods could be used to reduce costs and to plan infrastructural upgrades for sustainable operation and are applicable to any railroad operating an electrical fleet.

Another area to be considered in this study is the energy lost in the transmission lines which are used to deliver the electric power to the train. This is referred to as “line loss” and occur as a result of some energy being dissipated in the internal resistances of the transmission lines. Line losses occur when there is a transfer of electrical energy to the train from the substation or WESS, or from the train to the WESS. Therefore, the acceleration, cruising and (regenerative) braking regimes will incur line losses since these are the only regimes where there is a transfer of energy along the lines. The quantities of energy involved will be determined and included in the calculations so that an accurate value of the energy flow could be obtained.

1.4 Expected Results

The aim of this research is to determine if placing the energy storage units in strategic locations along the alignment could enhance the energy-saving performance of an electric

train. This was examined by using the optimal speed profile with and without WESS as inputs to a linear programming algorithm that was specially designed for this problem. Since the present research used inputs to the LP algorithm that were already optimal, this could only serve to improve on the accuracy of the current model. Besides, the WESS units need to be placed at locations where there will be most receptive. As such, locating them in positions to maximize net benefit would ensure a maximization of receptivity. The expectation is that the methods utilized in this study would maximize energy savings, thereby maximizing the net benefit to the operator. In so doing, environmental emissions would be mitigated, making the operation more environmentally and economically sustainable.

1.5 Dissertation Organization

This dissertation is organized into six chapters. Chapter 1 presents background information on rail energy consumption and the adverse effects associated with it. It also discusses the work scope and objectives of the research. Chapter 2 examines previous studies in the areas of rail energy usage, current energy-saving methods including programmed driving and energy recovery and storage applications. It then discusses the advantages and disadvantages associated with the current energy-saving technologies. Chapter 3 presents the development of the model for the purpose of energy optimization. It examines the motion regimes which the train experiences and the four operating scenarios examined in this research. Chapter 4 discusses the methodology associated with the models and results

that are expected from a theoretical point of view by operating the train in the manner outlined in the objectives and work scope. Chapter 5 presents a numerical example to apply the theories developed in the current research to a practical situation. It includes an analysis to determine the practicality of the proposed methods. Chapter 6 describes possible extensions of the current research and concludes the dissertation.

CHAPTER 2

LITERATURE REVIEW

2.1 Organization of the Review

This review examines previous studies conducted on the topic of rail energy conservation using coasting and regenerative braking and also studies centered on the optimization of the locations of WESS units for maximum energy capture. It provides some background information for the development of the methodology presented in the dissertation. The review consists of five sections: Section 2.2 discusses rail transportation energy usage in the North America, Europe and Asia which are essentially the three largest usage zones in the world, and the need to conserve energy. Section 2.3 focuses on energy-saving technologies currently in use including simulation and the optimization methods for programmed driving and energy recovery and storage. Section 2.4 discusses the advantages and disadvantages of the current energy-saving technologies while Section 2.5 summarizes and concludes the review.

2.2 Passenger Rail Energy Usage

Energy is one of the largest expenditures for the world transportation sector. For North American railroads it is second only to labor (Simpson, 2020). Therefore, a great deal of research has been conducted over the years on energy optimization in railroad operations, and on a wider scope in transportation operations, due to the numerous opportunities that

exist for increasing sustainability. The benefits derived from these initiatives serve to reduce operational costs as well as to reduce the emissions of greenhouse gases into the atmosphere.

Passenger rail plays a leading role in transportation sustainability and is the backbone of urban mobility. Rail vehicles have been known to have very high fuel efficiencies among various modes of transportation in terms of per passenger fuel consumption. This is illustrated in Table 2.1, which depicts the superiority of the efficiency of passenger rail over various other transportation modes. This is in part due to their low rolling resistance and large hauling capacities; the rolling resistance at the steel-to-steel wheel/rail boundary being about one sixth that of the asphalt/tire boundary for trucks (Barkan, 2007).

Table 2.1 Energy Efficiency of Urban Transportation Modes

Transportation Mode	**Occupancy (pass/veh)**	**Energy Efficiency (pass-mi/kWh)**
Automobile	1.2 - 2.8	1.2 - 4.6
Carpool	2.0 – 6.0	2.1 – 9.8
Bus Rapid Transit	10 - 70	3.5 - 42
Commuter Rail	15 - 200	2.9 - 125
Rail Rapid Transit	25 - 200	4.9 - 57

Source: Vuchic (2007)

Electric trains have the additional advantage of not emitting pollutants locally, which makes them ideal for subterranean operations. This is especially so for transportation

operations in heavily populated urban centers where at-grade rail operation is limited to trams and light rail vehicles. Despite their excellent fuel economy, the scale of operations of passenger rail dictates large fuel budgets. In 2018, the passenger rail ridership in the European Union reached 8 billion rail travelers on trains that consumed 0.268 quadrillion BTU of energy (Eurostat, 2020). In North America (US and Canada), there were 4.8 billion unlinked passenger rail trips in 2019 (APTA, 2020). The energy budget for the New York Metropolitan Transportation Authority, which is the largest transportation agency in the US, was $641 million in 2019 (MTA, 2019) whereas, Amtrak budgeted $260 million for fuel in 2019 (Amtrak, 2019). In Asia which has the largest passenger rail networks, the fuel budgets are even larger. The East Japan Railway (JR East) for example, has a ridership of 17 million passengers per day (JR East, 2020); while China and India being the two most populous countries in the world, have extensive and expanding rail networks (World Bank, 2015). The foregoing serves as a stark reminder of the need to reduce operating costs and to increase the attractiveness of rail travel to increase ridership and dissuade the use of personal vehicles.

2.3 Current Energy Saving Methods

There are several well-known methods by which rail propulsion energy can be reduced in order to reduce operating costs and mitigate environmental degradation. These methods are necessary to maintain the sustainability of rail operations which encountered immense competition from the automobile after the completion of the Interstate Highway System

(Transit Cooperative Research Program, 1997). Some energy saving methods currently practiced are outlined below.

2.3.1 Programmed Driving Methods

It is a well-known fact which is verified by extensive research over the years, that substantial energy savings could be realized by programmed driving of trains. This operation allows the train to be operated in accordance with a preset speed profile which is developed from the train specifications, the rail alignment parameters and allowable speed limits. There are several successful examples of programmed driving tools currently in use. The Locomotive Engineer Assist Display and Event Recorder (LEADER) for example, is an on-board GPS-based computer system that was developed by New York Air Brake Company for Norfolk Southern Railroad. It prompts the driver on the optimal throttling, speed and brake settings for maximum fuel efficiency and conserves energy by maintaining momentum and eliminating unnecessary braking. It also allows for the safe and efficient running of long, heavy trains to maximize asset utilization. Trains equipped with the LEADER system consume 5% less fuel on average and saves Norfolk Southern about 10 million gallons of diesel fuel per year (Norfolk Southern Sustainability Report, 2011).

GE's Trip Optimizer is very similar to the LEADER system but is capable of automated operation. It learns the characteristics of the train, for example, its weight, number of cars, origin and destination and creates an optimal trip profile. It then automatically controls the throttle and dynamic brakes to reduce fuel consumption and

ensure safe train handling. It boasts an average of 3~17% fuel savings and 10% emissions reduction (Vantuono, 2010).

Computer Aided Train Operation (CATO) calculates the most energy-efficient speed profile from the supplied data for the on-time arrival of the train at its destination. It is based on data communication between the train and the Traffic Control Center (TCC), together with a centralized system for the calculation of optimal train movements. It reportedly can reduce fuel consumption by 10~25% (United Nations Framework Convention on Climate Change, 2020).

The above-mentioned methods, while improving efficiency, involve the purchasing of expensive proprietary software packages, the contents of which are never disclosed to the purchaser. A less expensive yet effective method involves the introduction of coasting strategies into the operating regimes of the trains. The vehicles are accelerated to the maximum allowable speed, and if the station-to-station distance allows it, traction is switched off and the vehicle is allowed to run on the momentum already built up. Although the travel time increases, the fuel savings obtained are tremendous. When the coasting regime is included fuel savings are generally due to the low rolling resistance of steel wheels on steel rails. Actually, a steel wheel on rail has about a 6 to 10 times less coefficient of friction than a rubber tire on pavement by comparison, allowing a train to run much further with its engine switched off than is possible with a truck or other highway mode of transportation (Barkan 2007).

Being cognizant of the benefits of coasting, Milroy (1980) developed a study to obtain the optimal operating trajectory of a train for minimum energy usage while conforming to schedule. He determined the switching points between the operating regimes using iterative methods. Acceleration and braking were done at maximum permitted rates, and the trajectories for those regimes were determined. Since the cruising regime was initiated immediately after attaining maximum speed, the problem came down to determining the end point of the cruising regime (start point of coasting), and the end point of coasting (start point of braking). He developed an iterative algorithm to determine the minimum energy consumption when the train is running according to schedule or the minimum travel time if it is late.

Uher and Disk (1987) developed a computer-based simulation to determine the switching points of the operating regimes to minimize energy consumption. Their train operations model (TOM) model consisted of two simulators: a train performance simulator (TPS) and a train movement simulator (TMS). The TPS took as inputs, the physical characteristics of the alignment as well as the train specifications, and output the speed profile, position, and power consumption of the train. On the other hand, the TMS required the alignment condition including layout of the network, block and switch positions and speed profile information from the TPS. It was tasked with obeying all signals and commands on the track. Their methodology assumed that the movement consisted of three motion regimes, namely acceleration, cruising, and braking. They simulated the acceleration and cruising in the forward direction, and the braking regime in the reverse

direction. The intersection of the forward and reverse simulations trajectories was determined to be the optimal switching points in the speed profiles.

Liu and Golovitcher (2003) determined that energy-efficient speed profiles can be obtained through the calculation of the switching points of the coasting and braking phases of a train. Taking into consideration the limits to traction, braking and velocity, and the effects of extreme topographical elements on the motion of the train, they developed a program for finding the sequence of controls for optimal operation and schedules using the optimal control theory.

Jong and Chang (2005) proposed a mathematical model and numerical integration to calculate the speed profile of the train using two algorithms. The first used the speed of the train to determine voltage and current and calculate the power drawn by the train. The second model estimated the electric power drawn by considering the train velocity, the tractive effort and energy efficiency curves. Their methods yielded results similar to those obtained with commercially available software.

Most of the above methods did not take into consideration what action should be taken if the total travel time was varied such as that which obtains when the trains are in varying states of tardiness. This is of extreme importance since railroad operations normally place a great amount of importance in on-time performance, which is a primary performance measure of reliability. This problem was addressed by Kim and Chien (2011) who designed a Train Performance Simulator (TPS) which used a metaheuristic to arrive at an optimal speed profile. The optimization was performed while adhering to speed limits

and train schedule and took track alignment into consideration. Their aim was to achieve minimum energy consumption if the train was early or on schedule but endure minimum travel time if the train was late. They considered four motion regimes and designed a method which altered the duration of the acceleration and cruising regimes in order to achieve minimum energy consumption.

Allen and Chien (2014) developed a Hybrid Multi-Station (HMS) model in which they optimized the energy consumption subject to the train schedule using a deterministic simulator. They applied the simulator to an alignment section consisting of three alignment segments with different physical characteristics. The train speed at the end of the coasting regime was adjusted to suit the schedule of the train. Terminating the coasting regime at higher speeds lead to reduced travel time and the opposite was true when coasting was terminated at low speeds. Since coasting is the only motion regime that can be altered or completely eliminated to save time or recover from delays, this was given great consideration in their analysis. They proposed the inclusion of additional coasting when the train was early and less coasting if the train was running late to minimize travel time. Their strategy achieved energy savings of over 20%.

Haramina et al (2012) developed a model in which they obtained the minimum running time between two stations on a commuter rail line. They added supplemental times to the timetable and developed three running regimes. The first regime accelerated the train to maximum speed and maintained that speed until the brakes had to be applied in order to stop at the next station. The other regimes incorporated varying levels of coasting into the

run depending on the time available for the run so as to save energy while maintaining the train schedule. They then ran a simulator which chose a regime depending on the time available for the run and calculated the energy used during the run. The results of the simulation showed that the method for energy-optimal running profile calculation for commuter trains could save up to 10 % of energy consumed for traction purposes.

Parajuli (2005) did a comparative study modeling road and rail freight energy consumption and proposed changes to improve rail efficiency by adding slack time to schedules and including varying levels of coasting into the driving strategies. Three classes of trains were also modeled; a high-speed train, a commuter rail and heavy freight train. It was seen that the heavier trains realized greater energy saving by adopting a coasting strategy than lighter trains. This could be attributed to the larger momentum and thus, kinetic energy built up in a heavier vehicle travelling at a given speed than in a lighter one. Fuel efficiency was measured as being the number of units of freight moved per unit of fuel consumed as against the usual measure of the quantity of fuel consumed per passenger mile when dealing with passenger trains. The study found that energy efficiency varied considerably with alignment and train parameters including grade, train length, speed, mass, curvature of alignment and number of axles on the trains.

An innovative study conducted by Desprez and Djellab (2012) developed an algorithm to determine the optimal path for a single train on a track with regards to energy consumption and timetable constraints. In their model, they set out an optimal driving strategy with different target speeds to be followed by the driver on a given journey with

known alignment characteristics. They incorporated the four operating regimes, i.e. accelerating, cruising, coasting and braking. However, since accelerating and braking were done at the maximum allowable rates, more focus was placed on the cruising and coasting regimes, which are instrumental in energy saving. For both regimes for a given target speed which was less than the maximum speed, they determined coefficients “Eco” and “Ecr”. Eco is the energy saved if the train remained in “coast” for one additional time unit, while Ecr is the energy saved if the train remained in “cruise” mode for one additional time unit. They posited that the optimal operation was obtained if Eco = Ecr. Through their efforts, they achieved as much as a 59% reduction in energy consumption. They however did not consider signaling restrictions, so that the driver only had to obey speed limits and station stop locations.

These strategies place a lot of emphasis on coasting which causes the speed of the train to diminish due to the train resistance elements acting in opposition to its motion. As a result, travel time is extended, and most operators pad their schedules to allow extra time so that their on-time performance is not negatively impacted. Therefore, if there is no delay, the driver of the train can then use the extra time to adopt a more energy-efficient driving strategy. Although these studies do not require any large additional capital investment and therefore can be immediately implemented, no provision was made for energy storage or harvesting the braking energy of the train for further energy savings.

Some other studies reviewed in the literature involved the use of searching algorithms to find the optimal profile. Bigharaz et al. (2014) designed a dynamic model to

calculate the speed profiles of a train using a Non dominated Sorting Genetic Algorithm (NGSA-II) and a Multi Objective Particle Swarm algorithm. Their analysis stemmed from employing kinematics related to Newton's second law of motion while considering four motion regimes, namely acceleration, cruising, coasting, and braking. In their methodology, their proposed multi-objective method was used for the simultaneous optimization of the energy consumption as well as the travel time. A virtual braking process was also included once the speed profile entered the braking area to determine the exact braking point for minimal energy consumption.

Su et al. (2014) reduced energy consumption in high-speed rail at a specified running time using parallel multi-population Genetic Algorithms (PMPGA), which was performed alongside a standard GA. This process involves the simulation of gene isolation and gene migration in the biological evolution process. The population is divided into many sub-populations which have different gene patterns and independent genetic processes. They performed three PMPGA methods where, in each method, they either altered the number of sub-populations or gene lengths. Their method was deemed to converge more rapidly and accurately than the standard GA and avoided the premature convergence of the single-population evolutionary algorithms.

Amrani et al. (2018) used genetic algorithms (GA) to calculate a series of energy-efficient speed profiles for each interstation segment while considering operational constraints. The generation of these speed profiles was based on data obtained from on-board sensors which included speed, acceleration, electric current and voltage, passenger

weight and GPS positions. They then "cleaned" the data which involved the removal of invalid points or locations and compensated for missing information. They used a random forest model to completely automate the optimization, resulting in a 14% energy reduction.

Encountered in the literature were studies involving timetable optimization to address changes in passenger demands. Wong and Ho (2004) used hierarchical genetic algorithms (HGA) to identify several flexible coasting points according to traffic conditions and to minimize energy and regulate the train schedule. This method involved the inclusion of coast control to serve as a balance between energy consumption and run time. They pursued this method after finding that a flexible train control cannot be attained in GA with a fixed number of coasting points, even though they may deliver good performance under different conditions. They also included the Minimum Allele Reserve Keeper (MARK) as a genetic operator with the expectation that fitter solutions would be obtained.

Another study conducted by Li and Lo (2014), proposed a dynamic train scheduling framework to minimize energy while adjusting speed profiles to address changes in passenger demands. They forecast passenger demands, then determined the headway and cycle time for the next cycle and adjusted the reference timetable and speed profile accordingly. For instance, when passenger demand increased, they reduced the headway and/ or cycle time to accommodate that increase. Conversely, for low passenger demands, they increased cycle time/ and or headway to save energy. By implementing their dynamic

timetable methods, energy savings of almost 8% were achieved over the static timetable approach.

Feng et al. (2017) developed a simulation-based method to devise an off-peak energy-efficient control system. Their methods optimized timetable and control strategy while assigning a dwell time margin to run time due to uncertain passenger demands in off-peak periods. They found that with a small increase in run time obtained from reducing the dwell time, a significant amount of energy saving resulted, and cycle time remained the same. Their methods reduced energy consumption by 22%.

Some studies based their research on the modification of the timetable to synchronize the movements of two or more trains for greater regenerative braking receptivity. The capture and reuse of regenerative braking in trains can result in significant energy savings providing significant potential for sustainability improvement. It involves the braking energy from one train being used to power a simultaneously accelerating train. To effectively achieve this coordination, some researchers modify the dwell time of the trains in their studies. Tang et al. (2015) proposed a methodology where communication-based train control was used to synchronize the movements of two opposing trains in the same DC power section. Their primary objective was to maintain schedule while simultaneously optimizing the energy efficiency, thereby maximizing the reuse of regenerative braking energy from the braking train. To maximize the energy efficiency, an enhanced GA was used to optimize the speed profiles of the trains. This algorithm differed from the traditional GA in that it contained a combinatorial selection method, adaptive

probability, and a dual search loop. They achieved a 12% reduction in substation energy consumption by synchronizing the train speeds to improve regenerative receptivity. They found that even without regenerative receptivity, energy consumption could be reduced by 22% by delaying one of the trains for 20 to 100 seconds. In rapid transit, this travel time increase may not be tolerated, but in commuter rail where headways and dwell time are much greater, this may not be an issue.

These shortcomings were addressed by Jung et al (2013), where efficiency was improved by integrating the power outputs of different railway systems. They therefore reduced peak power consumption through the utilization of regenerative energy to supply power to an accelerating train and eliminated the need to extend the dwell time of a departing train to synchronize with a braking train. Their method, however, was constructed under the assumption that there would be minimal delays which is sometimes not the case, especially at peak periods.

Lin et al. (2016) proposed a multi-train model for energy savings by altering the dwell time of the trains at a station so that its acceleration coincides with a braking train. Using GA for the optimization, they considered minimized energy consumption as the objective function. Their methods achieved an 8% increase in regenerative braking rate along with an 8% reduction in energy consumption. This achievement was obtained with 29 second increase in running time. Another study conducted by Zhou and Xu (2012), proposed a multi-train, multi-objective dispatch method with safety and flexible time constraints to save energy and increase traffic volume in complicated lines. They included

multi-train coordination in their study as a means of saving energy and as a means of ensuring the safety constraints were not violated. The objective function of the study was based on minimizing the energy consumption rate and maximizing the traffic volume. Their results achieved over 70% increase in the utilization factor after optimization, and a further 10% increase after applying the train dispatch method.

Gong et al. (2014) used GA for timetable optimization by modifying the dwell time at each stop to enable train-to-train regenerative braking energy transfer. For instances where the train encountered disturbances that affected the optimized status, they applied a compensatory driving strategy algorithm (CDSA) to return the system to an energy saving state. With this strategy, if the time delay on the previous segment could not be made up on the present segment, then the train is driven at the maximum allowable speed to the next segment and the delay is made up on one or more subsequent segments. There is more priority based on punctuality, thus, when there is a delay, the emphasis is to get back on schedule, and energy saving takes a secondary role. After the train resumes on-time status, the energy-saving operation continues.

Su et al. (2020) promoted the increased use of regenerative braking by combining driving strategy and timetable optimization to reduce energy drawn from the substation. They designed a dynamic programming (DP) algorithm in conjunction with a simulation annealing (SA) algorithm to solve the problem. First, the DP was used to handle the eco-driving problem, which enhances the driving strategy and energy consumption. Then, SA was used to calculate the trip times and headway that minimize the energy drawn from the

utility. They found that their methods increased the regenerative braking energy use by over 160% for peak operation and almost 170% for off-peak operation. Luan et al. (2018) considered an integrated optimization method to reduce delay, while simultaneously targeting energy efficiency through management of train speed. They adopted a structural query language (SQL) approach for speed profile optimization and applied regenerative braking for additional energy savings. This resulted in 13.1 to 22% reduction in energy consumption.

Pena-Alcaraz et al (2011) designed timetables for subway travel which synchronized the arrival and departure of trains to optimize energy consumption by maximizing the use of regenerative energy. They developed a mathematical model which scheduled trains in such a way that a train braking to enter a station was synchronized with a train accelerating to leave the same station or one nearby which is connected to the same electrical grid. The schedules developed were tested on an existing underground system and the results were observed to be strongly correlated to the model. This method was advantageous in that, since the schedules were time-tabled, there were no adverse effects on the quality of service offered to passengers, and the implementation cost was minimal.

The disadvantages of the above studies included the need to synchronize the trains exactly for maximum savings through the use of regenerative energy, which may cause delays at rush hour and may be difficult to implement during off-peak hours. Such perfect synchronization of acceleration of one vehicle to the deceleration of another and exact coordination of movements is difficult to achieve depending on the time of day or

prevailing weather conditions. This is especially so for trains with ongoing connections. Failure to properly synchronize the trains results in a net loss of regenerative energy. On the other hand, the direct transmission of regenerated energy to an accelerating train, though much more economical in terms of cost of equipment, may not be achieved efficiently unless the receptivity of the system is high (Acikbas and Soylemez, 2007). In this instance, receptivity refers to the ability to efficiently harness the regenerated energy and may be improved by storing the energy in a wayside energy storage system (WESS) for subsequent reuse.

Those disadvantages were mitigated in a study done by Miyatake and Ko (2010). They developed speed profiles to save energy using optimal control techniques. Their method utilized Dynamic Programming (DP), the gradient method, and state of charge (SOC) of the energy storage devices. Using computer programs to administer the control techniques allows the equipment to more effectively mimic the developed model, and thus energy efficiency is maximized. The study involved the use of regenerative energy where the energy is stored and utilized in the next step to provide acceleration. This method eliminates the likelihood of failed regeneration which may occur in the absence of energy storage devices. However, the study lacked focus on timetable schedules and on alignment geometry.

The aspects of geometry of track alignments are of great importance for energy economy in terms of speed profile optimization. An extreme negative gradient could cause a train to accelerate downhill and save energy. Alignment geometry could also cause the

train to decelerate or even stop on positive gradients. Figure 2.1 shows a family of curves of resistance plotted against speed for various values of alignment gradient. The plots show that resistance increases with speed for positive, zero and negative gradients. For the speed of the vehicles to increase on a positive slope, there must be a tractive force propelling it on the uphill movement. For vehicles on a negative slope, the gravitational force may cause them to accelerate. As stated in Vuchic (2007), the point E on Figure 2.1 where the -6% curve intercepts the x-axis is the value of the speed to which the train would accelerate and maintain constant motion on a 6% downhill slope.

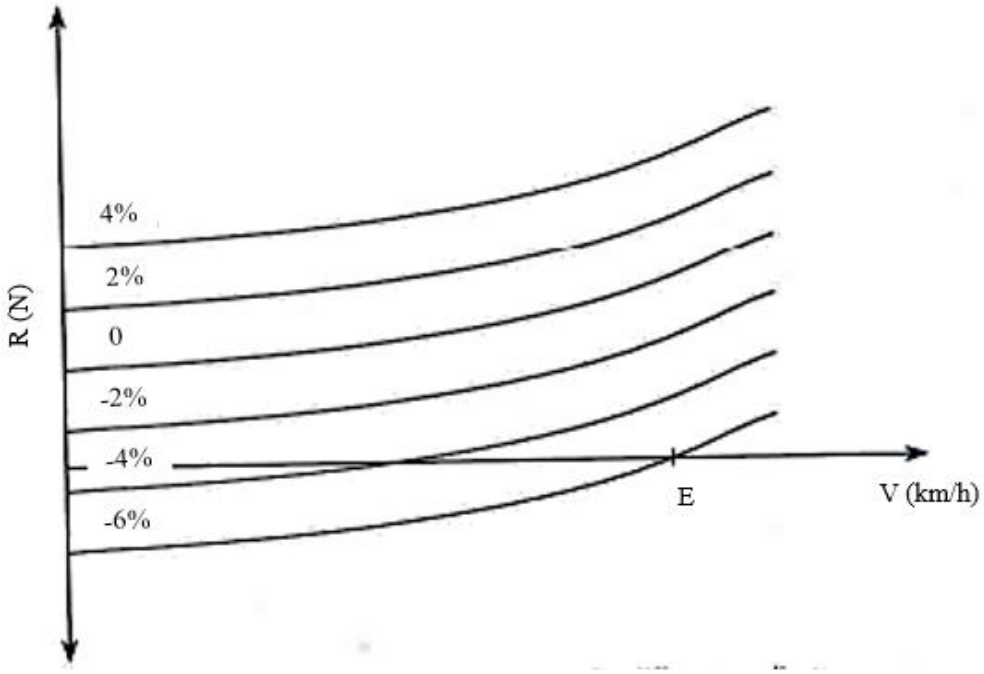

Figure 2.1 Resistance vs. speed for various gradients.
Source: Vuchic (2007)

Yeh (2003) also touched on the topic of track alignments in his study. He examined in his research, the advantages that can be obtained from the geometrical features of the

alignments which could aid in both acceleration and deceleration, leading to savings in energy and time. A dip in the alignment aids in acceleration by reducing total train resistance, while an incline aids in retardation. A simulation model was developed to compute all aspects of train motion and energy consumption on the alignment, with varying vertical profiles. Speed and coasting distances were optimized as well as cost savings. Yeh, in his study did not address speed limits and optimized only in one direction.

Kim and Chien (2011) demonstrated how the use of several operation methods could be adopted and incorporated into the driving pattern of trains to save large amounts of fuel and hence operational costs. They considered train schedule, track alignment and speed limits as constraints in their study and determined that varying amounts of fuel consumption could be obtained, depending on load factor, number of cars, the number of passengers and length of the coasting interval. They opted to develop a train performance simulator (TPS) which modeled the movement of the train and calculated all aspects of the movement in every simulation step, including, but not limited to, the tractive effort, resistance, speed, acceleration/deceleration and location. Their model consisted of three modules which worked in unison to accept train and alignment parameters and selecting the best combination of regimes when faced with the constraints of speed limits, alignment geometry and train schedules. They concluded that significant amounts of energy could be saved by their methods. However, they did not consider situations where stations were on different elevations which are generally the case especially with commuter rail where the trains encounter various geographical features along the way.

Kim and Schonfeld (2013) examined three different vertical alignments and developed a deterministic simulator to carry out an analysis of the train movement and the energy usage on the alignments being studied. They considered a baseline case as well as a dipped vertical alignment (DVA) and an undipped vertical alignment (UVA). They managed to minimize the cost of rail operation in both directions by optimizing the cruising speed while simulating the train operations on the proposed alignments. By use of a numerical example, they verified the model and tested sensitivities to various parameters including maximum gradients, station spacing, acceleration rates and passengers per car to the quantity of fuel consumed. They discovered that the largest percentage saving was obtained from the DVA model which saved a significant amount of travel time compared with the UVA model, which was in turn more efficient than the Baseline model.

It is well-known that energy is one of the largest expenditures for the world transportation sector and that the installation of storage devices could result in significant savings. Many studies have been conducted over the years on reducing energy consumption with or without WESS in railroad operations. The WESS units can capture and release the braking energy of the train on demand in a fast and efficient manner, which can yield 15% ~ 30% energy savings (Gonzalez-Gil, 2013). However, the placement of energy storage units is also of extreme importance. Wang et al. (2014) examined the energy-saving problem from multiple perspectives. They optimized the size and location of the WESS units to save energy (e.g., by 4.88%), improve voltage profiles and reduce operating costs. Meisner and Sauer (2019) found that 10% ~ 15% of energy can be saved with WESS. In

these studies, optimizing the speed profile as well as the number and locations of the WESS units which could further reduce energy consumption were not considered.

Some studies encountered combined regenerative braking with other strategies to save energy. For instance, Su et al. (2016) considered increasing maximum traction/braking force, reduction in train mass, and timetable optimization. The train-to-train regeneration through timetable optimization and train-to-wayside regeneration with WESS were investigated by simulation analysis. The results indicated that regenerative braking yielded 15% and 11% energy saving with and without the WESS, respectively. Allen and Chien (2018) synergized the energy-saving strategies of coasting and regenerative braking to a WESS for a given track segment. This minimized the energy consumed by an electric train and yielded 20% reduction in energy consumption. These findings encourage further research to optimize the WESS locations at a network level for greater benefits.

Considering energy cost, it is affected by the amount of usage and the utility related to the highest sustained power use in an interval (e.g., 15 or 30 minutes) during the billing cycle. The demand charge is a monthly fee that is paid as part of the cost of maintaining the electric utility's infrastructure required to deliver electricity to the customer and is separate from the actual cost of energy used. The peak demand charges during the peak billing periods are even higher and could be as much as five times the charges during the base or off-peak periods (New York State Energy Research and Development Authority, 2021). The peak power demand is calculated as the energy used during the peak period

divided by the duration. Therefore, significant savings can be expected through optimization of the speed profiles while utilizing energy from the WESS.

Table 2.2 Studies Reviewed on Programmed Driving

Year	Author	Objectives	Decision Variables	Solution Algorithm
1980	Milroy	Energy optimization	Speed, distance, time	Mathematical methods
1987	Uher and Disk	Energy optimization	Speed, distance, time	Iterative methods
2005	Jong and Chang	Speed profile optimization	Speed, distance, time	Object-oriented programming
2011	Kim and Chien	Speed profile optimization	Speed, distance, time	Simulated Annealing
2012	Desprez and Djellab	Speed profile optimization	Speed, distance, time	Simulation-based
2014	Allen and Chien	Energy optimization	Speed, distance, time	Analytical methods
2014	Bigharaz et al	Speed profile optimization	Speed, distance, time	Particle swarm, GA
2014	Li and Lo	Speed profile optimization	Timetable, headway, cycle time	Kuhn-Tucker conditions
2014	Su et al	Energy optimization	Speed, distance, time	Genetic algorithm
2014	Wong and Ho	Energy optimization	Speed, distance, time	Hierarchical GA, GA
2017	Feng et al	Timetable optimization	Dwell time, running time	Simulation-based method
2018	Amrani et al	Speed profile optimization	Speed, distance, time	GA, random forest method

2.3.2 Energy Recovery and Storage Methodologies

Some other studies involved energy recovery techniques which in this context refers to the capturing of the kinetic energy of a braking train, either for use immediately by an accelerating train, or to be stored in an appropriate medium for later use. The kinetic energy possessed by the train at the time of braking is converted to electrical energy to be used in the next acceleration phase. The conversion is accomplished after application of the brakes, by operating the traction motors as electrical generators. The regenerated energy can either be fed directly from a braking train to an accelerating train or stored in either an onboard location or in a wayside device for later use. Otherwise, if on application of the brakes, there is no adjacent accelerating train or energy storage device to absorb the regenerative energy, that energy is dissipated in the braking resistors of the train. Studies have shown that the use of an energy storage system can result in a 10% improvement in the energy efficiency of the system (Conti et al, 2015).

Gonzalez-Gil et al. (2013) examined several energy recovery strategies for the harvesting and management of braking energy. They found that between 15% and 30% energy savings could be achieved using electromechanical double layer capacitors (EDLC) for energy storage. Ianuzzi et al. (2013) explored the use of EDLCs for storage of regenerative energy for boosting line voltages and avoiding voltage sags at stations when a train accelerates. They found that with their methods the drop in voltage was reduced to 32% of that without EDLCs. Wang et al. (2014) examined the energy-saving problem from multiple perspectives. They devised a method to conserve energy in an ultra-capacitor

wayside energy storage system (WESS) by the optimization of the size and location of the storage device. Using genetic algorithms, they found that preferable sizes and locations of storage devices could be found as compromises between satisfying improved energy saving, voltage profiles and operating costs. They obtained and average energy saving of 4.88%, regenerative braking cancellation of 5.45% with an installation cost of $3.5 million. Meisner and Sauer (2019) achieved on average 10 to 15% savings by using WESS for improved energy efficiency.

Some studies used a combinatorial approach to the energy optimization problem with the expectation that combining the strategies would be more advantageous than using a single method. Allen and Chien (2018) conducted a study where coasting and regenerative braking were synergized to enhance their results. They achieved energy savings of over 20% of the case where no energy saving strategy was applied. Frilli et al. (2017) analysed interactions between the longitudinal dynamics of the train and the electrical characteristics of the power lines to optimize rail energy consumption. They also considered regenerative braking energy recovery in their approach and observed that about 33% energy savings could be obtained using their methods. In addition, above a certain braking request threshold, the effort could reach saturation and limit the recovered energy. Most other studies examined separate applications of energy-saving strategies. Hull (2009) in his research, obtained a 23% energy reduction using regeneration, and a 22% reduction through the application of coasting in addition to a 4% reduction through improved driving style. Su et al. (2016) considered operational strategies such as increasing maximum

traction/braking force, reduction in train mass, timetable optimization and optimized slope distances. They also examined train-to-train regeneration by timetable optimization and train-to-wayside regeneration by installing a WESS in separate simulations. The simulations involving regenerative braking yielded the greatest savings with 11% saving for regeneration without the WESS and 15% with the WESS.

Regeneration is possible during any brake application where the regenerative braking function of the train is active, however a suitable receptacle needs to be available to receive the regenerated energy. This receptacle could take the form of an accelerating train or a storage device containing less than its maximum capacity of stored energy. Power from these receptacles can supply energy to certain continuous loads at the stations such as heating/cooling, elevator/escalator, and lighting loads. In the absence of a storage medium, rheostatic braking dissipates the regenerated energy as heat in the braking resistors. Otherwise, if only conventional friction brakes are used, the kinetic energy lost due to deceleration can never be recaptured (Bracken and Selker, 2013). The use of 100% friction bakes is however reserved for stopping in emergency situations where the maximum possible deceleration rate is required.

The foregoing studies did not consider combinatorial solutions while adhering to schedules as in the present research and did not develop a course of action to be taken if an unexpected delay arose. In the present study, the algorithm would reduce the length of or eliminate the coasting regime if the train is behind schedule. It would also be able to

readjust the speed profiles in the case of service delays or rail traffic congestion which is a frequent occurrence at peak periods.

The storage devices for regenerated energy can be electrical such as ultra-capacitors, mechanical such as flywheels, or chemical such as batteries. They can be stored either inside of the train or on the wayside. Each method of storage and storage location has their respective advantages and disadvantages. For example, ultra-capacitor storage is highly desirable for its high charge and discharge rates and high-power densities but lacks the long-term storage capability or energy density of batteries. Flywheels store the translational kinetic energy of the train as rotational kinetic energy (Wang et al, 2012). These require large storage areas to locate the equipment and reinforced safety cages to protect against injury in the event the device breaks loose from its supports. The operational characteristics of several energy storage devices suitable for use in rail operations are illustrated in Table 2.3.

Table 2.3 Operating Characteristics of Various Energy Storage Devices

Storage Technology		**Energy Density** (Wh/kg)	**Power Density** (W/kg)	**Self-discharge Rate** (% of rated capacity)	**Life Cycle** (cycles)	**Efficiency** (%)
Super Capacitors (EDLC)		2.5 - 15	500 - 5000	14	$<10^6$	85 - 98
Flywheels		100	1000 - 5000	100*	10^5- 10^7	90
Batteries	Lead-acid	5 - 100	180	5	1200 - 1800	85 – 90
	Nickel types	50 - 80	80 - 150	10	1500 - 3000	65 – 80
	Lithium types	100 - 150	100 - 350	5	100	90 - 100

Source: San Martin (2011), Zablocki (2019) **Flywheels completely self-discharge within 24 hours*

2.3.3 Energy Storage Device Positioning

The braking energy could be stored in either an on-board energy storage system (OBESS) or in a WESS unit. Installation of OBESS units saves on transmission line losses but reduces the seating capacity of the train. In addition, the energy produced would only be available to the train producing it. WESS units free up space on the train and allows the energy to be used by any train within proximity of the storage location but are subject to line losses in the required transmission lines. The OBESS could increase recoverable regenerative energy to approximately 75% of the full amount available (Brown, 2013). With regards to energy consumption, the locations of the WESS units along the line are of extreme importance. Sub-optimal energy efficiency can occur when the units are not positioned to absorb maximum energy regenerated by a braking train. Besides, the procurement of WESS units require a significant outlay of capital and therefore the operator needs to avoid unnecessary installations.

It therefore would be advantageous to locate WESS devices close to positions where trains are most likely to brake and accelerate from, such as stations and stop signals. Either way, there are trade-offs which must be carefully examined to determine the most economically feasible option. A study by Lamedica et al. (2020) proposed an optimization algorithm to determine the size and location of WESS units on a dc rail line that maximize the economic benefits, considering instances where there was WESS installed, no WESS and train-to-train regenerative braking. They found 34% energy savings from train-to-train transmission and a further 8% savings by including WESS. Yet another study Xia et al.

(2015) proposed a method to simultaneously optimize the energy management, location, and size of the WESS units along a rail line. Their methods yielded an efficiency of over 19% compared to around 15% obtained by tradition methods.

Roch-Dupré et al. (2020) detailed a study to determine the siting and sizing of WESS for a DC railway line. They proposed a railway simulator with three separate modules to evaluate the different aspects of their optimization. They included a train module that considered the train specifications such as weight and motor power, a line module which included physical characteristics of the alignment and an automatic train operation (ATO) module. The purpose of the ATO module was to control the amount of traction or braking power to be sent to the traction motors by virtue of its position, speed limits and the programmed driving commands. Their methods involved testing a large number of WESS position configurations and calculating the net present value of each configuration to determine the optimal arrangement. To solve the problem, they used genetic algorithms GA, particle swarm (PS) and fireworks algorithms (FA) and likened it to the knapsack problem where the aim was to choose a set of items from a larger set to maximize the value. The headway was used to determine the train frequencies, but a single rate was used for the electricity charges. It must me noted that electricity costs vary with time of day, for example, peak and off-peak periods. Peak refers to the times when demand is high, and this is when the utility raises the rates. In addition, unlike the above studies, the present research first optimized the speed profiles of each alignment segment, so that

the energy inputs to the linear programming algorithm, were already optimal. This could only serve to improve on the accuracy and energy efficiency of the current model.

Table 2.4 Studies Reviewed on Energy Recovery

Year	Author	Objectives	Decision Variables	Solution Algorithm
2007	Acikbas and Soylemez	Energy optimization	Time, speed, distance	Computer simulator
2009	Hull	Energy optimization	Speed, time, distance	Analytical
2010	Miyatake and Ko	Charge and discharge cycle Optimization	State of charge	Sequential quadratic prog., dynamic prog.
2011	Pena-Alcaraz et al.	Timetable /Regen synchronization	Dwell time, speed, distance	Mathematical programming
2013	Bracken and Selker	Energy optimization	Braking control, duration	Computer simulation
2013	Jung et al.	Power output integration	Peak power	Analytical
2014	Wang et al.	Energy optimization	Size, location	Genetic algorithm
2016	Lin et al.	Dwell time optimization	Speed, time, distance	Genetic algorithm
2018	Allen and Chien	Speed profile optimization	Speed, time, distance	Computer simulation

2.4 Advantages and Disadvantages of Current Energy-Saving Technologies

On the question of energy optimization, railway companies benefit when the costs incurred to achieve the energy reduction are less than the savings from the reduced energy expenditure. As such, the technologies outlined in Section 2.3 contain numerous

advantages that support energy conservation and reduction in operational expenses. Coasting on a downgrade, for example, can aid in acceleration without the consumption of energy. It can also aid in braking on an incline, saving on the wear of brake shoes. This all adds up to savings in energy and brake maintenance costs. On the other hand, the flexibility of the coasting regime is invaluable to train operation since it is the only regime that can be eliminated to recover time when the train is running behind schedule.

Operational expenses could be further reduced by the implementation of regenerative braking where the net energy consumption is reduced by recovering the kinetic energy of the train during the braking regime. This strategy serves a dual purpose – (1) it decelerates the vehicle and (2) – it recovers energy in the process. Since the braking is electric, it also serves to save on mechanical wear of the brake components, so that the frequency and cost of maintenance are significantly reduced. When a WESS is included in the energy-saving process with regenerative braking, numerous advantages can be realized. For instance, system voltage regulation where the WESS could receive the energy from a braking train and prevent an area of high voltage at the point of regeneration. If a WESS is not present, protective circuit breakers are activated at the substation which causes the regenerative energy to be dissipated in the train braking resistors. If the train is accelerating, the large energy drawn from the utility would cause an area of low voltage to exist in that local area. Other trains passing the area may have to wait until the voltage recovers.

Peak demand reduction can also be achieved with WESS installation. This refers to the costs that the electric utility adds to a customer's electricity bill for using above a certain

amount of energy during the peak demand period. A WESS grants the opportunity for a train to use regenerated energy for acceleration instead of drawing from the utility and therefore energy costs are lowered, especially at peak periods. However, the storage device must be able to endure frequent and rapid charge and discharge rates to handle rapid transit or railroads with high frequencies.

The energy-saving strategies of coasting and regenerative braking, though important to the energy economy of railroad operation, are not without drawbacks. For instance, both methods are most effective when administered at high speeds and diminish significantly with speed. Coasting also causes the average speed of the train to be reduced, thereby increasing travel time, or in the case of a passenger train, increasing the in-vehicle time of passengers. Regenerative braking on the other hand will not completely stop the train or hold it at rest because once the train speed is below a critical value (approximately 6 mph), the traction motors cease to act as generators (Vuchic, 2007). Therefore, they lose their ability to transform the kinetic energy of the train to electrical energy and slow the train any further, and the stopping process is normally supplemented using friction brakes in a process known as blended braking (Kim and Schonfeld, 2010). In the blended braking process, as the dynamic brake drops off, the friction brakes are introduced in like quantities to achieve the intended retarding effect in a seamless manner. Pugi et al. (2013), conducted a study which predicted braking performance and underscored the importance of blending when electric and pneumatic brakes are applied in tandem. They predicted the stopping

distances while considering loading and operating conditions to meet prescribed safety standards.

2.5 Summary

Many previous studies focused on energy savings using only one optimization strategy; either coasting only (Kim and Chien, 2011; Allen and Chien, 2014), or regeneration only. The combining of different energy-saving methods serves to take advantage of the benefits of each strategy. Coasting proves to be a very successful method when administered in an optimal manner and when combined with regenerative braking, could reduce energy consumption by as much as 23% (Hull, 2009).

In some cases, it was assumed that there was only one of each operating regime whereby there was an acceleration regime followed by cruising, then a coasting regime followed by braking. However, there was not much consideration given to the fact that if a train must ascend an incline to get to the next station, then another acceleration regime may be necessary. Also, if the next station is on a decline, then depending on the maximum allowable speed, a cruising regime may have to be supplemented with a brake application to adhere to speed limits. It is therefore desirable to build a model that takes all the foregoing into consideration to accurately depict the different scenarios and get a true picture of the level of energy optimization that can be accomplished.

This study proposes a method to optimize the location of WESS units which maximize the benefit achieved with the inclusion of optimal speed profiles. Some studies

encountered in the literature maximized the regenerative braking energy to achieve maximum energy savings, while others maximized energy recovery through timetable optimization. However, few of them optimized the deployment of the WESS on a network basis considering practical constraints (e.g., operator's budget, time varying passenger demand, service frequency, and energy cost) to maximize the net benefit, which would be the focus of this study.

CHAPTER 3

MODEL DEVELOPMENT

3.1 Speed Profile Optimization

The speed profile optimization finds the operation method that consumes the least quantity of energy, while observing all safety measures and conforming to schedule. It would first utilize any available regenerated energy for acceleration and would operate through the motion regimes as dictated by the train simulator designed for this purpose. In the development of the model, four distinct scenarios will be examined to assess the effectiveness of the proposed methodology. Those scenarios are described below.

3.2 Simulation Scenarios

In the development of the model, four distinct scenarios will be examined to assess the effectiveness of the proposed methodology. First, the baseline scenario where no energy-saving strategy is applied will be examined. Then coasting only, where there is a tradeoff between energy consumed and travel time, will be applied. The third scenario is regenerative braking only, where the energy from regenerative braking is maximized. The fourth scenario will be the optimal combination of both coasting and regenerative braking. Those scenarios are described below.

3.2.1 Scenario I: The Baseline Scenario

This scenario serves as a yardstick for measuring the level of optimization achieved in the other three scenarios. It has the least travel time of the Scenarios discussed and does not involve energy optimization but calculates the level of energy consumption experienced in the absence of an energy-saving strategy. A typical operation in the baseline scenario is shown in Figure 3.1. It illustrates the event where the train is running behind schedule and either there is no receptacle available at the destination station to capture the regenerated energy or that the receptacles are not receptive. Receptivity here refers to the ability of the receptacle (either a WESS or accelerating train) to receive the energy being regenerated by the braking train.

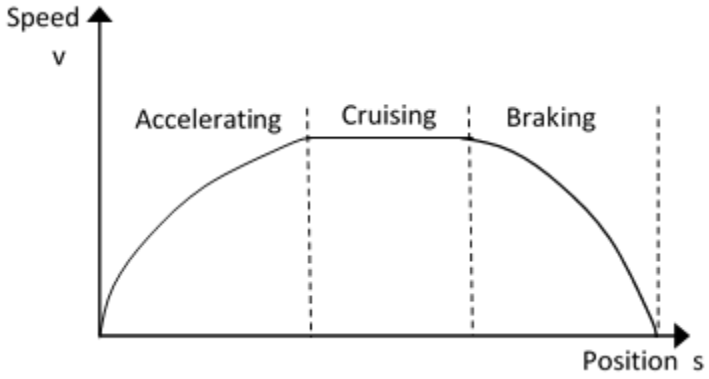

Figure 3.1 Scenario I **(**The baseline scenario).

In this scenario, the train undergoes maximum acceleration along with a cruising regime to the point where the brakes must be applied to stop at the next station. Therefore, the coasting regime is not included, and the braking energy is dissipated in the braking

resistors of the train as heat. It is then radiated to the atmosphere and can never be recaptured.

3.2.2 Scenario II: Coasting only

In railroad operations, the operator pads their schedules with extra time to absorb perturbations of the operations which may cause delays and affect their on-time performance. If on a given leg of the trip the extra time is not needed, it could be used to add a coasting regime to the operation or extend an already planned coasting regime and save energy. In this scenario the train is accelerated to maximum allowable speed and may or may not endure a minimal constant speed regime to a point where maximum coasting is included before the brakes must be applied to stop at the next station. This is illustrated in Figure 3.2.

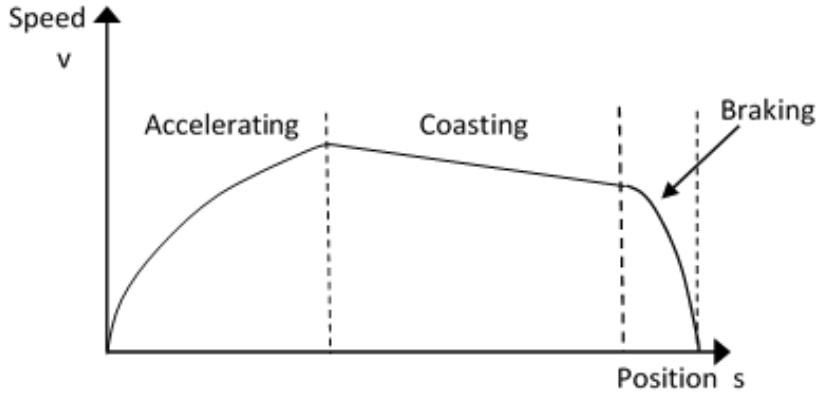

Figure 3.2 Scenario II (Coasting only).

3.2.3 Scenario III: Regenerative Braking Only

In this scenario, after accelerating to maximum speed, the train remains at maximum speed until the brakes must be applied to stop at the next station. However, in this case, regenerative braking is applied so that the kinetic energy is captured and converted to electrical energy on application of the brakes. This Scenario simulates the case where the train is running behind schedule and therefore must minimize the run time. This scenario bears a striking similarity to the baseline (Scenario I) in that the operating method of the train and travel time in both scenarios are the same. The only difference being that in this case, there is an existing receptacle available to capture the braking energy and therefore the operator can derive some cost savings.

3.2.4 Scenario IV: Both Coasting and Regenerative Braking

The train is accelerated to maximum speed and then begins a cruising regime. There are pre-determined points at which cruising will end and coasting will begin, and where coasting will end, and braking will begin, to stop at the next station. However, by inputting the train specifications and alignment parameters in the simulator, all the regimes are automatically calculated by the algorithm in a synergistic manner, so that the energy consumption is optimized. The acceleration curve is always the same in length and shape for a particular maximum operating speed on a given alignment section but depending on the value of the coasting termination speed, the cruising, coasting and braking regime plots will vary in lengths (duration). The value of the coasting termination speed would depend on the train schedule and the available time remaining to arrive at the next station. If the

time is short, then the coasting regime would be shortened to decrease the travel time and reduce delay. A typical operation in Scenario IV is illustrated in Figure 3.3.

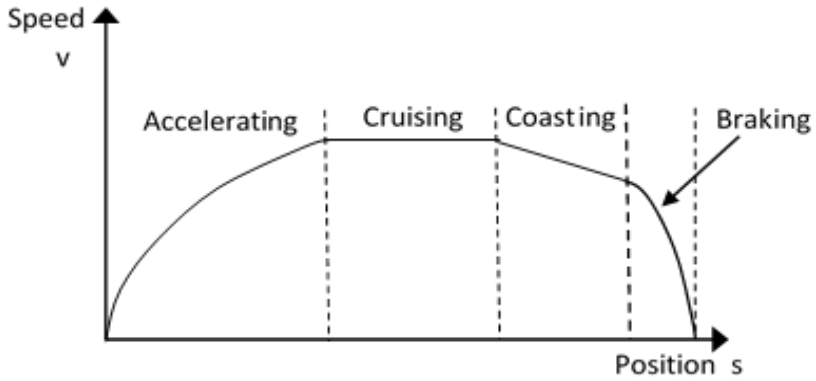

Figure 3.3 Scenario IV: Coasting and Regenerative Braking

3.2.5 Summary

The preceding Sections 3.2.1 through 3.2.4 described the four scenarios examined in the optimization of the speed profiles in this study. In Scenario I, no energy-saving strategy is applied, and it is used as a reference to assess the levels of benefits derived from the application of the other scenarios. For example, Scenario II where coasting is the only energy-saving strategy applied increases the travel time and would only be applied when the train is ahead of schedule. The extra time could therefore be used to save energy. Scenario III where regenerative braking is the only method of energy saving is only applied when the train is behind schedule to save time. Scenario IV where both coasting and regenerative braking are synergistically applied will ensure that minimum energy is drawn from the substation and that the schedule of the train is maintained.

3.3 Optimization of WESS Locations

The WESS units store the energy regenerated by a braking train. First of all, the train has to be in motion and in braking mode for regeneration to take place. The WESS is stationary, and therefore there is constant relative motion between the energy source and the intended destination. Therefore, two conditions must be satisfied for maximum energy transfer; the WESS must have the capacity to accommodate all the energy being transferred to it, and it must be within a certain optimal range to receive the transferred energy. To maximize the net benefit, the alignment section must be able to produce enough regenerative braking energy considering the prevailing electricity rates and considering the train frequencies, to offset the WESS costs.

The foregoing arguments form the basis for the development of the model for the optimization of the WESS locations. The quantified benefits with and without the WESS will be assessed, from which the net benefits could be determined for each alignment segment. The problem entails finding the optimal combination of units that maximize the total net benefits for the entire line. In order to do this, a linear programming algorithm will be developed to determine the number and locations of the units that maximize the net benefits and the dollar value annual net benefits.

CHAPTER 4

METHODOLOGY

The methodology of this research is based on the modelling of the movement of the train and the optimization of the energy consumed using the train specifications and the alignment parameters. The development of the optimization model, the evaluation of the optimal criteria and their solutions via a heuristic algorithm are discussed in this section. The proposed energy consumption model is dynamic, in that it varies with the speed and location on the track over time. The acceleration was assumed to be constant within each time step with very short duration (e.g., 0.01 second). Consequently, motion equations were developed for the acceleration, cruising, coasting and braking regimes.

4.1 Motion Regimes

The regimes were characterized by a high acceleration followed by a period of cruising, followed by a period of coasting and maximum comfort-limiting braking. Propulsion is only active during the acceleration and cruising regimes, and as such, these are the only instances where energy was consumed as indicated in Table 4.1. The coasting regime consumed no energy because propulsion is disabled. On the other hand, regeneration occurs only during the braking regime, where energy is returned to the system for subsequent re-use. The following sections outline the equations describing the movement of the train and the resulting consumption of energy.

Table 4.1 Propulsion and Brake Statuses of the Motion Regimes

Regime	Propulsion status	Brake status
Acceleration	Active	Inactive
Cruising	Active	Inactive
Coasting	Inactive	Inactive
Braking	Inactive	Active

4.1.1 Acceleration

The acceleration of the train over an arbitrary alignment segment at time *t* is denoted as the sum of the tractive effort and the train resistance divided by the equivalent mass of the train. This is the mass adjusted for additional weight of the rotating components, denoted as M_e. The deceleration of the train over the same segment is the sum of the braking force and the train resistance divided by the equivalent mass of the train. These relationships are depicted in Figure 4.1.

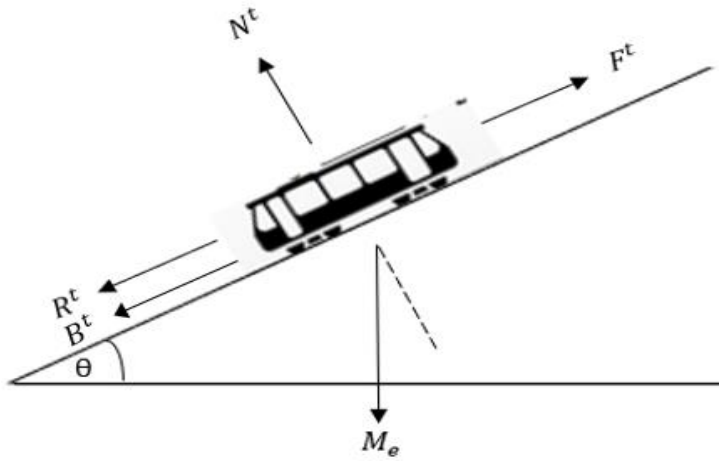

Figure 4.1 Forces acting on a body in motion.

The forces typically acting on an accelerating train are the train resistance R^t, the Braking force B^t, the equivalent mass M_e the normal reaction to its weight N^t and tractive effort F^t. The tractive effort is the mechanical force exerted on the wheels of the train by the traction motors to achieve acceleration and is a major consumer of energy when accelerating from rest. After reaching about 8 mph, the necessary tractive effort decreases drastically with speed as shown in Figure 4.2.

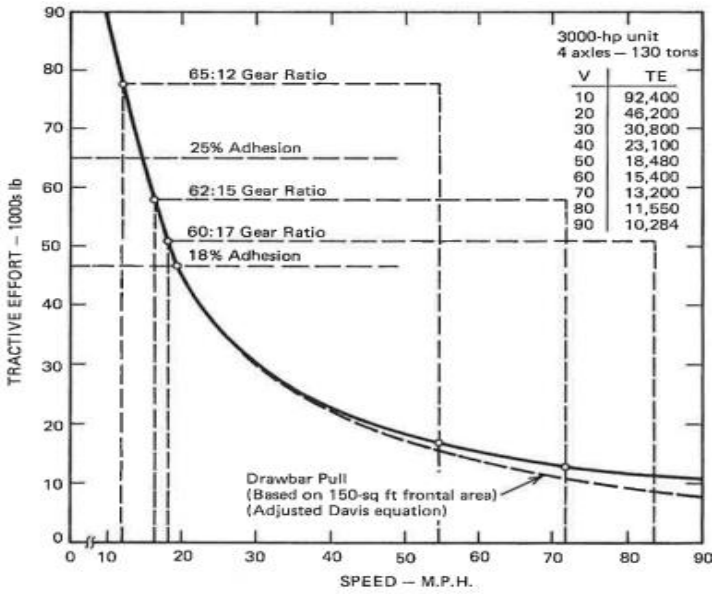

Figure 4.2 Tractive effort vs. speed curve.
Source: Hay (1982)

The train cannot be in a powering and braking mode at the same time, and thus the tractive effort and braking force cannot be simultaneously applied (Table 4.1). The acceleration a^t of a train at time *t* is formulated in Equation (4.1) as the tractive effort F^t less the resistance R^t and then divided by the equivalent mass of the train M_e. Thus,

$$a^t = \frac{F^t(v) - R^t(v)}{M_e} \qquad \forall t \tag{4.1}$$

The speed and cumulative distance travelled in the next time step are represented by Equations (4.2) and (4.3), respectively:

The unit train resistance R_u^t represented by Equation (4.4) was suggested by the Association of American Railroads (Vuchic, 2007):

$$R_u^t = \left(0.65 + 10G^t + \frac{129}{w} + 0.009v^t + 0.0716A\left(v^t\right)^2 \right) \qquad \forall t \tag{4.2}$$

where G^t is the percentage gradient at time *t*, *w* is the weight per axle (tons), v^t is the speed at time *t*, and *A* is the cross-sectional area of the train. Therefore, the total train resistance is the product of the unit resistance, the weight per axle, and the number of axles denoted as *n*. Thus,

$$R^t = R_u^t.w.n \qquad \forall t \tag{4.3}$$

The applied tractive effort F^t between the wheels and the running rails at time *t* is the minimum of the force exerted by the traction motors, denoted as F_m^t, and the adhesive force, denoted as F_a^t, formulated as Equations (4.6) and (4.7), respectively.

Therefore,

$$F^t = \min\left\{F_m^t, F_a^t\right\} \qquad \forall t \tag{4.4}$$

$$F_m^t = \frac{375\eta P_r}{v^t} \qquad \forall t \tag{4.5}$$

375 is a conversion factor, η is the motor efficiency P_r is the motor power and v^t is the train speed at time *t* (Hay, 1982).

The adhesive force acting on the train is:

$$F_a^t = \mu^t M_e \cos\theta^t \qquad \forall t \tag{4.6}$$

where μ^t is the coefficient of adhesive friction and θ^t (rad) is the inclination angle of the train to the horizontal at time *t*.

the inclination angle to the horizontal is equal to the arctangent of the gradient divided by 100. Thus,

$$\theta^t = \arctan\frac{G^t}{100} \qquad \forall t \tag{4.7}$$

For horizontal curvature, the American Railway Engineering Association (AREA) has adopted a recommended value of 0.8lb/ton/degree of curvature (Hay, 1982). In this research, the alignment consisted of mostly straight mainline and as such horizontal curvature was not considered.

The coefficient of friction is inversely proportional to the speed of the train and also varies with the condition of the rail. For example, the presence of moisture, leaf film in the fall season, ice or grease all has a significant impact on the adhesive friction coefficient. The adhesive coefficient for dry tunnels as represented in (APTA, 2012) is:

$$\mu^t = \begin{cases} 0.3 - 0.0015 \times 1.609 v^t & \text{for } v^t \leq 62.15 \\ 0.15 & \text{for } v^t > 62.15 \end{cases} \tag{4.8}$$

The available acceleration rate denoted as a_{av}^t is the applied tractive effort less the train resistance, multiplied by the acceleration due to gravity and then divided by the product of the rotating mass coefficient and train weight. Thus,

$$a_{av}^t = \frac{(E_a^t - R^t)g}{\rho W} \qquad \forall t \tag{4.9}$$

The train should accelerate at the maximum rate which is tolerable to the passengers. A study conducted by Hoberock (1976) concluded that the maximum comfort-limiting longitudinal acceleration /deceleration rate is:

$$a_{\max} = -0.15g \le a \le 0.15g \tag{4.10}$$

For the comfort and safety of passengers, the longitudinal acceleration is limited to ± 0.1~0.15g. The applied acceleration rate denoted as a_{ap} is determined as the minimum value of a_{av}^{t} and $a_{\max}$:

$$a_{ap} = \min\left\{a_{av}^{t}, a_{\max}\right\} \tag{4.11}$$

The mechanical power consumed at time *t* is:

$$P^{t} = \frac{v^{t}.F^{t}}{375\eta} \qquad \forall t \tag{4.12}$$

The incremental energy consumed by the train at time t is given by:

$$e^{t} = P^{t}\,\frac{t}{3600}.\frac{1}{1.341} \qquad \forall t \tag{4.13}$$

where the 3600 converts seconds to hours and the 1.341 converts horsepower to kilowatts. Finally, the energy consumed during acceleration E_a is formulated as:

$$E_a = \sum_{t=0}^{t_a} e^t \qquad \forall t \tag{4.14}$$

where t_a is the duration for acceleration regime.

4.1.2 Cruising

In the cruising regime, the speed remains constant subject to the maximum operating speed. The tractive forces effectively balance the resistive forces. Thus:

$$F^t = R^t \qquad \forall t \tag{4.15}$$

The energy consumed is the sum of the respective amounts consumed during t_c. Thus,

$$E_c = \sum_{t=t_a}^{t_c} e^t \qquad \forall t \tag{4.16}$$

The total energy consumed without the WESS denoted as $E_T^{'}$ is equivalent to that consumed during the acceleration and cruising regimes.

Therefore,

$$E_T^{'} = E_a + E_c \tag{4.17}$$

4.1.3 Braking

On the application of the brakes, the motors are forced to run as generators thereby converting the kinetic energy of the train to electrical energy. This generated electrical

energy is fed to a wayside energy storage system (WESS) by way of the network transmission lines, to be stored until it is needed in the next acceleration cycle. The power flow during regenerative braking and the energy storage in a WESS is illustrated in Figure 4.3.

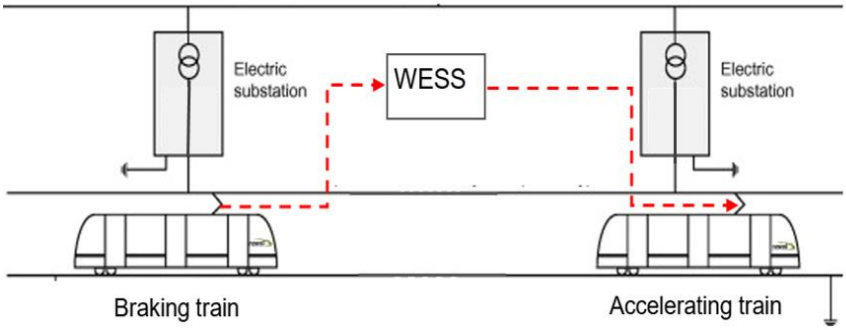

Figure 4.3 Wayside energy storage system (WESS).

It shows how energy flows from a braking train to power an accelerating train through the WESS represented by the dashed line in the Figure. The two trains must be located within the same electrical section with the WESS for achieving the illustrated transfer and even when this is so, there will be inefficiencies that must be considered. A regeneration coefficient that compensates for the inefficiencies of the charge and discharge cycles of the WESS as well as the traction motor inefficiency is factored into the energy equations to improve accuracy. In this dissertation, the regeneration coefficient is taken to be 0.82.

The braking rate b^t, which greatly influences the total recoverable kinetic energy from the train is equal to the sum of the braking force B^t and train resistance divided by the equivalent mas of the train M_e. Thus,

$$b^t = \frac{B^t + R^t}{M_e} \qquad \forall t \tag{4.18}$$

where B^t is equal in magnitude to the adhesive force stated in Equation (4.8).

Equation (4.21) represents the regenerated energy produced at time *t* when the train brakes (Sivanagaraju et al., 2010). Thus,

$$e_r^t = \left[0.01072m\rho\left[\left(v^t\right)^2 - \left(v^{t+1}\right)^2\right] + 27.25\left(s^{t+1} - s^t\right)mG^t - \left(0.2778R^t\left(s^{t+1} - s^t\right)\right)\right]\eta_r \ \forall t \tag{4.19}$$

where e_r^t is the regenerated energy G^t is the percentage gradient experienced by the train at time *t*, *m* is the mass of the train in tons, R^t is train resistance, s^t is the incremental distance travelled and η_r is the regeneration coefficient. The regenerative braking serves a dual purpose; it decelerates the train, and it generates energy. It is the kinetic energy of the train that is harvested and stored in the WESS, and since it depends only on the mass and speed of the train, then a decrease in kinetic energy translates to a decrease in speed. The total energy returned to the network through regenerative braking can be written as:

$$E_r = \sum_{t=t_c}^{t_b} e^t \qquad \forall t \tag{4.20}$$

The aim here is to minimize net consumed energy, denoted as E_T, and is equal to the difference of $E_T^{'}$ and E_r. Thus,

$$E_T = \min\left(E_T^{'} - E_r\right) \tag{4.21}$$

4.1.4 Transmission Line Losses

During consumption and regenerative braking, energy is lost due to dissipation in the electrical resistances of the transmission line segments. Considering the location of a train between a pair of stations with station spacing *S* at time *t* as illustrated in Figure 4.4, the length of the downstream segment of the alignment (Segment 1) is s^t and thus the upstream segment (Segment 2) is $S - s^t$.

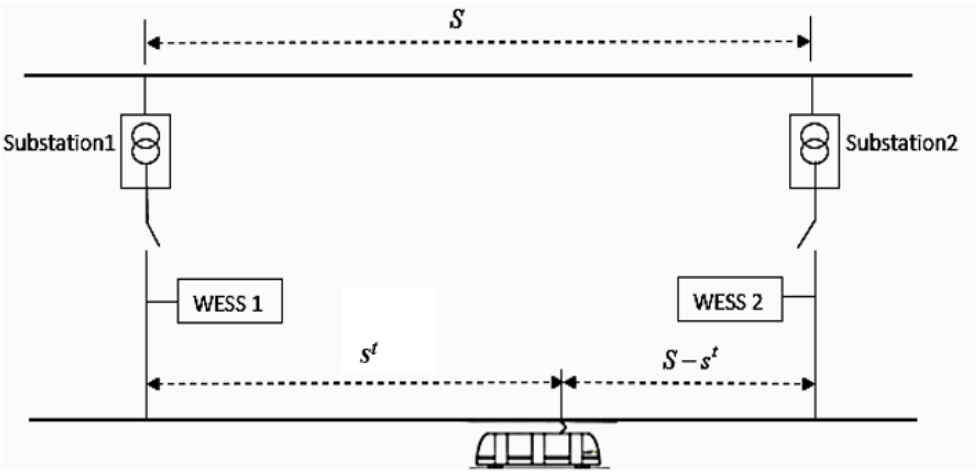

Figure 4.4 The Alignment Represented as Electrical Resistances

Since a WESS is positioned at each of the stations, the electrical resistance between the train and each WESS is the length of the transmission line between the segment multiplied by the unit resistance of the transmission line. The resistance for the sections of

the line upstream and downstream of the train conforms with the following piecewise equation:

$$r^t = \begin{cases} s^t r_u \text{ for } s^t \leq 0.5S \\ \left(S - s^t\right) r_u \text{ for } s^t > 0.5S \end{cases} \quad \forall t \tag{4.22}$$

where r^t is the line resistance at time t and r_u is the resistance per foot of the transmission line. The power lost at time t denoted as P_L^t is the product of the square of the current (I^t) drawn and line resistance r^t, where I^t is equal to the power consumed P^t divided by the line voltage V. Thus:

$$P_L^t = \left(\frac{P^t}{V}\right)^2 . r^t \qquad \forall t \tag{4.23}$$

Finally, the energy dissipated in the transmission line denoted as e_L^t at time t is:

$$e_L^t = \sum_{t=0}^{t_b} P_L^t . t \qquad \forall t \tag{4.24}$$

where t is the index of time steps.

4.2 System Constraints

In this research, there were some constraints that were adhered to for the objective function to remain in the feasible region. For instance, the train cannot exceed the speed limit for the respective sections as indicated by Equation (4.28). Equation (4.29) indicates

that the cumulative sum of the individual distances travelled over the various alignment segments cannot exceed the length of the station spacing. Equation (4.30) states that the total time travelled cannot exceed the maximum allowable travel time.

The objective function is therefore:

$$\min\left\{ E_T - e_L^t \right\} \qquad \forall\, t \tag{4.25}$$

st:

$$v^t \le v_{\max} \qquad \forall\, t \tag{4.26}$$

$$\sum_{t=0}^{T} s^t = S \qquad \forall\, t \tag{4.27}$$

$$t \le T \qquad \forall t \tag{4.28}$$

The following boundary conditions were observed during the simulation. They indicate the values of the decision variables at the start and end of the simulation. Equation (4.31) indicates that at the start of the simulation, the clock is set to zero and at the end of the run, the time will be equal to the total travel time *T*.

$$t = 0: \quad t = T \tag{4.29}$$

$$s^0 = 0: \quad s^T = S \tag{4.30}$$

In Equation (4.32), the train starts at the origin station where the travelled distance is zero and ends at the destination station where the travelled distance is equal to the station spacing *S*. It is important that the train stops and lines up exactly with the station platform,

since an overrun could result in a dangerous situation. As such there are alignment markers which guide the train driver on the correct position depending on the number of cars in the train consist.

Equation (4.33) states that the train speed at the start of the simulation is zero (at rest) and it would also be zero after arriving at the destination station.

$$v^0 = 0: \quad v^T = 0 \tag{4.31}$$

4.3 Solution Algorithms

This study comprises two models which were used in conjunction to solve the problem. The first used Genetic Algorithms (GA) to optimize the speed profile of a rail segment. In the process, values of the decision variables, namely travel speed, travel time and the coasting termination speed (speed at which braking begins) which minimize the net energy drawn from the substation were determined. This optimization method using GA was selected because of its ability to arrive at global optima in complex multi-dimensional search spaces.

The second model determined the locations of the WESS units that maximized the net benefit to the operator. The problem at hand was a non-linear multi-dimensional undertaking involving variables that were constantly changing. Due to its combinatorial nature, analytical methods were not sufficient to obtain a solution. The methods used to formulate the first model are detailed below. In this section, the formulation of the GA is discussed

4.3.1 Solution Method for Speed Profile Optimization

4.3.1.1 Genetic Algorithms. GAs are based on the principles of natural genetics and consist of the basic elements of reproduction, crossover and mutation. The solution of the problem in this study was achieved by using GA to optimize the speed profiles of each rail segment, where a randomly generated initial population was obtained from the minimized energy function stated in Equation (4.23). The GA determined values of the duration of the acceleration, coasting, cruising and braking regimes and the travel speeds involved. Since there is a tradeoff between travel time and coasting duration, and another between coasting and the quantity of energy regenerated to the WESS, the GA performs complex calculations to minimize the energy consumption and the cost to the operator. GA starts with a randomly generated initial population formed with a priori knowledge of the problem. In this way, the optimization starts with a set of approximately known solutions for faster convergence, then the following genetic operators are applied sequentially: Reproduction (Selection), Crossover, and Mutation.

The accelerations for each interstation movement can be described as:

$$a = \left[a_1 \; a_2 \; a_3 \; .... \; a_{l-1} \; a_l \right] \tag{4.32}$$

where l is the total number of time steps and each $a_i \left(i \in 1, 2, 3....l \right)$ is the acceleration rate at the i^{th} time step. The distance travelled during acceleration is determined similarly as:

$$s = \left[s_1 \; s_2 \; s_3 \; .... \; s_{l-1} \; s_l \right] \tag{4.33}$$

A series of cells in a chromosome contain the acceleration rates in a series of time steps of various speed regimes (i.e., acceleration, cruising, coasting, and braking). The length of the chromosome denoted as l, and the number of cells, is equal to scheduled travel time T divided by the duration of time step ΔT. Thus,

$$l = \frac{T}{\Delta T} \tag{4.34}$$

Whenever the train arrives ahead of schedule, the chromosome will be of the same length as stated in Equation (4.36), but the cells for the time steps that exceed the actual travel time would be empty.

4.3.1.2 Reproduction. This involves the selection of strings with above average properties from the current population and inserting them into the mating pool based on the probability of them producing even better offspring. A string is selected with a probability that is proportional to its fitness.

4.3.1.3 Crossover. The crossover operation randomly selects two individuals from the mating pool and exchanges portions of the strings, creating new strings. In the example below, for two parent strings (Parent 1 and Parent 2), if the crossover is on the third digit, they would exchange the digits after the third and yield Offspring 1 and Offspring 2.

(Parent 1) $X_1 = \{010|1001101\}$ → (Offspring 1) $X_3 = \{010|0010010\}$

(Parent 2) $X_2 = \{101|0010010\}$ → (Offspring 2) $X_4 = \{101|1001101\}$

4.3.1.4 Mutation. In this operation, the diversity of the strings is ensured, and premature convergence is prevented. A child string is produced from a single parent string by inverting a digit in a randomly selected position. That is, changing a one to zero or vice versa. As shown below, the fifth digit in the old string is inverted to form the new string.

Old string $\{1100010011\}$
New string $\{1100110011\}$

Note that a high mutation rate may lead to instability, while a low rate may introduce difficulty in reaching a solution and cause the process to be trapped in local optima.

The important parameters in GA are the size of the population, crossover rate and mutation rate. Large populations could mean simultaneous handling of many solutions and could increase computation time. However, this would increase the likelihood of convergence to a global optimum since many samples from the search space are used. Crossover frequency is used to discover a promising region for convergence. A low crossover rate slows convergence, while a high crossover rate leads to saturation around one solution. For mutation, a high rate may lead to instability while a low rate may introduce difficulty in reaching a solution.

In this study, mutation rate was set to 0.01, probability of mutation 0.1 and probability of crossover 0.8. The GA options are the user-selected termination criteria, for which a population size of 10 was used, in addition to maximum generation number of 20,

8 for maximum stall generations, and a maximum run time of 1000 seconds. The model framework for the speed profile optimization is presented in Figure 4.5 below.

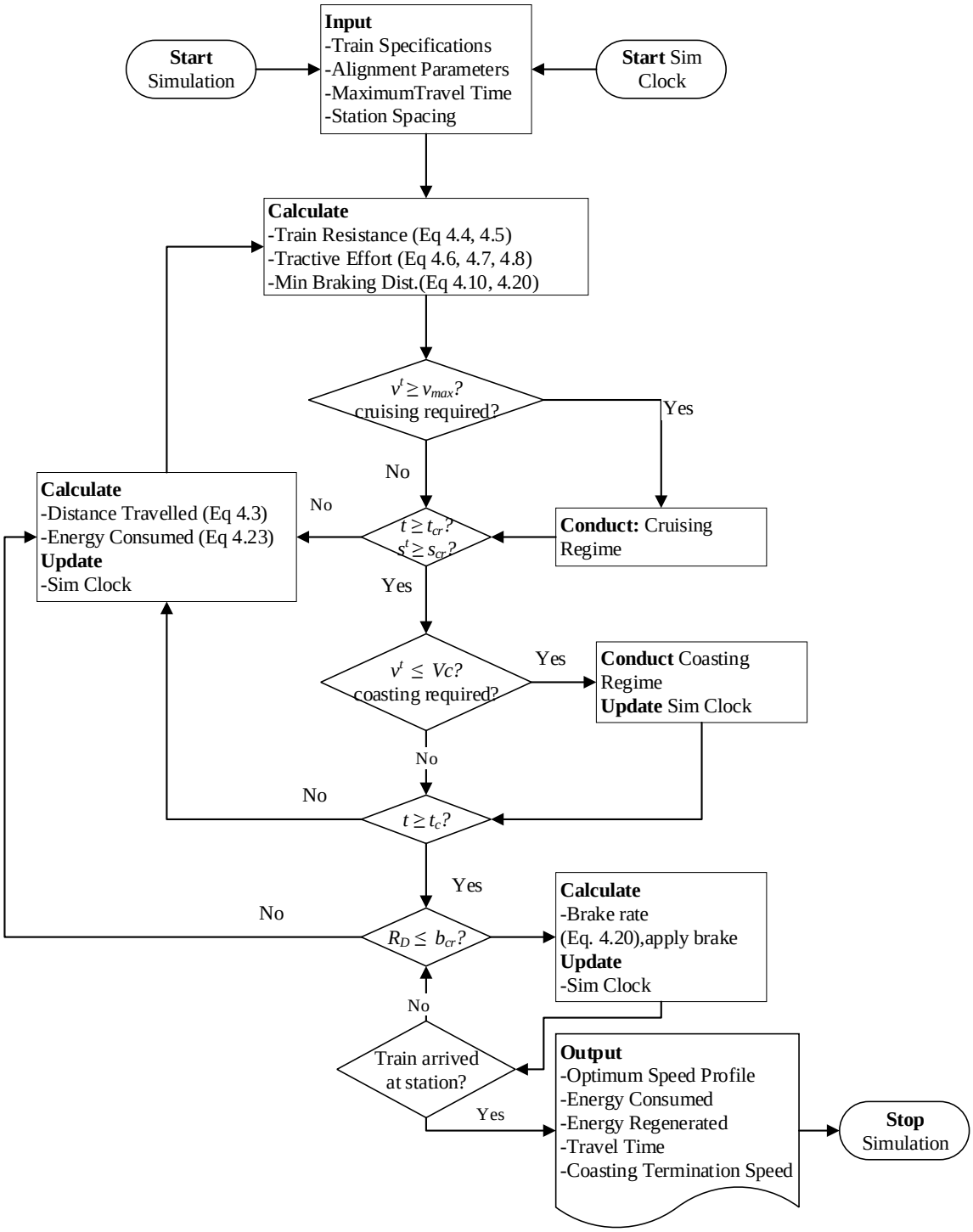

Figure 4.5 The simulation algorithm (Speed Profile Optimization).

The steps used to develop the model are listed below:

1. Input train specifications and alignment parameters into the simulator at time $t = 0$, set the maximum allowable trip time T and station spacing S.

2. Calculate the Train resistance R, tractive effort F, the minimum braking distance (b_{cr}) using Equations (4.4), (4.5), (4.6), (4.7), (4.8), (4.1) and (4.2) respectively. Accelerate train to maximum allowable speed.

3. Check if current travel speed has reached the maximum allowed and conduct cruising regime if needed, if not return to step 2.

4. Check if elapsed time and distance are greater than that allotted for the cruising regime and conduct coasting regime if needed; otherwise return to Step 3.

5. If the speed reaches the coasting termination speed V_c determine the braking rate required; if not, return to Step 4.

6. Conduct a braking regime and regenerate the braking energy to the WESS; otherwise return to Step 5.

7. If the train arrived at the station, stop the simulation and generate speed profiles; otherwise, return to Step 6.

8. Output the coasting termination speed V_c, the energy consumed E_t, the energy regenerated E_r and total travel time T.

4.3.2 Assumptions

For the purpose of the model development and clarity of the proposed model, the following assumptions were made:

1. The train is treated as a point mass and since all axles are self-propelled, the powering and braking commands are assumed to reach each car simultaneously.

2. Acceleration and braking occur at maximum comfort-limiting rates.

3. The rails are clean, dry and free of debris and therefore no slipping or sliding occurs.
4. Regenerative energy is stored on the wayside for use by accelerating trains.

4.3.3 Solution Methods for Optimization of WESS Locations

This section outlines the methods used to develop the second model in this research. It optimizes the number and locations of WESS units that maximize the annual net benefit (*NB*), which is annual benefit (*TB*) less annual cost (*TC*). Here, the mathematical relationships between the variables are developed. The model framework is given in Figure 4.6.

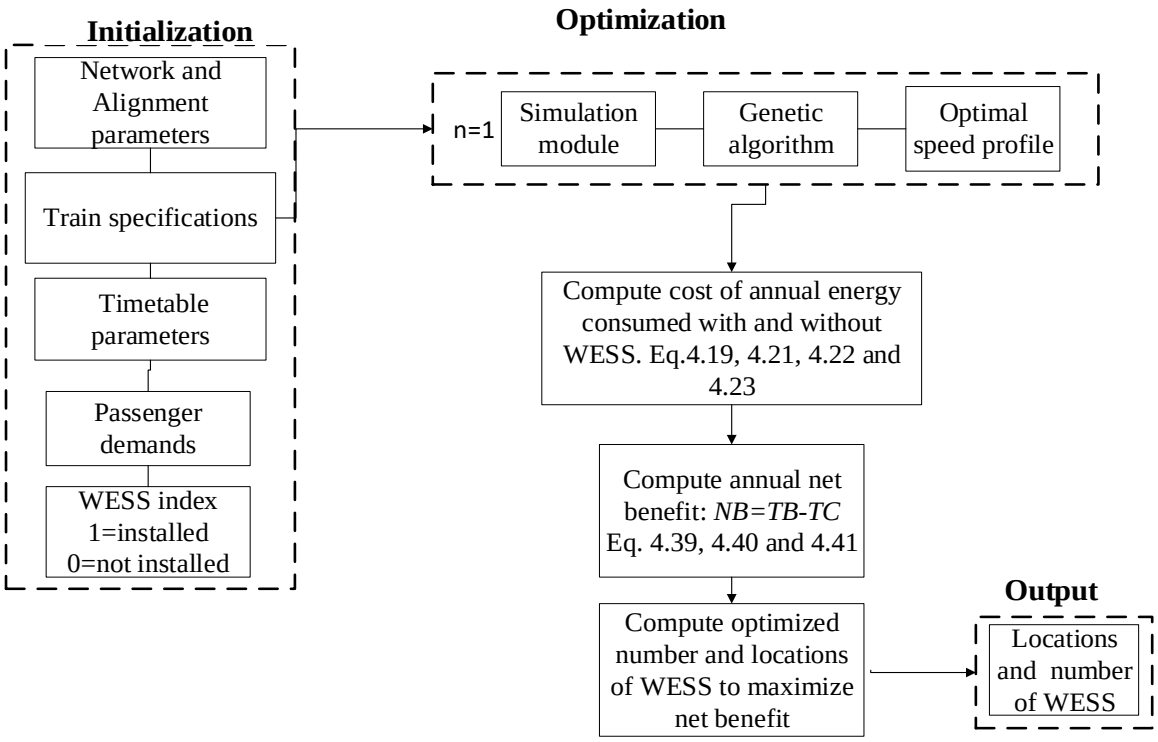

Figure 4.6 Optimization model framework (WESS Locations).

The following are the steps used to develop the model framework:

1. Initialize network and alignment parameters, train specifications, timetable parameters passenger demands and WESS index, and input into the optimization module; the output is the optimal speed profiles with and without the WESS for each segment.

2. Determine the frequency of trains within the different electricity rate periods e.g. summer peak, winter peak and off-peak, and calculate the annual cost of energy with and without WESS.

3. Compute the annual benefit *TB* as the annual cost of energy without WESS less annual cost of energy with WESS.

4. Calculate the annual cost of WESS (*TC*) as the number of units installed multiplied by the sum of the annual maintenance and installation costs

5. Determine the net benefits (*NB*) as $NB = TB - TC$.

6. Optimize the number and locations of WESS units that maximize *NB* and output the result.

4.3.3.1 Optimization of WESS Locations. At this point we recall from Equation (4.27) that the net energy consumed is the energy consumed during the generation of the optimal speed profile. This value is the input to the simulator in this section.

The cost of each WESS, denoted as *C*, is calculated on an annual basis, consisting of installation cost C_I and maintenance cost C_M. Thus,

$$C = C_I + C_M \tag{4.35}$$

Note that C_I is determined based on an interest rate for the lifecycle period of the WESS.

The total annual benefit, denoted as *TB*, is defined as the annual energy cost saving after operation of WESS. Thus,

$$TB = C_E - C_{E'} \tag{4.36}$$

where $C_{E'}$ and C_E are energy costs with and without WESS, respectively. C_E is determined by the train frequencies and operation in periods with different electricity rates. Thus,

$$C_E = \sum_{j=1}^{M} (e_{ij})(f_N r_N + f_1 r_1 + f_2 r_2) \tag{4.37}$$

where M is the number of track segments on the line, e_{ij} (kWh/year) is the energy consumed by train *i* on section *j* without WESS, f_N, f_1 and f_2 are the annual train frequencies during off-peak, summer-peak, and winter-peak electric consumption periods, respectively, while r_N, r_1 and r_2 represent the corresponding unit costs.

$C_{E'}$ ($/year) is obtained from the train frequencies during the summer-peak, winter-peak, and off-peak billing periods and is heavily dependent on the number of WESS units installed as shown in Equation (4.40).

$$C_{E'} = \sum_{j=1}^{M} (e_{ij}(1-y_j) + e'_{ij}\, y_j) f_N r_N + (e_{ij}(1-y_j) + e'_{ij}\, y_j) f_1 r_1 + (e_{ij}(1-y_j) + e'_{ij}\, y_j) f_2 r_2 \tag{4.38}$$

where e'_{ij} (kWh/year) is the energy consumed by train *i* on section *j* with WESS installed and y_j is a binary index for WESS installation on segment *j*; if y_j is 1, then a WESS is installed. Else, if y_j is 0, then no WESS is installed. The sum of all the indexes for WESS

installation should not be greater than the total number of rail segments under study which is represented by *M.* For instance, if no WESS is installed, the sum of the indexes will be zero. Moreover, if WESS units are installed on all ten segments, then that sum would be ten.

The total cost *TC* for the entire line includes the installation and maintenance cost for all installed WESS units. It is denoted as:

$$TC = \sum_{j=1}^{M} y_j \left(C_I + C_M \right) \tag{4.39}$$

The net benefit NB ($/year) is the total benefit TB ($/year) less total cost TC. Thus:

$$NB = TB - TC \tag{4.40}$$

The number of WESS units that can be procured would depend on several factors including the fuel budget and the price per WESS unit. The highest yearly cost of the WESS units must be less than the budget allowance. Therefore:

$$TC \leq B \tag{4.41}$$

where *B* is annual budget allowance.

The objective function is therefore:

$$\text{Max: } NB = TB - TC \tag{4.42}$$

$$\text{st: } \quad TC \leq B \tag{4.43}$$

$$\sum y_i \leq M \tag{4.44}$$

The problem at hand and is computationally intensive, consisting of all linear inputs and requiring integer outputs. As such, a linear programming algorithm was chosen to find the solution. First, a GA was used to optimize the speed profiles for each line segment with and without WESS, and those results along with the train frequencies and the electricity rates were used to determine the annual benefit. It is expected that the optimization of the location of the WESS units would further decrease the total energy consumed by the train and therefore increase the benefit to the operator.

CHAPTER 5

NUMERICAL EXAMPLE

In this chapter, a numerical example that transforms the theoretical model into a practical situation is presented. In this case, the section of alignment between two stations, Jamaica, and East New York, on Long Island Rail Road's Hempstead branch were chosen as a simulation platform for the first proposed model to optimize the speed profiles. This section of alignment was chosen because its gradients vary intensely from level to gentle to extreme. The extreme gradients allow for the rigorous testing required for the validation of the model and the problem was solved using Genetic Algorithms (GA). As an extension to this model, a multi-segment rail line stretching from Jamaica station in Queens to Seaford station in Suffolk County was selected to maximize the net benefit derived from installing the energy storage devices on the line. This was contained in a second model which is also described below.

5.1 Equipment used and Technical Specifications

The equipment used in the simulation is a Bombardier M7 type railcar which came into service in the late 1990s and is presently the backbone of Long Island Rail Road's electric railcar operations. These cars are extremely reliable with a current Mean Distance Between Failures (MDBF) in excess of 724,000 km (450,000 miles). The railcars were manufactured in married pairs which are then coupled with other pairs to form a train. The exterior

dimensions of one car are illustrated in Figure 5.1, and at this point it should be noted that the exterior dimensions of each member of the married pairs is the same.

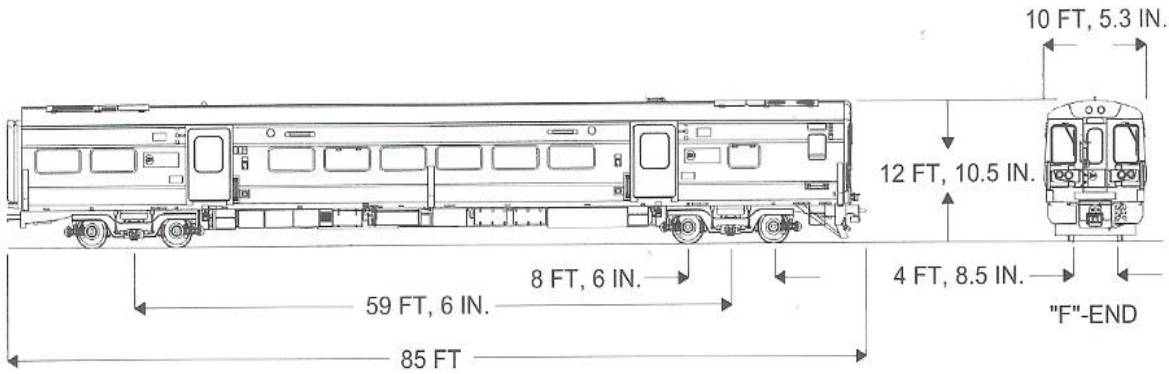

Figure 5.1 M7 railcar dimensions.
Source: Bombardier Transportation

Each car is powered by four 256 hp motors, each with rated voltage of 750V which is supplied by a third rail located a ground level. The mass of the train is 630,455 kg and its maximum allowable speed is 33 m/s with a comfort-limiting acceleration rate of 0.9 m/s^2; their deceleration rate is 1.3 m/s^2. A list of the railcar technical specifications is presented in Table 5.1. Two stations, Jamaica, and East New York approximately 8 km apart, separated by a dip in the alignment on Long Island Rail Road's Hempstead branch were chosen to demonstrate the model; the extreme gradients located on this section of alignment being one of the criteria for the choice. The branch has 29 westbound trains serving this station daily with average headway of 44 minutes, peak ridership of 1500 passengers per train and 750 passengers per train off-peak. Weekend service on this line matches the off-peak headway and ridership.

Table 5.1 Train Technical Specifications

Train specifications		**Values**
Number of cars per train		10
Number of traction motors		4 units/car
Motor power		265 hp
Weight per car		63,045 kg
Passenger weight*	Peak	122,727 kg
	Off peak	61,364 kg
Maximum allowable speed		33 m/s
Approximate headway		2640 s
Maximum acceleration rate		0.9 m/s^2
Maximum deceleration rate		1.3 m/s^2
Air resistance coefficient		0.07
Regeneration coefficient		0.82
Coeff. of rotating masses		1.04

** Passenger weight estimated at 82kg per passenger*

The alignment topography over the study segment is shown in Figure 5.2, consisting of two stations at approximately equal elevations separated by a convex parabolic spacing. The alignment consists of double track; one eastbound and one westbound.

Figure 5.2 Alignment gradient vs. distance.

5.2 Case Study 1: Speed Profile Optimization

Two case studies are presented; one for each of the models formulated. In this section the development of the speed profile optimization model is presented.

5.2.1 Background Specifications

Passenger rail operation has a reputation of being safe and reliable. Safety referring to the well-being and comfort of the passengers and reliability referring to the train being operated according to schedule with high level of service. There are numerous driving strategies that can be followed to get the train to its destination depending on the remaining time. Moreover, regardless of the remaining time for the trip, the operator endeavors to achieve the most energy-efficient strategy while maintaining schedule.

On-time performance is the number a priority of passenger rail service and the operator would take steps to ensure that this is maintained. The travel speed could be increased to make up time if the train is late, provided that speed restrictions are not violated. If the train is running early, it can add coasting to the movement, and if a WESS is available, it could benefit from regenerative braking energy recovery. Both coasting and regenerative braking are most effective at high speeds, indicating a tradeoff between the two strategies. For instance, except on a negative gradient, coasting reduces the speed of the train. On the other hand, if braking is applied at a high speed to maximize regenerative braking energy, then the time available for coasting would be reduced, since the two

strategies cannot be applied simultaneously. The middle ground is the development of the optimal speed profiles where the advantages of each strategy is exploited.

5.2.2 Optimal Results and Discussion

The simulation analysis was conducted under four distinct scenarios for peak hour operation. Each scenario was meant to simulate different values of the remaining travel times for the trip. For example, Scenarios I and II were meant to depict when the train is late, so that the coasting regime is eliminated to save time. Scenario III maximizes energy saving from coasting, and Scenario IV generates the optimal speed profile by synergizing the coasting and regenerative braking strategies. The simulation scenarios are outlined below:

- **Scenario I (Baseline run) –** Travel time was minimized without applying coasting and regenerative braking. The train was accelerated to the maximum operating speed where it remained until the brakes had to be applied to stop at the next station.
- **Scenario II (Coasting only) –** The train was accelerated to the maximum operating speed, then it maximized the coating regime before the brakes had to be applied for the train to stop at the next station.
- **Scenario III (Regenerative braking only) –** The train was operated like Scenario I. However, on application of the brakes, the regenerated energy was captured and stored in a WESS for later reuse.
- **Scenario IV (Coasting and regenerative braking) –** Regenerative braking was combined with the coasting in a synergistic manner to optimize the energy consumed by the train.

For the powering regimes (acceleration and cruising) a forward simulation was performed and for the coasting and braking regimes, a reverse simulation was performed;

similar to a method outlined in (Uher and Disk, 1987). The switching point between powering and deceleration occurs where the forward and reverse simulations intersect as shown in Figure 5.3. This point indicates the moment that the cruising regime can end and coasting can begin.

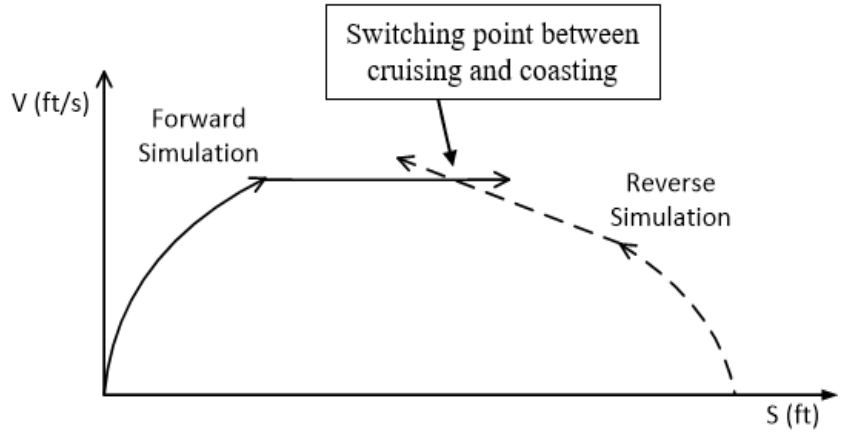

Figure 5.3 Switching Point between Powering and Non-powering Regimes.

The peak hour optimal speed profiles are shown in Figure 5.4 (a), where travel speed is plotted against distance travelled. These plots indicate an operating strategy that could be followed for safe, comfortable and efficient operation of the train. Scenario II with the lowest average speed incurs the longest travel time, followed by Scenario IV. The plots for Scenarios I and III are superimposed on each other since they both operate according to the shortest travel time, which translates to the fastest average speed and is shown in Figure 5.4 (b). The only difference between them is that Scenario III includes the

regenerative braking feature, which does not affect the travel time, but incurs less net energy consumption.

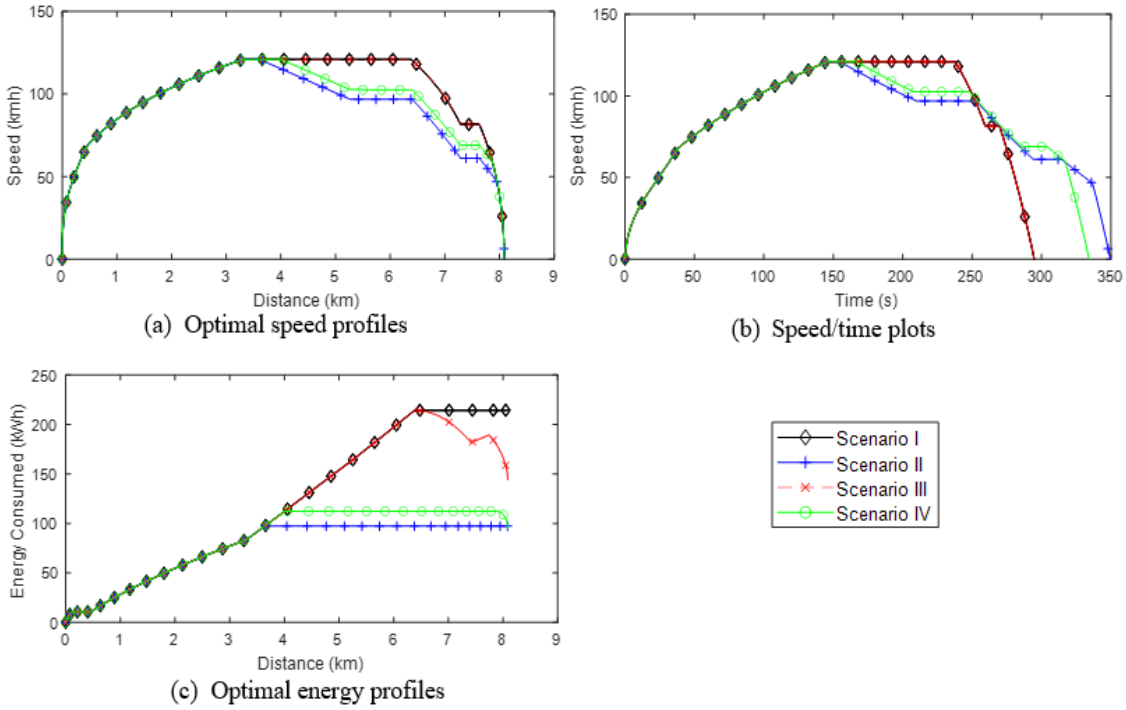

Figure 5.4. Optimal speed and energy profiles over space and time for various scenarios (peak).

The comparative cumulative energy consumption for the four Scenarios is illustrated by the energy profiles in Figure 5.4 (c), where the energy consumption is plotted against the distance travelled.

For Scenarios I and II where no regenerative braking is applied, the sections of the plot for the acceleration and cruising regimes are represented by positively sloping sections followed by horizontal sections representing the cruising (if included) and braking regimes.

In Scenarios III and IV the acceleration and cruising regimes are also represented by upward sloping sections on the plots and a horizontal one for cruising. The regenerative braking energy, being energy returned to the system, is regarded as a negative consumption, and is represented by the negatively sloping sections of the plots after the cruising regimes.

According to Table 5.2, for the peak operation, Scenario IV consumed 44% of the energy consumed in Scenario I, but the incurred travel time was 13% longer. Scenarios II and III consumed 45% and 67% of the energy consumed in Scenario I respectively, and the travel time for Scenario II was 18% greater than that of Scenario I.

Table 5.2 Optimized Results with Various Scenarios during Peak and Off-peak Periods

Scenario	Peak		Off-peak	
	Energy Consumed (kWh)	**Travel Time (s)**	**Energy Consumed (kWh)**	**Travel Time (s)**
I	214.4	294.8	207.7	290.8
II	97.2	349.5	99.5	349.1
III	144.1	294.8	143.1	290.8
IV	95.1	334.2	91.1	349.8

Note: Train empty weight 753,182 kg; peak passenger volume 1500 passengers' off-peak passenger volume 750 passengers

Since the inclusion of regenerative braking does not affect travel time, the travel times for Scenarios I and III were identical. In addition, since in railroad operations, punctuality is priority, Scenarios II and IV with the highest travel times would only be included when the train is running ahead of schedule, even though they consume the least energy. In the off-peak operation, speed profiles obtained were similar to those obtained with the peak period

passenger volume since the added passenger weight is minimal compared with the train weight. Scenario IV consumed 43% of the energy consumed in Scenario I, but its travel time was 20% greater. Scenario IV and Scenario II consumed similar amounts of energy and incurred similar travel times. The energy consumed by Scenario IV was 57% less than that consumed by Scenario III, but its travel time was 20% greater.

Generally, without the WESS (Scenarios I and II), the travel time plays an important role in energy consumed by the train. For instance, with Scenario II, as travel time for a particular travel segment is increased, more coasting is added to the operation which results in reduced consumption. On the other hand, the inclusion of the WESS brought a significant reduction in the energy consumption by synergizing coasting and regenerative braking, thereby reducing the cost to the operator and increasing the sustainability of the service. The train undergoes a shorter coasting regime and utilizes the regenerative braking to optimize the operation. For instance, WESS installation (Scenario IV) resulted in less energy consumption at the off-peak and peak periods, respectively, than when coasting was the only option (Scenario II) to reduce energy consumption. WESS inclusion reduced travel time at peak periods, which allows for increased capacity and elevates the level of service (LOS). Another benefit of WESS installation is to provide backup power to take the train to a location where it is safe to evacuate the passengers if there is a loss of power. It can also be used to power continuous station loads such as escalators, lighting, heating/cooling and charging stations for electric vehicles.

5.2.3 Sensitivity Analysis

The following section examines the input and output of the model and the processes occurring in between and identifies the key parameters in the input that would influence the value of the output. In this instance, changes in the optimized speed profiles (the outputs) are observed when maximum speeds, passenger volumes at peak and off-peak periods and maximum allowable travel times were varied.

5.2.3.1 Energy Consumption and Travel Times vs. Maximum Speed (peak periods).

Figure 5.5 displays the optimum speed profiles obtained from the simulation for various maximum operating speeds. These plots indicate to the train driver, the different maximum speeds that can be reached and the different speeds that should be maintained for the train to safely travel while minimizing energy consumption. They also indicate to the driver what operational profile can safely be maintained while retaining the ability to stop at the next station. At higher speeds, the train would face increased air resistance and initially consume more energy on acceleration. After reaching the maximum operating speed, there is opportunity to include optimal amounts of coasting and regenerative braking to reduce overall energy consumption. Therefore, as the maximum operating speed increases, the overall energy consumed decreases since in addition to exerting less tractive effort, the train can apply coasting where possible to save energy.

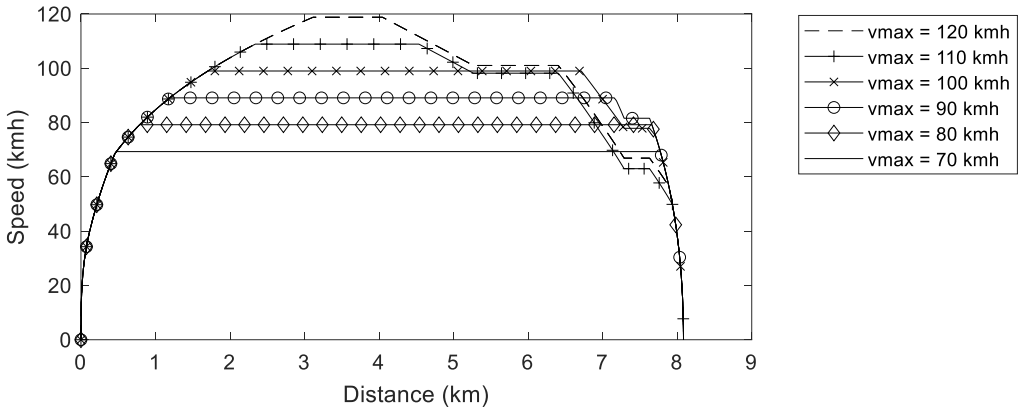

Figure 5.5 Optimized speed profiles for various maximum speeds (peak).

On the other hand, at lower operating speeds, the increased energy consumption stems from the fact that in order to not violate the time constraint, travel in the cruising regime is sustained for longer periods. This is also because at lower speeds, there is little or no opportunity to apply coasting as could be seen in Figure 5.5 in instances where *vmax* values are 70 and 80 kmh. These optimal speed profiles could be used for trains to recover from service delays that are typical with adverse weather conditions, track maintenance or signal malfunctions.

5.2.3.2 Energy Consumed and Travel Time vs. Maximum Operating Speed. In addition to reduced tractive effort causing reduced energy consumption at increased maximum operating speeds, the opportunities for prolonged coasting if the train is early or increased regenerative braking present themselves. These decreases in energy consumption are indicated in Figure 5.6(a) and may be made even greater by the unevenness of the alignment.

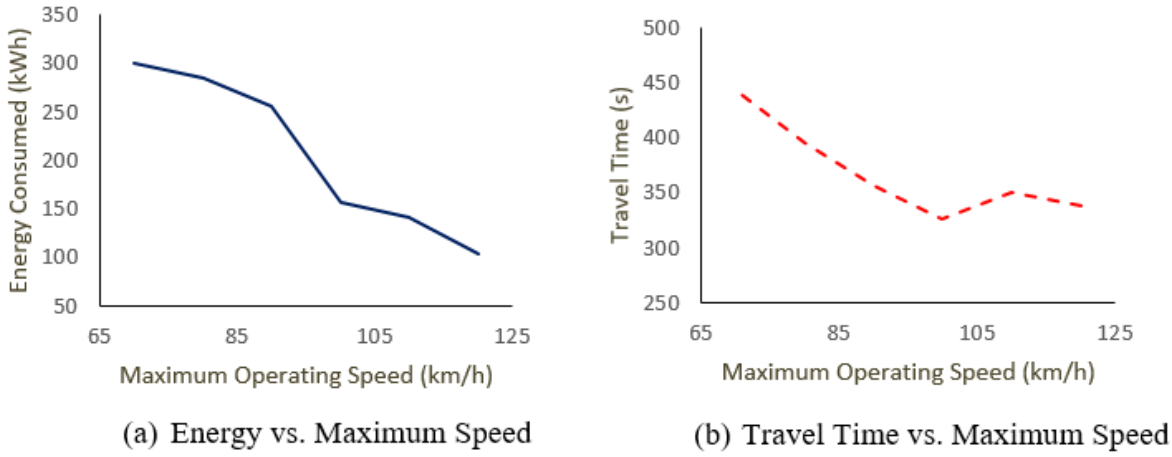

(a) Energy vs. Maximum Speed (b) Travel Time vs. Maximum Speed

Figure 5.6 Minimized energy consumption and travel time vs. maximum operating Speed.

With regards to the total travel time, as shown in Figure 5.6(b), there was an initial decrease in travel time as the maximum operating speed was increased. This was an expected occurrence. However, with the maximum operating speed at around 105 km/h, the simulator included coasting into the operation to save energy and caused the travel time to increase. Beyond 112 km/h, the cruising is reduced in favor of regenerative braking so as not to exceed the maximum allowable travel time, resulting in a decrease in travel time. In summary, when the maximum operating speed is low, the train compensates for the lower average speed by operating with minimal coasting to save time. At higher operating speeds, if punctuality is not a concern, coasting is applied to reduce energy consumption, and this results in a reduction of the average speed and increase in travel time. Since there is a tradeoff between energy saved by coasting and that saved by regenerative braking, there is a critical point while increasing the maximum operating speed where the energy

wise saving through regenerative braking is greater than that saved through coasting. At that point, the simulator reduces the length of the coasting regime, thereby decreasing the travel time and increasing the length of the braking regime and the regenerative braking energy.

5.2.3.3 Optimal Speed Profiles for various Allowable Travel Times (Peak). This Section demonstrates how the optimal speed profiles vary as the expected travel time varies and how the energy consumption of each train could change as a result of padding the train schedule with extra time. The schedule was altered by adding time in 60 second increments as well as subtracting time from it in 60 second increments. The resulting optimal speed profiles for each allowable travel time at peak periods are presented in Figure 5.7.

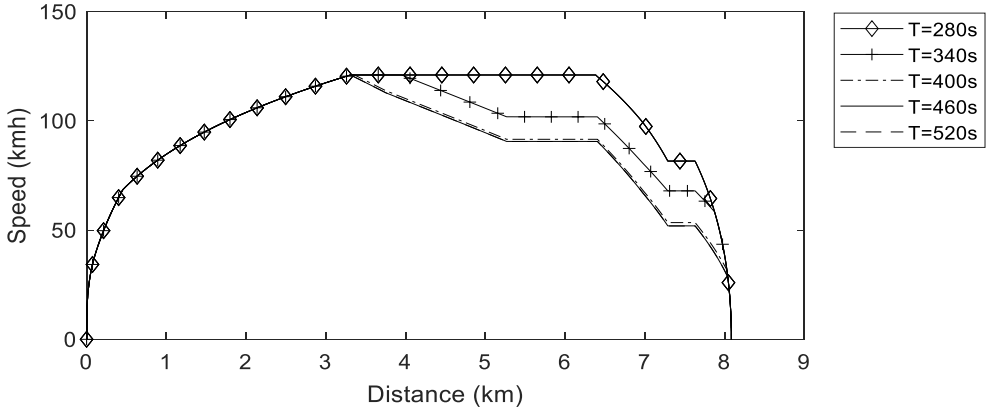

Figure 5.7 Optimized speed profiles for various expected travel times (seconds).

When the available travel time was significantly reduced below the scheduled time, the train opted for the operation mode according to Scenario III. In this case, the travel time was minimized, and although regenerative braking was included, the resulting energy

consumption was substantial. As the available travel time was increased, the train underwent varying levels of coasting along with regenerative braking, thereby reducing the energy consumption. When the available time exceeded the scheduled time, where the speed profile generated was optimal in terms of travel time and energy consumption, as expected, the speed profiles closely resembled the optimal profile. The result is seen in Figure 5.7 for values of the total travel time (T) equal to 400 s, 460 s and 520 s almost coinciding.

Table 5.3 lists the energy consumption of the train with and without the use of the WESS under various values of expected travel times. It also includes the actual travel times with and without the WESS. The results indicate that with the WESS included, the actual travel times are shorter since the train could include regenerative braking to save energy and this reduces the length of the coasting regime and hence the travel time. However, without the WESS, coasting is the only energy-saving strategy that could be utilized, and therefore the coasting regime is maximized as much as permitted by the schedule. In addition, since no further energy savings could be obtained from increasing the available travel time, any added time is used to absorb delays caused by service disruption or to facilitate passenger connections to other lines in the network.

Table 5.3. Minimized Energy Consumption for Various Travel Times

Expected Travel Time (s)	Energy Consumed (kWh)		Regenerated Energy (kWh)	Actual Travel Time (s)	
	With WESS	No WESS		With WESS	No WESS
280	144.1	214.4	70.3	294.8	294.8
340	92.8	106.1	15.8	337.2	339.3
400 (sched.)	84.2	83.7	7.7	346.8	375.6
460	84.2	83.7	3.8	373.8	426.9
520	84.2	83.7	3.8	374.0	427.8

Note: The maximum operating speed v_{max} is 120 km/h.

5.2.3.4 Energy Consumed per Car vs. Changes in Train Length. A change in length of a train varies the train weight, which includes the weight of the equipment, passenger weight and the weight of the crew. This analysis was carried out using peak hour data, where the occupancy was approximated at 150 passengers per car and the average weight of each passenger was 82 kg. The train was operated in order to obtain the minimized consumption while progressively varying its length. At this point it must be stated that increasing the train length also increases its total power, since all four axles on each car are powered on this model of train. It follows that as the number of cars per train increases, the total energy consumed on a given inter-station spacing will increase due to increased weight and additional traction motors. Figure 5.8 shows a plot of the energy consumed per car vs. the number of cars per train and total energy consumed by the train. It was observed that a non-linear relationship exists between the energy per car and the number of cars per

train. This indicates that as the number of cars on the train increases, less energy per car is consumed, and this relationship shows that the operator could benefit from economies of scale by operating longer trains.

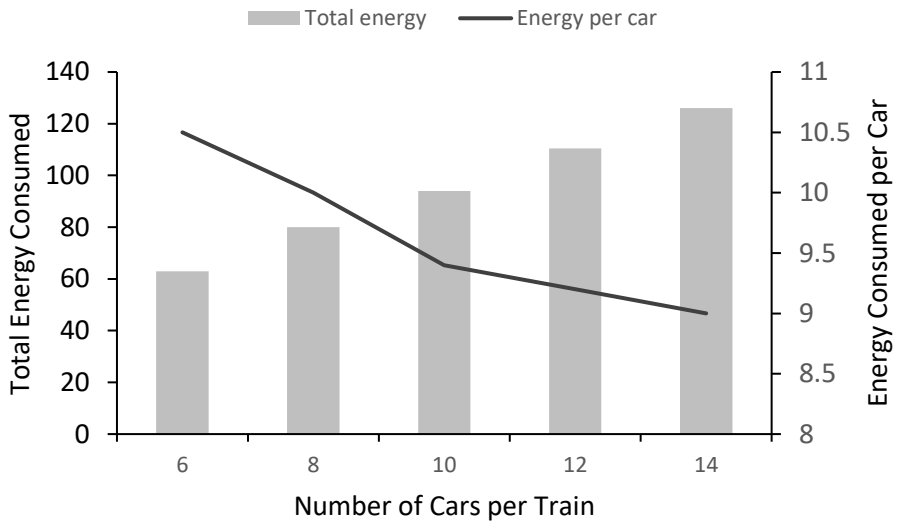

Figure 5.8 Minimized energy consumed per car vs. number of cars per train.

However, after the point where the length of the train is 10 cars, the decrease in energy consumption is marginal and it may not be advisable to operate trains above this length unless passenger volume is high, and the extra cars are necessary. As expected, the total energy consumed increases because of the additional weight and motor consumption. Another benefit of a heavier train is that on acceleration, its momentum is greater, and it is therefore, able to save more energy through coasting and regenerative braking.

5.2.3.5 Energy consumed vs. changes in V_c . Increases in the speed at which coasting ends (V_c) results in higher energy consumption as indicated in by the plot in Figure 5.9. A

higher V_c indicates that more cruising and thus less coasting is added to the movement, which leads to higher energy consumption, provided that the maximum speed is held constant.

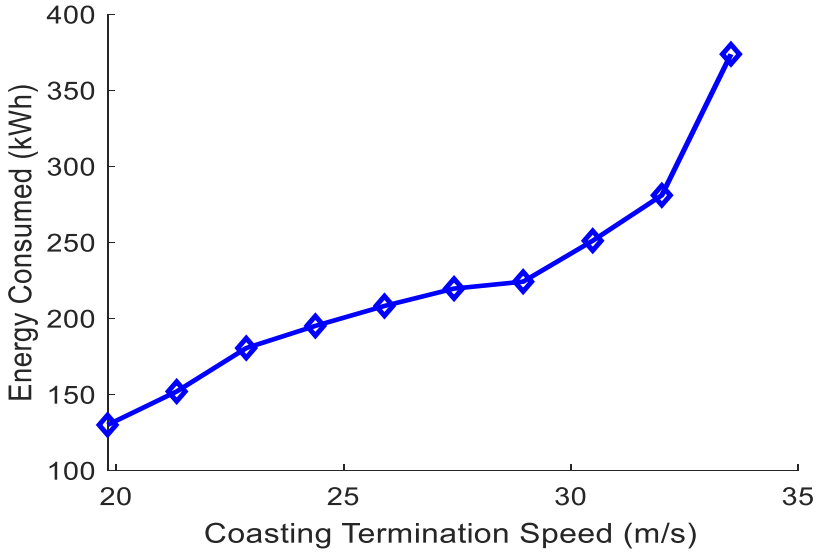

Figure 5.9 Minimized energy vs. coasting termination speed.

The plot indicates that the relationship between V_c and energy is linear up to a V_c value of approximately 27.75 m/s after which there is an exponential increase in the energy consumed. Although at the greater V_c value the train can recover more regenerative braking energy, the time constraint on the movement progressively reduces the coasting time. It was previously indicated in Table 5.3 that coasting, when synergized with regenerative braking could lead to minimum energy consumption for a given trip. Therefore, increasing

the coasting termination speed leads to a sub-optimal condition where the energy consumed increases.

5.2.4 Summary and Suggestions

The case study sought to demonstrate how the determination of the optimal speed profile could result on energy savings for the operator and reduction in greenhouse gas emissions thereby mitigating the effects of climate change. It achieved an energy saving of 125% over the baseline scenario at peak time and 127% at off-peak. Its travel time was 13% longer than the baseline at peak and 19% longer at off-peak periods. The model adopted four scenarios of which Scenario II incurred the longest travel time. Its energy savings were comparable with the optimal profile at peak time, but its travel time was 5% greater. At off-peak, the travel times between Scenario II and Scenario IV (optimal) were comparable, but its energy consumption was almost 10% greater. The energy consumption in Scenario III was 48% less than that of the baseline at peak and 45% less at off peak.

The results obtained from operation in Scenario II are very similar to those obtained from Scenario IV in terms of both energy consumption and travel time. On the contrary, although the travel times were identical for Scenarios I and III, their energy consumptions were much different. The operator may want to look into the positioning of the WESS at another location for better WESS capture, since Scenarios I and III may not be used often and coasting is very desirable for energy efficiency. Otherwise, a combination of locations with additional WESS units may achieve greater energy savings.

5.3 Case Study 2: Optimization of Locations of WESS Units

A second case study was conducted on a commuter rail line to verify the model formulated to assess the economic benefit of the WESS deployment to supplement the energy savings with optimized speed profiles. The WESS can absorb the electrical energy supplied to it if it in electrical proximity of the regenerating train. The benefit derived from the installation of a WESS unit depends on the energy recovered compared with the cost to have it installed at that particular location. It is a measure of the difference between the total benefits and total costs. If it is found that the total costs outnumber the total benefits, then it would not be profitable to install a unit at that location. This case study explores all the possible locations for WESS installation and determines the combination of installations that maximizes the net benefit.

5.3.1 Background and Specifications

The rail line which consists of 11 stations along Long Island Rail Road's Babylon branch starts at Jamaica and runs eastward to Seaford as represented in Figure 5.10. This section of track was chosen due to its widely varying station spacing and gradients which avails the opportunity for two very important factors in rail energy consumption to be thoroughly examined.

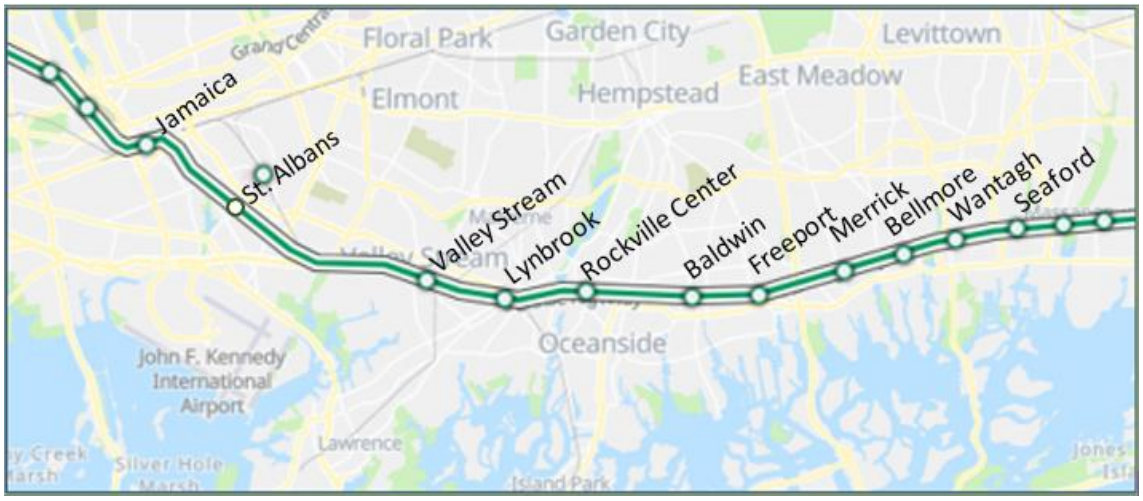

Figure 5.10 Schematic of rail line in the case study.

Long station spacing allow the train to operate at higher speeds and therefore accumulate more kinetic energy. A steep negative gradient causes the train to accelerate without consuming energy. A steep positive gradient allows the train to drastically reduce speed with minimal use of the brakes saving on brake maintenance in the process. The average track gradients and station spacing vary in lengths over the route are indicated in Table 5.4. The average gradients are obtained by multiplying the length of each segment by its percentage gradient, adding them to each other and then diving the result by the total station spacing.

There are 23,172 eastbound trains serving this this route annually which consume energy at costs depending on electricity rates at different periods. To calculate the annual energy cost, the “time of use” rates from Con Edison Inc. were used. It names two peak periods: June to September, weekdays 8am to 10pm (Summer peak), and all other months,

weekdays 8am to 10pm (Winter peak). All other times are off-peak. According to the schedule, the summer peak period accounts for 4,299 trains (MTA Long Island Rail Road, 2022). Trains during this period consume electricity at the most expensive rate.

Table 5.4 Station Spacing and Average Gradient

Segment ID	**Distance (ft)**	**Average Gradient (%)**
1	3541.04	0.7
2	6517.76	0.002
3	804.66	0.36
4	4707.31	0.03
5	3459.97	0.02
6	2051.89	0.1
7	2856.57	0.08
8	2011.67	0.07
9	1770.25	0.13
10	2132.36	0.014

The winter peak period is the second most expensive period and sees 8,597 trains. The off-peak periods have 10,286 trains scheduled and are the most inexpensive rate periods. The passenger demands peak at different periods to those of the electricity rates. For instance, morning peak periods for passenger demand occurs from 6am to 10pm and evening peak from 4pm to 10pm on weekdays (except holidays). All other times are considered off-peak Table 5.5 lists the passenger demands for the different travel periods along with the train frequencies and electricity rates for the summer peak, winter peak and off-peak rate periods. used in this case study.

Table 5.5 Passenger Demand, Train Frequency, and Electricity Rates in Different Time Periods

Passenger Demand		Electricity Rates		Train Frequency	
Daily periods	**Number of passengers/yr.**	**Electricity rate periods**	**Rates ($/kWh)**	**Travel periods**	**Frequency (trains/year)**
Morning Peak	1,492,008	Summer peak	0.35	Summer peak	4,299
Evening Peak	3,635,400	Winter peak	0.17	Winter peak	8,597
Off-Peak	6,361,047	Off-peak	0.013	Off-peak	10,286

Note: *morning peak is 6am to 10 am and evening peak 4pm to 10pm weekdays except holidays. Off-peak: all other times.*

The simulations were performed on the model in accordance with the train specifications in Table 5.6 to determine the annual energy consumed with and without the WESS.

There are several costs associated with the installation of WESS units at the railway stations. The one-time costs include the installation and the equipment costs. In addition, there are recurring costs for operation and maintenance which may be contracted out on an annual basis.

Table 5.6 Train Configuration for Location Optimization

Parameters	**Values**
Maximum operating speed	120 km/h
Maximum acceleration rate	3.2 km/h/s
Maximum deceleration rate	4.8 km/h/s
Regeneration coefficient	0.82
Net weight per car	63,045 kg
Coefficient of rotating masses	1.04
Air resistance coefficient	0.07

These costs shown in Table 5.7 were based on a single WESS installation with 2% interest rate. Note that maintenance cost was not financed, and therefore, not subject to interest. The interest was calculated using the compound interest formula in Equation 5.1:

$$A_T = P\left((1+r)^q - 1\right) \tag{5.1}$$

where A_T is the total interest to be paid (\$), P is the principal (\$), r is the interest rate as a decimal, and q is the repayment period.

Table 5.7 Costs per WESS unit

Cost per unit (\$)	Interest over 15 years (\$)	Yearly cost per unit (\$)	Maintenance (\$/year)	Annual cost (\$/year)
979,738	338,860	87,906	28,921	116,827

For the calculation of the average annual cost, the cost per unit was added to the interest accrued over 15 years at 2% interest. The result was divided by the payback period (e.g., 15 years) and then added to the annual maintenance cost.

5.3.2 Optimal Results and Discussion

The aim of this research was to optimize the number and locations of WESS units to maximize the net benefit (*NB*) on a commuter rail line. Initially, a simulation was conducted on each segment of the line using GA to obtain the optimal speed profile with and without the WESS. Then, those results were used to determine the total benefits while considering the electricity rates during the respective travel periods. Finally, a linear programming algorithm was developed to determine the number of WESS units and their locations along the alignment that maximize the operator's net benefit.

5.3.2.1 Energy Consumption, Saving and Avoidance of CO_2 Emissions. The optimal speed profiles were obtained without WESS by adding varying levels of coasting to the movement and with the WESS by adding optimal coasting and regenerative braking. The level of coasting added depended on the schedule, since coasting decreases the travel speed. Table 5.8 lists the energy consumed at the evening peak periods on each segment with and without the WESS along the entire line.

The inclusion of WESS in the network resulted in significant energy savings, and as a consequence, the avoidance of significant quantities of carbon dioxide (CO_2) into the atmosphere. According to the US Energy Information Administration (2021), each kilowatt hour (kWh) of energy saved, results in the avoidance of 0.85 lbs. of CO_2. The segment that consumed the highest quantity of energy without the WESS was St. Albans to Valley Stream, which is the longest at just over 1.1 miles. The train could therefore travel at the maximum allowable speed to maintain schedule and potentially recover more regenerative braking energy. In this way, it delivers greater energy savings when operating with WESS installed and greater CO_2 avoidance as is evident in Table 5.8. However, traveling at maximum speed, the motion resistance would increase, and it would consume more energy. The opposite was true for the Valley Stream to Lynbrook segment which was the shortest and therefore consumed the least energy with and without the WESS. The largest consumption with WESS was observed on Segment 1 (Jamaica to St. Albans), which also consumed a large amount without WESS.

Table 5.8 Energy Consumed and CO_2 Emissions per Evening-Peak Train

Segment ID	Energy consumed without WESS (kWh)	Energy consumed with WESS (kWh)	Energy saving with WESS (kWh)	*CO_2 Emissions Avoided (lbs)
1	160.3	151.1	9.2	7.8
2	269.0	104.0	165.0	140.2
3	27.5	18.0	9.5	8.0
4	76.0	60.9	15.1	12.8
5	135.5	43.0	92.5	78.6
6	86.4	80.7	5.7	4.8
7	104.5	45.9	58.6	49.8
8	43.0	40.7	2.3	2.0
9	76.0	63.4	12.6	10.7
10	56.0	30.1	25.9	22.0

*One kWh of electricity consumed produces 0.85 lbs of CO_2

This resulted in a small energy saving compared with Segment 2 (St. Albans to Valley Stream). The reason could be the larger positive gradient on Segment 1 which resulted in larger train resistance and lower regenerative braking production.

5.3.2.2 Linear Programming Optimization. A linear programming optimization was performed to determine the number and locations of WESS units to maximize the net benefits. The destination station on each segment is viewed as a potential location. For example, the location of the WESS on Segment 1 would be at the St. Albans station. From the LIRR schedules, the annual train frequencies in the summer peak, winter peak and off-peak periods were determined. These values along with the electricity rates for the

respective periods and the budget allowance were input into an LP algorithm designed especially for this optimization problem. The results stated in Table 5.9 indicate that placing three units at the stations on Segments 2, 5 and 7 would maximize the net benefit, giving a value of $629,380 annually.

Table 5.9 Optimized WESS Locations

Segment ID	Segments	WESS index*
1	Jamaica – St. Albans	0
2	St. Albans – Valley Stream	1
3	Valley Stream – Lynbrook	0
4	Lynbrook – Rockville Center	0
5	Rockville Center – Baldwin	1
6	Baldwin – Freeport	0
7	Freeport – Merrick	1
8	Merrick – Bellmore	0
9	Bellmore – Wantagh	0
10	Wantagh – Seaford	0

** 1 = WESS installed; 0 = no WESS installed*

All other configurations would take the system into varying states of infeasibility as indicated by the optimized WESS index values of "0" in Table 5.9. This translated into significant benefit for the operator and the environment due to the avoidance of fossil fuel usage. There was also considerable energy recovered from regenerative braking; this is an indication that there is great benefit to deploying the WESS in the energy recovery process.

5.3.2.3 Net Benefit. Subtracting the energy consumed using the WESS from the energy consumed without the use of the WESS yields the energy savings derived from WESS usage. An analysis was conducted to determine to merits of deploying WESS at the various stations considering a 15- year lifecycle. The results shown in the Table 5.10 indicate that all configurations appear to be feasible.

Table 5.10 WESS Annual Net Benefit

Number of WESS	WESS Cost ($/year)	Energy Consumed		Total Benefit ($/year)	Net Benefit ($/year)
		With WESS (MWh/yr)	Without WESS (MWh/yr)		
1	116,827	23,453.0	23,964.5	511,477	394,650
2	233,655	23,167.3	23,964.5	797,215	564,560
3*	350,481	22,984.6	23,964.5	979,861	629,380*
4	467,308	22,904.3	23,964.5	1,060,148	592,840
5	584,135	22,893.5	23,964.5	1,070,955	522,820
6	700,962	22,818,5	23,964.5	1,146,022	445,060
7	817,789	22,789.0	23,964.5	1,175,469	357,680
8	934,616	22,760.5	23,964.5	1,203,986	269,370
9	1,051,443	22,742.8	23,964.5	1,221,653	170,210
10	1,168,270	22,191.0	23,964.5	1,228,789	60,519

**Note: optimized number of WESS that maximized net benefit*

In addition, as more units were added, the WESS costs rose more rapidly than the benefits obtained, so that there was a non-linear positive correlation between the WESS cost and the total benefit. The net benefits on the other hand, which was calculated as the

total benefits less the WESS costs, rose initially up until three units were installed, after which it steadily declined. The reason for the decline is that there is a tradeoff between the total cost and benefit. However, there is a greater cost per unit installed than benefit as the number of units increases beyond the optimized number.

Figure 5.11 illustrates the variations in the net benefits observed with changes in the number of installed WESS units in a graphical form. These results indicate that installing three units delivers the maximum net benefits, which verifies the linear programming algorithm discussed previously. The operator could use the results to make an informed decision on the number of units to install depending on budget, so that costs are reduced to a minimum.

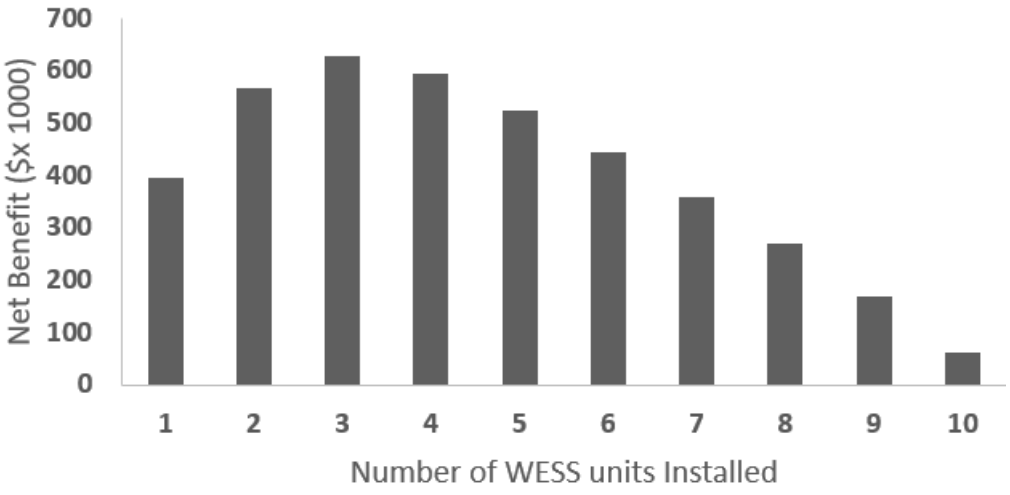

Figure 5.11 Annual net benefit vs. number of WESS units installed.

5.3.3 Sensitivity Analysis

This section identifies the reaction of the output as a result of changes in some of the input variables with all other variables remaining constant. It is an indicator of the robustness of the results obtained in the study and gives an indication of how the model would perform under different scenarios.

5.3.3.1 Electricity costs vs. Number and Locations of WESS. This section investigates how increases in electricity costs affects the number and locations of units, and what needs to be done to re-optimize the system. The electricity rates for summer peak, winter peak and off-peak periods were increased in 20% increments with the total number of units constant, and the optimal locations of the units and the net benefits were computed. The results are listed in Table 5.11.

Table 5.11 Percent Electricity Rate Increase vs. Optimal WESS Locations and Net Benefit

Percent rate increase (%)	Optimal locations	Net benefit ($/yr)
20	2,5,7	825,351
40	2,5,7	1,021,330
60	2,5,7,10	1,228,230
80	2,5,7,10	1,460,950
100	2,5,7,10	1,653,310
120	2,5,7,10	1,865,033
140	2,5,7,10	2,077,077
160	2,4,5,7,10	2,183,253

The numbers listed under “optimal locations” refer to the positions of the stations along the line. For instance, “2,5,7” means that the optimal locations are on the second, fifth and seventh alignment segments. The results indicate that substantial increases in energy rates could require, in some instances, the installation of additional WESS units to return the line to an optimized state. For instance, with a 20 – 40% increase in rates, 3 units were needed at stations 2,5 and 7. However, for a 60 – 140% rate increase an additional unit was necessary at station 10 and yet another unit was needed for a 160% increase. The net benefit on the other hand, showed a linear correlation with the increases in rates.

5.3.3.2 Train Frequency Change vs. Net Benefit. This section tests the reaction of the optimal net benefits and locations of WESS units to the changing of train frequencies. This indicates what action can be taken by the operator if passenger demands drop to unsustainable levels or rises to levels resulting in crowded trains.

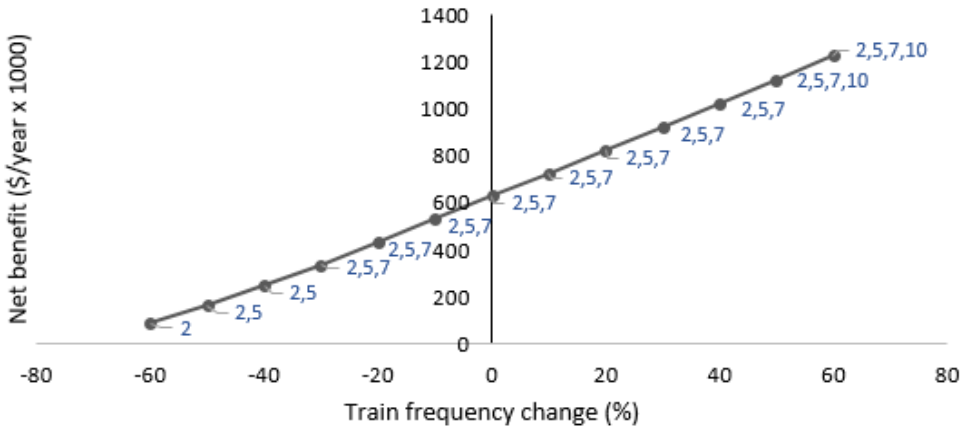

Figure 5.12 Train frequency vs. optimal WESS locations and max. net benefit.

The passenger frequencies were decreased, and then increased in 10% increments while the electricity rates were held constant. From the results indicated in Figure 5.12, there is a linear relationship between the frequency and net benefits when electricity rates are unchanged. The number of units required to optimize the travel, indicated by the data labels in the Figure, remained constant for most passenger frequency changes except very large increases or reductions. Here, the cost, as indicated by reduction in required WESS units, and annual net benefits are greatly reduced when the train frequency is reduced. Likewise, increases in train frequencies tend to result in increasing annual net benefits and total costs.

5.3.3.3 Budget Allocations vs. Optimal Net Benefits. This section examines how budget reductions affect the optimal net benefit. Each budgeted amount was entered in the linear programming algorithm and WESS units were only installed at the optimal locations allowed by budget. The resulting optimal net benefit along with the resulting number and locations of units were tabulated. Starting with a $600,000 budget, the optimization results were obtained to determine what changes would result when the budget was progressively reduced. The results in Table 5.12 show that reducing the budget allowance in $100,000 increments down to $400,000 did not change the optimal net benefit, location or number of units required.

Table 5.12 Budget vs. Optimal Number and Locations of WESS units and Max. Net Benefit

Budget ($x 1,000)	Optimal No. of WESS units	Optimal Locations	Max. Net Benefit ($/yr)
600	3	2,5,7	629,380
500	3	2,5,7	629,380
400	3	2,5,7	629,380
300	2	2,5	564,560
200	1	2	394,650
100	0	0	0

However, with a further 25% reduction to $300,000, the optimal net benefit decreased 10% and needed only two units to optimize the system. With an additional 25% reduction to $200,000, the optimal benefit showed a 37% decrease.

5.3.3.4 Interest Rate vs. Net Benefit for Changing Electricity Rates. The interest rate is one of the decision variables that could have a significant impact on any capital project. They influence company's capital structure by affecting its debt capital. It is the cost the company has to pay for the privilege of accessing the borrowed funds and causes the borrower to repay more than the amount borrowed. This section examines the reaction of the net benefit due to changes in the interest in capital borrowed and concurrent changes in electricity rates. The results are shown in the plot of Figure 5.13.

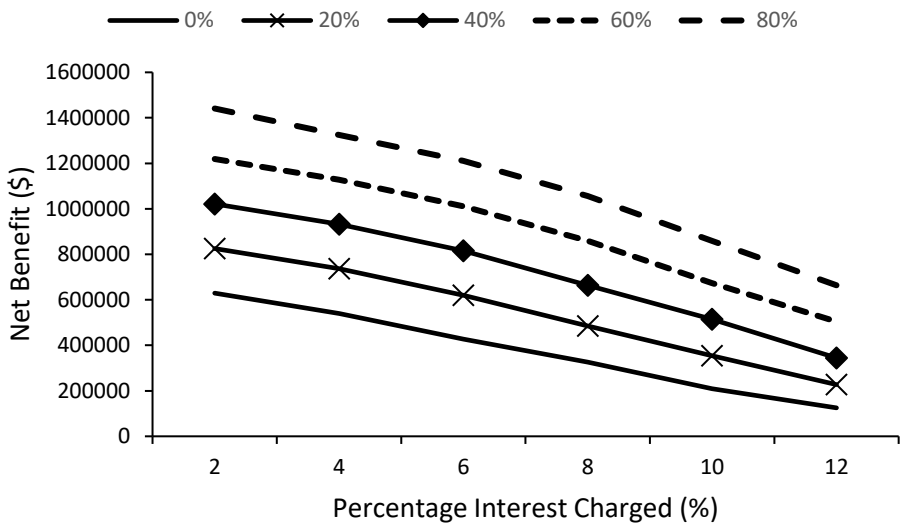

Figure 5.13 Interest rate vs. net benefit and WESS locations.

The interest rates were varied from 2% through 12%, and the electricity rates were varied from 0% through 80%. Increases in the interest rate causes the net benefit to decrease. This means that as it becomes more expensive to acquire capital funding, the net benefit from the project to the borrower decreases. This is both a logical and an expected result, but the plot also shows that as the percentage rate for electricity increases, the net benefit decreases at a faster rate. This results in the apparent convergence of the plots for the electricity rate increases. This tendency stems from the increased expenses incurred by the electricity increases being added to those of interest rate increases. The decrease in net benefits is expected to continue to the point where the interest rate would be so high that it would not make economic sense to borrow capital. At that point, the net benefit would be zero.

Another observance noted as the interest and electricity rates were varied, was that the locations for installation of WESS units for maximum net benefit sometimes changed. The changes are noted in Figure 5.14.

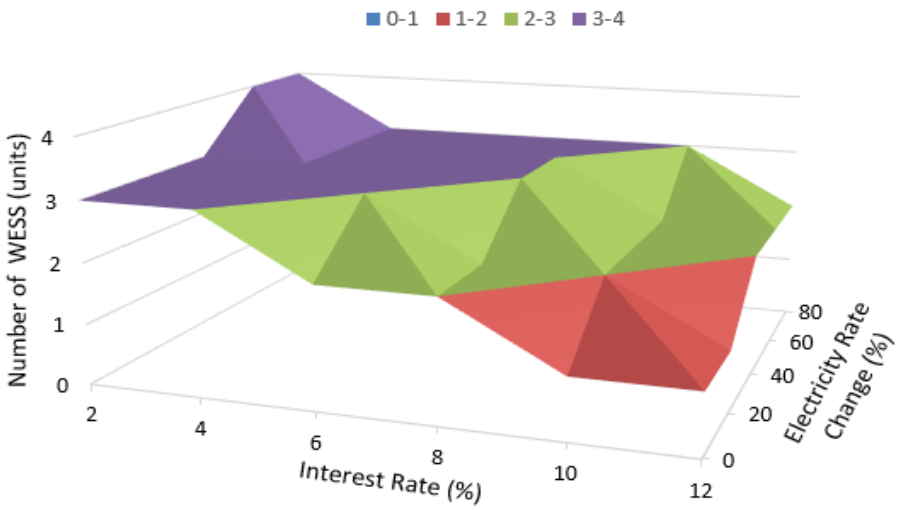

Figure 5.14 Number of WESS units vs. interest rate and electricity rate

By observing the trends in Figures 5.13 and 5.14, it can be seen that the highest net benefit is characterized by the lowest interest rates and the highest electricity rates. The reason for this is that when interest rates rise, the cost of borrowing increases, and this causes a reduction in benefits. One the other hand, when electricity rates increase, the energy saved by through the strategies adopted become more valuable, adding to the operator's net benefit. In addition, the lowest net benefit was seen where electricity rates were low and interest rates were concurrently high.

5.3.4 Summary and Suggestions

This case study sought to verify the model and to find the combination of WESS installations that would maximize the net benefit to the operator. The input of the simulator was the output of the speed profile optimization so that the process was starting with inputs that were already optimized. The optimization was accomplished using a linear programming model which output the number and locations of the WESS units for maximum economic benefit. An optimized annual net benefit of $639,380 was determined as well as the avoidance of emission of over 300 lbs of CO_2.

A sensitivity analysis conducted showed that increases in electricity rates as well as train frequency increases cause increases in the net benefit, but interest rates increases causes it to decrease. Another sensitivity of the number of WESS units required vs. electricity and interest rates indicated that low interest rates and high electricity rates characterize higher number of WESS units which in turn indicate higher net benefits.

It is suggested that the operator tries to negotiate the best interest rate on loans and use the excess regenerative braking energy to power high-consuming non traction loads such as escalators, heating and cooling units. In addition, they may try to increase regenerative braking production in the summer peak periods by non-WESS methods such as coasting and timetable optimization if possible. These methods are suggested because of the high costs of additional WESS installation.

CHAPTER 6

CONCLUSIONS AND FUTURE REASEARCH

6.1 Conclusions

This study aimed to maximize the net benefit obtained from installing WESS units along the alignment for the capture and re-use of regenerative braking energy. It determined firstly, how the locations of the WESS units could supplement the energy savings obtained from the speed profile optimizations in an existing rail network. Secondly, the quantified benefits obtained from the cost savings due to the amount of energy captured by the WESS units by maximizing the net benefits.

The results indicate that significant quantities of energy could be recuperated by installing WESS units, and the benefits could be further increased by optimizing their locations thereby reducing the user costs. User cost referring to the cost incurred by the operator through the use of the capital assets (trains and WESS units). The key contributions of this study are the novel method of combining speed profile optimization with optimized number and locations of WESS to maximize the net benefits. The optimization of the locations of WESS units minimizes some of the user costs by maximizing the economic benefit resulting from their installation. In addition to cost reductions for the operator, the environmental impact is further mitigated with the methods presented. The analysis indicates that almost 337 lbs. of CO_2 could be avoided due to the energy savings achieved using the methods outlined in this study.

In case study 1, the speed profile operation in Scenarios I and III could be applied if the train is running late to recover from slowdowns due to service disruptions or emergencies. In case study 2 it was also shown that the operator may have to deploy increased number of units to respond to increased electricity rates to re-optimize the operation. In addition, a decrease or increase in train frequency could result in the deployment of less or more units respectively to re-optimize the operation. In relation to interest rates on loans, greater benefits are achieved from having the lowest rates possible. These results could be used in construction planning for infrastructural upgrades to set the maximum number of WESS units to be deployed according to budget. They can also be used to determine what action should be taken if there is a change to any input variable, such as a rate increase for electricity.

6.2 Future Research

Further research may be conducted in the future on an expanded network where multiple trains are operating from the stations and to determine the likelihood of using the speed profile optimization method for recovery from perturbations of the train service. With a single train, this was shown to be possible in Section 5.2.3.2, but would be much more involved when considering multiple scheduled trains on a larger network. The optimal speed profiles could be applied in a realistic situation where the on-board computer of the train could receive live updates about the traffic ahead and rail condition, speed restrictions etc. and adjust the speed profiles to obtain optimal operation. It would be difficult to apply

manually because human interaction may introduce errors due to inattentiveness and reaction time of the driver to execute commands. With adequate funding and approval, railroads such as the Long Island Rail Road could implement these strategies with ease.

In addition, tractive effort in a train is a large consumer of energy when it starts from rest, and coasting is a great strategy for conserving energy. Maybe some research on a trip with multiple acceleration and coasting regimes after the train reaches maximum operating speed where tractive effort is low, could be valuable.

APPENDIX

MATLAB SOLUTION ALGORITHM

The following code written in Matlab was used to generate the speed profile optimization mentioned in Section 3.1 through 3.25.

```
% function
[t,TCr,TCo,TB,s,sC,s3f,sf,v,vC,v3f,vf,EEAc,EECr,EECo,EEBr,Travel_Time,T
otal_Energy] = EnergyCalc(vmax,Vc,tmax)
function [Total_Energy] = EnergyCalcGA(V,Tmax,S)
%%
persistent Iter
if isempty(Iter)
    Iter = 0 ;
end
Iter = Iter + 1 ;

%%
mg=1387000;
mgt=mg/2000;          %?
Pr=10600;             %?
eta=0.82;             %?
rho=1.04;             %?
g=32.15;              %?
G=0;                  %?
amax=4.8;
w=17.34;              %?
num=40;               %?
Dt=0.01;

%%
vmax = V(1);     %Vmax= 65 - 105
Vc = V(2);       %Vc= 75 - vmax (the upper limit is the vmax value)
tmax = Tmax;    % tmax= 340 - 425
%%
EET = 0 ;
%%
%% Braking
bmax=-4.8;

j=1;
tb(j)=0;
b(j)=4.8;
sb(j)=0;
vb(j)=0;
```

```
mub(j)=0.3-0.002413.*vb(j).*(3600/5280);     %? Why minus? Shouldn't be
plus
Gb(j)=0.5;                                   %?
Rb(j)=((0.65+
(129/w*9.96)+0.009.*(vb(j)*1.09)*mgt*9.96)+(0.0716.*(vb(j)*1.09).^2)...
    +(mgt*9.96*10).*Gb(j))*0.225; Fba(j)=0; Fb=0;Vb(j)=0;Sb(j)=0; %?

while vb<=Vc
    j=j+1;
    tb(j)=tb(j-1)+Dt;
    %%
    if b(j-1)<0
        b(j-1)=0;
    end
    %%
    vb(j)=vb(j-1)+b(j-1)*Dt;
    sb(j)=sb(j-1)+((vb(j)+vb(j-1)/2).*Dt);
    tbt=tb(end)-tb(1);
    sbt=sb(end)-sb(1);
    Vb(j)=vb(j)^2-vb(j-1)^2;
    Sb(j)=sb(j)-sb(j-1);

    if sb(j)>0 && sb(j)<= 1506.8
        Gb(j) = 0.5;
    elseif sb(j)> 1506.8 && sb(j) <= 2640.0

        Gb(j) = -1;
    elseif sb(j)>2640.0 && sb(j) <= 3677.14
        Gb(j) = 0.6;
    elseif sb(j)> 3677.14 && sb(j) <= 5562.85
        Gb(j) = 0.65;
    elseif sb(j)> 5562.85 && sb(j) <= 7448.56
        Gb(j) = -0.37;
    elseif sb(j)> 7448.56 && sb(j) <= 9334.0
        Gb(j)= -0.2;
    elseif sb(j)> 9334.0 && sb(j) <= 14337.7
        Gb(j) = 0.16;
    elseif sb(j)> 14337.7 && sb(j) <= 16222.7
        Gb(j)=0.27;
    elseif sb(j)> 16222.7 && sb(j) <= 16887.7
        Gb(j) = -0.8;
    elseif sb(j)> 16887.7 & sb(j) <= 18674.1
        Gb(j) = -0.75;
    elseif sb(j)> 18674.1 && sb(j) <= 21408.4
        Gb(j) = -0.58;
    elseif sb(j)> 21408.4 && sb(j) <= 25368.1
        Gb(j) = -0.2;
    elseif sb(j)> 25368.1 && sb(j) <= 25552.47
        Gb(j) = -2.9;
    elseif sb(j)> 25552.47 && sb(j) <= 26499.53
```

```
        Gb(j) = -0.5;
    elseif sb(j)> 26499.53 && sb(j) <= 26770.0
        Gb(j) = 0;
    end


    mub(j)= 0.3-0.002413.*vb(j).*(3600/5280);
    Fba(j)=(mg)*mub(j)*((1-Gb(j).^2)/2);

Rb(j)=((0.65+(129/w*9.96)+0.009.*((vb(j)*1.09-vb(j-
1)*1.09))*mgt*9.96)+(0.0716.*((vb(j)*1.09).^2-(vb(j-
1)*1.09.^2))+(mgt*9.96*10).*Gb(j))*0.225);
    Fbc(j)= (bmax*mg*rho/g)+Rb(j);
    Fb=max(Fba,Fbc);
    b(j)=((Fb(j)+Rb(j))./(rho*mg/g));

    er(j)=(0.01072*(((mg*rho)/2.2)/mgt).*((vb(j).*1.09).^2-(vb(j-
1)*1.09).^2))+(27.25.*((sb(j)*0.0003048-sb(j-1)*0.0003048)).*Gb(j))-
(0.2778*4.45*0.0003048*(Rb(j)-Rb(j-1)).*(sb(j)-sb(j-1))/mgt)*0.82;
    E_Brake(j) = sum(er)/1000 ; %%%
end
%     figure(1)
%
plot(tb',[Fba',Fbc',Fb',Rb',(Fb+Rb)']);legend('Fba','Fbc','Fb','Rb','Fb
+Rb')
%     figure(2)
%     plot(tb',sb')
%     figure(3)
%     plot(tb',er')

Er=(sum(er))/1000;
V_Brake = flip(vb) ;
S_Brake = flip(-sb) ;
S_Brake = S_Brake-S_Brake(1) ;
T_Brake = tb ;
%% Acceleration

n=1;
t(n)=0;
a(n)= 4.8;
s(n)=0;
v(n)=0;
s(n)=0;
R(n)=2061.5;
mu(n)= 0.3;
Fa(n)= mu(n)*mg;
Fp(n)= inf; %%%?
F(n)= min(Fa(n),Fp(n));
while v(n) <=vmax
```

```
    n=n+1;
    v(n)=v(n-1)+a(n-1)*Dt;
    t(n)=t(n-1)+Dt;
    s(n)=s(n-1)+((v(n)+v(n-1))/2)*Dt;
    tt=t(end)-t(1);
    vt=v(end)-v(1);
    st=s(end)-s(1);

    if s(n)>0 && s(n)<= 186.5
        G(n) = 0;
    elseif s(n)> 186.5 && s(n) <= 370.87
        G(n) = 0.5;
    elseif s(n)>370.87 && s(n) <= 1502.3
        G(n) = 2.9;
    elseif s(n)> 1502.3 && s(n) <= 5462.0
        G(n) = 0.2;
    elseif s(n)> 5462.0 && s(n) <= 8196.3
        G(n) = 0.58;
    elseif s(n)> 8196.3 && s(n) <= 9983.4
        G(n) = -0.75;
    elseif s(n)> 9983.4 && s(n) <= 10647.7
        G(n) = 0.8;
    elseif s(n)> 10647.7 && s(n) <= 12532.7
        G(n) = -0.27;
    elseif s(n)> 12432.7 && s(n) <= 17436.4
        G(n) = -0.16;
    elseif s(n)> 17436.4 && s(n) <= 19321.84
        G(n) = 0.2;
    elseif s(n)> 19321.84 && s(n) <= 21207.55
        Gn = 0.37;
    elseif s(n)> 21207.55 && s(n) <= 23093.26
        G(n) = -065;
    elseif s(n)> 23093.26 && s(n) <= 24130.4
        G(n) = 0.3;
    elseif s(n)> 24130.4 && s(n) <= 25263.6
        G(n) = 1;
    elseif s(n)> 25263.6 && s(n) <= 26770
        G(n) = -0.5;
    end

    mu(n)= 0.3-0.002413.*v(n).*(3600/5280);
    Fa(n)= (mu(n).*(1-(G(n).^2)/2))*mg;
    Fp(n)=(375*Pr*eta)./v(n).*(3600/5280);
    F(n)=min(Fa(n),Fp(n));
    if F(n)<=0
        F(n)=0;
    end
    R(n)=((0.65+
(129/w*9.96)+0.009.*(v(n)*1.09)*mgt*9.96)+(0.0716.*(v(n)*1.09).^2)+(mgt
*9.96*10).*G(n))*0.225;
```

```
    a(n)=(Fp(n)-R(n))./(rho*mg/g);
    P(n)=(Fp(n).*v(n))./(375*eta);
    e(n)=P(n).*Dt.*(0.7457*(1/3600));
    E_Acc(n)=sum(e);
end
Ea=sum(e) ;

%     figure(1)
%     plot(t',Fp')
%     figure(2)
%     plot(t',s')
%     figure(3)
%     plot(t',EEE')
T_Acc = t ;
S_Acc = s ;
V_Acc = v ;

%% Coasting

k=1;
tc(k)=tb(j);
vc(k)=vb(j);
sc(k)=sb(j);
Rc(k)=Rb(end);
ac(k)=b(j);
Gc(k)=Gb(j);
muc(k)= mub(j);
tct = 0 ;
E_Coast = 0 ;
while  vc(k) <=vmax  && sc(k)<(S-sb(j));
    k=k+1;
    tc(k)=tc(k-1)+Dt;
    %%
    if ac(k-1)<0
         ac(k-1) = 0 ;
    end
    %%
    vc(k)=vc(k-1)+ac(k-1)*Dt;
    muc(k)= 0.3-0.002413.*vc(k).*(3600/5280);
    tct = tc(end)-tc(1);

    sc(k)=sc(k-1)+((vc(k)+vc(k-1))/2)*Dt;
    sct=sc(end)-sc(1);


    if sc(k)>0 && sc(k)<= 1506.8
        Gc(k) = 0.5;
    elseif sc(k)> 1506.8 && sc(k) <= 2640.0
```

```
        Gc(k) = -1;
    elseif sc(k)>2640.0 && sc(k) <= 3677.14
        Gc(k) = 0.6;
    elseif sc(k)> 3677.14 && sc(k) <= 5562.85
        Gc(k) = 0.65;
    elseif sc(k)> 5562.85 && sc(k) <= 7448.56
        Gc(k) = -0.37;
    elseif sc(k)> 7448.56 && sc(k) <= 9334.0
        Gc(k) = -0.2;
    elseif sc(k)> 9334.0 && sc(k) <= 14337.7
        Gc(k) = 0.16;
    elseif sc(k)> 14337.7 && sc(k) <= 16222.7
        Gc(k)=0.27;
    elseif sc(k)> 16222.7 && sc(k) <= 16887.7
        Gc(k) = -0.8;
    elseif sc(k)> 16887.7 && sc(k) <= 18674.1
        Gc(k) = 0.75;
    elseif sc(k)> 18674.1 && sc(k) <= 21408.4
        Gc(k) = -0.58;
    elseif sc(k)> 21408.4 && sc(k) <= 25368.1
        Gc(k) = -0.2;
    elseif sc(k)> 25368.1 && sc(k) <= 25552.47
        Gc(k) = -2.9;
    elseif sc(k)> 25552.47 && sc(k) <= 26499.53
        Gc(k) = -0.5;
    elseif sc(k)> 26499.53 && sc(k) <= 26770.0
        Gc(k) = 0;
    end

    Rc(k)=((0.65+
(129/w*9.96)+0.009.*(vc(k)*1.09)*mgt*9.96)+(0.0716.*(vc(k)*1.09).^2)+(m
gt*9.96*10).*Gc(k))*0.225;
    ac(k)= ((Rc(k)/.225)./(rho*((mg/g)/2.2)))/3.28;
    E_Coast(k) = 0 ;
end
 %     figure(1)
%     plot([tb';tc'],[vb';vc'])
T_Coast = tc-tc(1) ;
S_Coast = flip(-sc+sc(end)) ;
V_Coast = flip(vc) ;


 %% Cruising
m=1;
vC(m)=v(n);
tC(m)=t(n);
sC(m)=s(n);
ec = 0 ;
tCt = 0 ;
E_Cruise = 0 ;
```

```
while vC(m) == v(n) && sC(m)>= s(n) && sC(m) <=(S-max(sc))
    %v(n) > vmax-0.001 & s(n) < (S-max(sc))

    m=m+1;
    tC(m)=tC(m-1)+Dt;
    vC(m)=vC(m-1);
    sC(m)=sC(m-1)+((vC(m)+vC(m-1))/2)*Dt;
    tCt=tC(end)-tC(1);
    vCt=vC(end);
    sCt=sC(end)-sC(1);

    if sC(m)>0 && sC(m)<= 186.5
        GC(m) = 0;
    elseif sC(m)> 186.5 && sC(m) <= 370.87
        GC(m) = 0.5;
    elseif sC(m)>370.87 && sC(m) <= 1502.3
        GC(m) = 2.9;
    elseif sC(m)> 1502.3 && sC(m) <= 5462.0
        GC(m) = 0.2;
    elseif sC(m)> 5462.0 && sC(m) <= 8196.3
        GC(m) = 0.58;
    elseif sC(m)> 8196.3 && sC(m) <= 9983.4
        GC(m) = -0.75;
    elseif sC(m)> 9983.4 && sC(m) <= 10647.7
        GC(m) = 0.8;
    elseif sC(m)> 10647.7 && sC(m) <= 12532.7
        GC(m) = -0.27;
    elseif sC(m)> 12432.7 && sC(m) <= 17436.4
        GC(m) = -0.16;
    elseif sC(m)> 17436.4 && sC(m) <= 19321.84
        GC(m) = 0.2;
    elseif sC(m)> 19321.84 && sC(m) <= 21207.55
        GC(m) = 0.37;
    elseif sC(m)> 21207.55 && sC(m) <= 23093.26
        GC(m) = -065;
    elseif sC(m)> 23093.26 && sC(m) <= 24130.4
        GC(m) = 0.3;
    elseif sC(m)> 24130.4 && sC(m) <= 25263.6
        GC(m) = 1;
    elseif sC(m)> 25263.6 && sC(m) <= 26770
        GC(m) = -0.5;
    end


    muC(m)= 0.3-0.002413.*vC(m).*(3600/5280);
    RC(m)=((0.65+
(129/w*9.96)+0.009.*((vC(m)*1.09)*mgt*9.96)+(0.0716.*((vC(m)*1.09).^2)+
(mgt*9.96*10).*GC(m))*0.225));
%      RCC(m) = RC(m) ; %%
    if RC(m)<0
```

```
        RC(m)=0;
    end

    PC(m)= ((RC(m).*vmax)./375).*eta;
    ec(m)=(PC(m).*Dt).*(0.7457*(1/3600));
    E_Cruise(m) = sum(ec) ;
end

% plot(tC-tC(1),RCC) ;
ec(ec<0)=0;
EC = sum(ec) ;

S_Cruise = sC-sC(1) ;
V_Cruise = vC ;
T_Cruise = tC-tC(1) ;

%     figure(1)
%     plot(tC',vC')
%     figure(2)
%     plot(tC',sC')
%     figure(3)
%     plot(tC',EEE')


%%
T_Tot = [T_Acc'] ;
T_Tot = [T_Tot;T_Cruise'+T_Tot(end)] ;
T_Tot = [T_Tot;T_Coast'+T_Tot(end)] ;
T_Tot = [T_Tot;T_Brake'+T_Tot(end)] ;

S_Tot = [S_Acc'] ;
S_Tot = [S_Tot;S_Cruise'+S_Tot(end)] ;
S_Tot = [S_Tot;S_Coast'+S_Tot(end)] ;
S_Tot = [S_Tot;S_Brake'+S_Tot(end)] ;

V_Tot = [V_Acc'] ;
V_Tot = [V_Tot;V_Cruise'] ;
V_Tot = [V_Tot;V_Coast'] ;
V_Tot = [V_Tot;V_Brake'] ;


E_Tot = [E_Acc'] ;
E_Tot = [E_Tot;E_Cruise'+E_Tot(end)] ;
E_Tot = [E_Tot;E_Coast'+E_Tot(end)] ;
E_Tot = [E_Tot;-E_Brake'+E_Tot(end)] ;
%%
Total_Energy = E_Tot(end) ;
```

```
Travel_Time= T_Tot(end) ;




if Travel_Time > tmax
    Total_Energy = 1000 + (Travel_Time-tmax)^2 ;
    fprintf('Travel Time: %1.2f sec, so this set of [Vmax,Vc] is not
acceptable.\n',Travel_Time) ;

else
    fprintf('Travel Time: %1.2f sec, so this set of [Vmax,Vc] is
acceptable.\n',Travel_Time) ;
end

fprintf('           Iteration Number: %1.0f\n',Iter) ;
fprintf('   Total Energy Consumption: %1.2f\n',E_Tot(end)) ;
fprintf('Regenerative Braking Energy: %1.2f\n',-E_Brake(end)) ;
fprintf('                       Vmax: %1.2f\n',V(1));
fprintf('                       Vc  : %1.2f\n',V(2));
% fprintf('Vel Diff: %% %1.2f\n',(V(1)-V(2))/V(1)*100) ;
fprintf('|-+-+-+-+-+-+-+-+-+-+-+-+-+-+-+-+-+-+-+-+-+-+-+-+-+-+-+-+-+-|\n') ;
fprintf('|-+-+-+-+-+-+-+-+-+-+-+-+-+-+-+-+-+-+-+-+-+-+-+-+-+-+-+-+-+-|\n') ;



%%
% clf(figure(1));
figure(1)
subplot(2,2,2) ;
plot(S_Tot,V_Tot);
xlabel('Distance') ;
ylabel('Velocity') ;
%%
% figure(2)
subplot(2,2,1) ;
plot(T_Tot,S_Tot);
xlabel('Time') ;
ylabel('Distance') ;
%%
% figure(3)
subplot(2,2,3) ;
plot(T_Tot,V_Tot);
xlabel('Time') ;
ylabel('Velocity') ;
str = ['Total Energy Consumption: ',num2str(E_Tot(end),'%1.2f')];
title([str]) ;
hold on;
plot([T_Acc(1);T_Acc(1)],[0;120],'-.b','LineWidth',1) ;
```

```
% plot([T_Acc(end);T_Acc(end)],[0;120],'-.b','LineWidth',1) ;
plot([T_Acc(end)+T_Cruise(1),T_Acc(end)+T_Cruise(1)],[0;120],'-
.g','LineWidth',1) ;
%    plot([T_Acc(end)+T_Cruise(end),T_Acc(end)+T_Cruise(end)],[0;120],'-
.g','LineWidth',1) ;

plot([T_Acc(end)+T_Cruise(end);T_Acc(end)+T_Cruise(end)],[0;120],'-
.k','LineWidth',1) ;
%
plot([T_Acc(end)+T_Cruise(end)+T_Coast(end);T_Acc(end)+T_Cruise(end)+T_
Coast(end)],[0;120],'-.k','LineWidth',1) ;

plot([T_Acc(end)+T_Cruise(end)+T_Coast(end)+T_Brake(1);T_Acc(end)+T_Cru
ise(end)+T_Coast(end)+T_Brake(1)],[0;120],'-.r','LineWidth',1) ;
%
plot([T_Acc(end)+T_Cruise(end)+T_Coast(end)+T_Brake(end);T_Acc(end)+T_C
ruise(end)+T_Coast(end)+T_Brake(end)],[0;120],'-.r','LineWidth',1) ;

ylim([0 120])
legend('','Ac Start','Cr Start','Co Start','Br Start',...
       'location','south','FontSize',8,'Box','off') ;
hold off;
%%
% figure(4)
subplot(2,2,4) ;
plot(T_Tot,E_Tot);
xlabel('Time') ;
ylabel('Energy Consumption') ;

EM = 10*ceil(max(E_Tot)/10*1.2) ;
hold on;
plot([T_Acc(1);T_Acc(1)],[0;EM],'-.b','LineWidth',1) ;
% plot([T_Acc(end);T_Acc(end)],[0;EM],'-.b','LineWidth',1) ;

plot([T_Acc(end)+T_Cruise(1),T_Acc(end)+T_Cruise(1)],[0;EM],'-
.g','LineWidth',1) ;
%     plot([T_Acc(end)+T_Cruise(end),T_Acc(end)+T_Cruise(end)],[0;EM],'-
.g','LineWidth',1) ;

plot([T_Acc(end)+T_Cruise(end);T_Acc(end)+T_Cruise(end)],[0;EM],'-
.k','LineWidth',1) ;
%
plot([T_Acc(end)+T_Cruise(end)+T_Coast(end);T_Acc(end)+T_Cruise(end)+T_
Coast(end)],[0;EM],'-.k','LineWidth',1) ;

plot([T_Acc(end)+T_Cruise(end)+T_Coast(end)+T_Brake(1);T_Acc(end)+T_Cru
ise(end)+T_Coast(end)+T_Brake(1)],[0;EM],'-.r','LineWidth',1) ;
```

```
%
plot([T_Acc(end)+T_Cruise(end)+T_Coast(end)+T_Brake(end);T_Acc(end)+T_C
ruise(end)+T_Coast(end)+T_Brake(end)],[0;EM],'-.r','LineWidth',1) ;

ylim([0 EM])



plot([0,T_Tot(end)]',[E_Tot(end),E_Tot(end)]','-.m','linewidth',0.5) ;
STR = ['Braking Energy: -',num2str(E_Brake(end),'%1.2f')] ;
title(STR)
hold off;
pause(0.02) ;

f = figure(1);
% f.WindowState = 'maximized';
```

REFERENCES

Acikbas, S. and Soylemez, M. T. (2007), "Parameters Affecting Braking Energy Recuperation Rate in dc Rail Transit", *Proceedings of the Joint Rail Conference, ASME/IEEE*, pp. 263-268, ASME Transportation Div., ASME ICE Division, New York, NY, 2007.

Allen, L., and Chien, S. (2014). "Optimization of Rail Energy Conservation Through the Adoption of Varying Coasting Strategies: A Case Study of the Long Island Rail Road's Flatbush Branch", *Proceedings of the 93rd Annual Meeting Transportation Research Board*, Washington, USA.

Allen, L., and Chien, S.,(2018), Rail Energy Efficiency Improvement by Combining Coasting and Regenerative Braking", *International Journal of Railway Technology*, 7(4), 1-22, 2018. doi:10.4203/ijrt.7.4.1.

American Public Transportation Association, (APTA, 2011), "Potential Impact of Gasoline Price Increases on U.S. Public Transportation Ridership", Washington, DC, 2011. http://www.apta.com/resources/reportsandpublications/Documents/APTA_Effect_of_GasPrice_Increase_2011.pdf Accessed November 16, 2014.

American Public Transportation Association (APTA, 2012), "Public Transportation Fact Book", Washington, DC, 2012.http://www.apta.com/resources/statistics/Documents/FactBook/APTA_2012Fact%20Book.pdf . Accessed April 8, 2013.

American Public Transportation Association (APTA, 2015), Washington, DC. http://www.apta.com/mediacenter/pressreleases/2015/Pages/150309_Ridership.aspx Accessed September 13, 2015.

American Railway Engineering and Maintenance of Way Association (AREMA, 2003), "Railway Electrification", A Practical Guide to Railway Engineering, *AREMA*, Lanham, MD.

Amrani, A., Hamida, A., Liu, T., and Langlois, O. (2018), "Train Speed Profile Optimization using Genetic Algorithm based on a Random-Forest Model to Estimate Energy Consumption", *Proceedings of the 7th Transport Research Arena TRA 2018*, Vienna, Austria.

Amtrak (2019), Office of the Inspector General, National Railroad Passenger Corporation, "Quality Control Review of the Independent Audit of Amtrak's Consolidated Financial Statements for the Fiscal year ended 2020", *National Railroad Passenger Corporation*, Washington, DC, 2020.

Barkan, C., (2007) "Railroad Transportation Energy Efficiency", *Technical Presentation*, University of Illinois, Urbana-Champaign, IL, 2007.

Bigharaz, M., Afshar, A., Suratgar, A. and Safaei, F., (2014), "Simultaneous Optimization of Energy Consumption and Train Performances in Electric Railway Systems", *Proceedings of the 19th World Congress, The International Federation of Automatic Control*, Cape Town, South Africa, 2014.

Bombardier Transportation, Suburban and Regional Transportation, Design Data for Electrical Multiple Units- M-7., Bombardier Transportation, St. Bruno, Canada. http://www.sonic.net/~mly/Caltrain-Electrification/2000-08-Rolling-Stock-Draft/a6.pdf Accessed August 7, 2019.

Bracken, J. and Selker, G., "Regenerative Braking: Decelerating for the Future", *University of Pittsburgh, Swanson School of Engineering*, Session B 3077.

Brown, D. T., "Feasibility Study of On-Car Regenerative Braking System for Electrical Rail Applications", *Dayton T. Brown Inc., Engineering and Test Division*, Bohemia, NY, 2013.

Consolidated Edison Inc. (2021), Time-of-Use-Rates. https://www.coned.com/en/accounts-billing/your-bill/time-of-use. Accessed February 28, 2022.

Conti, R., Galardi, E., Meli, E., Nocciolini, D., Pugi, L. and Rindi, A., "Energy and Wear Optimization of Train Longitudinal Dynamics and of Traction and Braking Systems", *Vehicle System Dynamics*, 53 (5), pp. 651-671, (2015), doi: 10.1080/00423114.2014.990466.

Desprez, C. and Djellab, H. (2012), "Traction Energy Saving by Speed Profile Optimization. *In Compendium of Papers for the Euro Working Group of Transportation*, Paris, France, 2012.

Eurostat (2020), "Passenger Transport Statistics", Statistical Office of the European Union, 2020, Luxembourg City, Luxembourg. https://ec.europa.eu/eurostat/statistics-explained/index.php?title=Passenger_transport_statistics#Maritime_passengers. Accessed May 10, 2021.

Eurostat (2021), "Final Energy Consumption in Europe by Mode of Transport", Energy Consumption in Transport, Fig. 4, Statistical Office of the European Union, 2021, Luxembourg City, Luxembourg. https://www.eea.europa.eu/data-and-maps/indicators/transport-final-energy-consumption-by-mode/assessment-10. Accessed May 10, 2021.

Feng, J.; Li, X.; Liu, H.; Gao, X.; Mao, B., "Optimizing the Energy-Efficient Metro Train Timetable and Control Strategy in Off-Peak Hours with Uncertain Passenger Demands". *Energies* 2017, *10*, 436. https://doi.org/10.3390/en10040436.

Frilli, A., Meli, E., Nocciolini, D., Pugi, L., Rindi, A., Romani, B., Ceraolo, M. and Lutzemberger, G., (2017), "The Tesys Rail Project: Innovative Models to Enhance the Energetic Sustainability of Railway Systems", *International Journal of Railway Technology, Vol. 6, Issue 4, pp. 1-28, doi: 10.4263/ijrt.6.4.1*, Saxe-Coburg Publications, 2017.

Ghaviha, N., Campillo, J., Bohlin, M. and Dahlquist, E., (2017), "Review of Application of Energy Storage Devices in Railway Transportation", *Proceedings of the 8th International Conference on Applied Energy*, Elsevier Energy Procedia 105 (2017) 4561-4568.

GE Optimizer, General Electric Corporation, Boston, MA, 2014. https://www.predix.com/sites/default/files/tripoptimizer.pdf. Accessed May 8, 2021.

Gong, C., Zhang, F., Zhang, J. and Wang, X. (2014). "An Integrated Energy-Efficient Operation Methodology for Metro Systems Based on a Real Case of Shanghai Metro Line One", *Energies*, 7, 7305-7329; doi:10.3390/en7117305.

Gonzalez-Gil, A., Palacin, R. and Batty, P., (2013), "Sustainable Urban Rail Systems: Strategies and Technologies for Optimal Management of Regenerative Braking Energy", Amsterdam, Netherlands: *Elsevier, Energy Conservation and Management*, 75 (2013) 374-388.

Gonzalez-Gil Palacin, R and Batty, P., (2014), "Optimal Energy Management of Urban Rail Systems: Key Performance Indicators", Amsterdam, Netherlands: *Elsevier, Energy Conservation and Management,* 90 (2015) 282-291.

Grisby, D. C., "A New Partnership: Rain Transit and Convention Growth", American Public Transportation Association, Washington DC, USA, September 2013.

Haramina, H., Mandić, M., and Nikšić, M. (2012). "New Method for Energy-Efficient Train Operation on Commuter Rail Networks". *Tehnicki Vjesnik*. 19. 801-806.

Hay, W. W., (1982), "Railroad Engineering 2nd Edition", New York, NY: *John Wiley & Sons Inc.*

Hoberock, L. L. (1976), "A Survey of Longitudinal Acceleration Comfort Studies in Ground Transportation Vehicles", *Research Report 40*, Department of Transportation, Office of Research, Washington, DC.

Howlett, P. G. and Pudney, P. J., (1995), "Energy-efficient Train Control", London, UK: *Springer-Verlag Ltd.*

Hull, G. J., "Simulation of Energy Efficiency on Commuter Railways", *Master's Thesis*, University of Birmingham, UK, 2009.

Ianuzzi, D., Pagano, E. and Tricoli, P., (2013), "The Use of Energy Storage Systems for Supporting the Voltage Needs of Urban and Suburban Railway Contact Lines", *Energies,* 2013,6, 1802-1820; doi: 10.3390/en6041802.

International Energy Agency, (2013), "CCS is a Necessity for a World Hooked on Fossil Fuels", International Energy Agency, Paris, France. www.iea.org/newsroomandevents/news/2013/january/name,34527,en.html. Accessed April 22, 2013.

International Energy Agency (2021), "Rail", IEA, Paris. https//: www.iea.org/repoerts/rail. Accessed December 5, 2021.

International Union of Railways, "Evaluation of Energy Efficient Technologies for Rolling Stock and Train Operation of Railways" *Deutsche Bahn AG, Railway Environmental Centre, Berlin Institute for Future Studies and Technology Assessment*, Berlin, Germany, 2003.

Jong, J. and Chang, S., "Algorithms for Generating Train Speed Profiles", *Journal of the Eastern Asia Society for Transportation Studies*, Vol.6, pp. 356-371, 2005

JR East (2020), “East Japan Railway company, Corporate Data, 2020. https://www.jreast.co.jp/e/data/index.html?src=gnavi. Accessed May 10, 2021.

Jung S., Lee, H., Jung, H. and Kim, H., (2013). A Study on Peak Power Reduction using Regenerative Energy in Railway Systems through DC Subsystem Interconnection, *Journal of Electrical Engineering Technology* Vol. 8, No. 5: 1070-1077, 2013. http://dx.doi.org/10.5370/JEET.2013.8.5.1070.

Kim, K., and Chien, S., (2011), “Optimal Train Operation for Minimum Energy Consumption Considering Track Alignment, Speed Limit and Schedule Adherence”, *Journal of Transportation Engineering,* Vol. 137, 2011, pp. 665-674.

Kim, M., Schonfeld, P. and Kim, E., (2013), “Simulation-Based Rail Transit Optimization Model”, *Transportation Research Record: Journal of the Transportation Research Board,* No. 2374, pp. 143-153, Transportation Research Board of the National Academies, Washington, D.C., 2013. Doi: 10.3141/2374-17.

Lamedica, R., Ruvio, A., Plagi, L. and Mortelliti, N., “Optimal Siting and Sizing of Wayside Energy Storage Systems in a DC railway Line”, *Energies,* 2020, 13, 6271, doi: 10.33901/en 13236271.

Lamontagne, C., (2013) “Advanced Wayside Energy Storage Systems for Rail Transit”, Final Report for Transit Idea Project 66, *Transportation Research Board of the National Academies*, National Research Council, Washington, DC.

Li, X., and Lo, H. (2014), “Energy minimization in dynamic train scheduling and control for metro rail operations”, *Elsevier, Transportation research Part B* 70 (2014) 269-284.

Lin, F., Li, X, Zhao, Y and Yang, Z., “Control Strategies with Dynamic Threshold Adjustment for Supercapacitor Energy Storage System Considering the Train and Substation Characteristics in Urban Rail Transit”, *Energies,* (2016), 9, 257.

Lin, F., Liu, S., Yang, Z., Zhao, Y., Yang, Z. and Sun, H., “Multi-train Energy Saving for Maximum Usage of Regenerative Energy by Dwell Time Optimization in Urban Rail Transit Using Genetic Algorithms”, *Energies* 2016, *9*(3), 208; https://doi.org/10.3390/en9030208.

Liu, R. and Golovitcher, I. M. (2003), “Energy-efficient operation of rail vehicles”, *Elsevier Transportation Research,* Part A, 37 (2003) 917–932.

Luan, X., Wang, Y., De Schutter, B., Meng, L., Lodewijks, G. and Corman, F., "Integration of real-time traffic management and train control for rail networks - Part 2: Extensions towards energy-efficient train operations", *Transportation Research Part B: Methodological*, Volume 115, 2018, Pages 72-94, ISSN 0191-2615, https://doi.org/10.1016/j.trb.2018.06.011.

Meisner F., and Sauer, D. (2019), "Wayside energy recovery systems in DC urban railway grids", *Elsevier*, https://doi.org/10.1016/j.etran2019.04.001.

Metropolitan Transportation Authority, Adopted Budget February Financial Plan 2019-2022.
https://new.mta.info/sites/default/files/2019-03/MTA-2019-Adopted-Budget-February-Financial-Plan_2019-2022.pdf. Accessed May 10, 2021.

Milroy, I. P., "Aspects of Automatic Train Control", *PhD Thesis*, Loughborough University of Technology, July 1980.

Miyatake, M. and Ko, H. (2010), "Optimization of Train Speed Profile for Minimum Energy Consumption", *IEEJ Trans Elec Electron Eng*., 5: 263–269, 2010. doi: 10.1002/tee.20528.

New York State Energy Research and Development Authority, "Understanding Demand Charges". https://www.nyserda.ny.gov/All-Programs/Programs/Energy-Storage/Energy-Storage-for-Your-Business/Understanding-Demand-Charges. Accessed September 28th, 2021.

Northeast Maglev (2018), 'The Decline of the American Passenger Railroad".
https://northeastmaglev.com/2018/10/23/the-decline-of-the-american-passenger-railroad/.
Accessed May 01, 2021.

Nowak, W., and Savage, I., "The Cross Elasticity Between Gasoline Prices and Transit Use: Evidence from Chicago", *Transport Policy* 29 (2013) 38-45.
https://doi: 10.1016/jtranpol.2013.03.002.

Norfolk Southern (2011), "Norfolk Southern Sustainability Report 2011Norfolk Southern Railroad Company.
http://www.nscorp.com/content/dam/nscorp/get-to-know-ns/impact/environment/sustainability-reports/ns-sustainability-report-2011.pdf.
Accessed November 20, 2015.

Parajuli, A., 2005. "Modelling Road and Rail Freight Energy Consumption: A Comparative Study", *Master's Thesis*, Queensland University of Technology, Queensland Australia. https://eprints.qut.edu.au/16193/. Accessed August, 2015.

Pena-Alcaraz, M., Fernandez, A., Cucala, A. P., Ramos, A. and Pecharroman, R., . (2011), 'Optimal Underground Timetable Design based on Power flow for Maximizing the Use of Regenerative-Braking Energy", *Proceedings of the Institution of Mechanical Engineers, Part F: Journal of Rail and Rapid Transit*, doi: 10.1177/0954409711409411, Sage Publications, UK.

Pew Research Center (2014), "Attitudes About Aging: A global perspective". https://www.pewresearch.org/global/2014/01/30/chapter-4-population-change-in-the-u-s-and-the-world-from-1950-to-2050/#fn-29181-33. Accessed March 26, 2022.

Pugi, L., Malvezzi, M., Papini, S., and Vettori, G., (2013), "Design and Preliminary Validation of a Tool for the Simulation of Train Braking Performance", *Journal of Modern Transportation*, 21(4), pp. 247-257, (2013), doi: 10.1007/s40534-013-00276.

Rackley, S., "Power Cut", *The Rail Engineer*, December 2009.

Roch-Dupré, D., Gonsalves, T., Cucala, A., Pecharroman, R., Lopez-Lopez, A. and Fernandez-Cardador, A., (2021), "Determining the Optimum Installation of Energy Storage Systems in Railway Electrical Infrastructure by means of Swarm and Evolutionary Optimization Algorithms" *Elsevier*, Electrical Power and Energy Systems 121 (2021) 106295.

San Martin, J. I., Zamora, I., San Martin, J. J., Aperribay, V and Eguia, P., (2011), 'Energy Storage Technologies for Electric Applications", Conference of the European Association for the Development of Renewable Energies, Environment and Power Quality, *Proceedings of the International Conference on Renewable Energies and Power Quality*, Las Palmas, Spain.

Simpson, S. (2020), "A Primer on the Railroad Sector", Sectors and Industries Analysis, Investopedia.https://www.investopedia.com/articles/stocks/11/primer-on-railroad-sector.asp Accessed August 4, 2020.

Sivanagaraju, S., Reddy, M. B. and Srilata, S., (2010), "Generation and Utilization of Electrical Energy", Uttar Pradesh, India: *Pearson Education*.

Su, R., Gu, Q. and Wen, T. (2014), "Optimization of High-Speed Train Control Strategy for Traction Energy Saving Using an Improved Genetic Algorithm", *Journal of Applied Mathematics*, Hindawi Publishing Corporation, Volume 2014, Article ID 507308.

Su, S., Tang, T. and Wang, Y. (2016), 'Evaluation of Strategies to Reducing Traction Energy Consumption of Metro Systems Using an Optimal Train Control Simulation Model", *Energies* 2016, 9, 105.

Su, S., Wang, X., Cao, Y. and Yin, J. (2020), "An Energy-Efficient Train Operation Approach by Integrating the Metro Timetable and Eco-Driving", IEEE Transactions on Intelligent Transportation Systems, Vol. 21, No. 10, Oct. 2020.

Tang, H., Dick, T. and Feng, X., (2015). "Optimization of Train Speed Profiles for a Metro Transit System by Genetic Algorithms",

Texas Transportation Institute, (2011) "Urban Mobility Report,2011". http://mobility.tamu.edu/ums/media-information/press-release. Accessed 1/26/13.

Thomas, C. E., (2015), "Sustainable Transportation Options for the 21st Century *A Comprehensive Comparison of Alternatives to the Internal Combustion Engine*", Springer International Publishing, Switzerland, 2015.

Transit Cooperative Research Program, (1997), "Consequences of the Development of the Interstate Highway System for Transit", *Research Results Digest*, August, 1997, No. 21.

Uher, R. A., Disk, D. R., "A Train Operations Computer Model", Rail Systems Center, Carnegie Mellon University, Pittsburgh, USA, Union Switch & Signal Company, American Standard Inc., Pittsburgh, PA, USA, 1987.

United Nations Framework Convention on Climate Change (2020), "Computer Aided Train Operation-Sweden".
https://unfccc.int/climate-action/momentum-for-change/activity-database/computer-aided-train-operation. Accessed September 2020.

United States Energy Information Administration (2021). "*Energy explained* Electricity generation, capacity and sales in the United States". https://www.eia.gov/energyexplained/electricity/electricity-in-the-us-generation-capacity-and-sales.php. Accessed April 2021.

United Stated Energy Information Administration (2021), "How much Carbon Dioxide is Produced per Kilowatt-hour of Electricity Generation?".

https://www.eia.gov/tools/faqs/faq.php?id=74&t=11. Accessed April 2022

United States Energy Information Administration, (2021), "Today in Energy", U.S. Renewable Energy Consumption by Source and Sector 2020. https://www.eia.gov/todayinenergy/detail.php?id=48396. Accessed November 13, 2021.

U.S. Energy Information Administration, (2014) "Short-term Energy Outlook 2014". http://www.eia.gov/forecasts/steo/report/global_oil.cfm Accessed November 12, 2014.

U.S. Energy Information Administration, (2020). Energy and the Environment Explained, 2020. https://www.eia.gov/energyexplained/energy-and-the-environment/where-greenhouse-gases-come-from.php. Accessed May 6, 2021.

United States Environmental Protection Agency, (EPA, 2011), "Climate Impact on Ecosystems", 2011. http://www.epa.gov/climatechange/impacts-adaptation/ecosystems.html Accessed April 22, 2013.

United Stated Energy Information Administration (EIA) (2010), "Energy trends in the New Policies Scenario, Primary Energy Demand", World Energy Outlook 2010. http://www.iea.org/publications/freepublications/publication/weo2010.pdf Accessed August 20, 2015.

Vantuono, W. C., "GE Transportation Touts Trip Optimizer", Railway Age Magazine, October 13, 2010. https://www.railwayage.com/news/ge-transportation-touts-trip-optimizer/. Accessed March 25, 2017.

Vuchic, V. R., 2007. *Urban Transit: Systems and Technology*, John Wiley and Sons, Hoboken, NJ, USA.

Wang, Z., Palazzolo, A. and Park, J. (2012), "Hybrid Train Power with Diesel Locomotive and Slug Car–Based Flywheels for NOx and Fuel Reduction", *American Society of Civil Engineers, Journal of Energy Engineering*, December 2012.

Wang, B., Yang, Z., Lin, F. and Zhao, W. (2014), "An Improved Genetic Algorithm for Optimal Stationary Energy Storage System Locating and Sizing", *Energies* **2014**, *7*, 6434-6458; doi:10.3390/en7106434.

Wong, K. K. and Ho, T. K., "Dynamic coast control of train movement with genetic algorithm", *International Journal of Systems Science*, volume 35, numbers 13-14, 2004, pp. 835-846.

World Bank Group, "World Development Indicators", World Databank, 2015 http://databank.worldbank.org/data/reports.aspx?source=2&country=&series=IS.RRS.TOTL.KM&period Accessed September 13, 2015.

Worldwatch Institute http://www.worldwatch.org/global-fossil-fuel-consumption-surges. Accessed September 8, 2016.

Xia, H., Chan, H., Yang, Z., Lin, F and Wang, B., "Optimal Energy Management, Location and Size for Stationary Energy Storage System in a Metro Line Based on Genetic Algorithm", *Energies* 2015,8(10), 11618-11640; doi: 10.3390/en81011618.

Yeh, S., (2003), "Integrated Analysis of Vertical Alignments and Speed Profiles for Rail Transit routes", *Master's Thesis*, University of Maryland, College Park.

Zablocki, A., (2019), "Fact Sheet: Energy Storage (2019)", *Environmental and Study Institute*. https://www.eesi.org/files/FactSheet_Energy_Storage_0219.pdf Accessed June 25, 2020